May 2006

"Luminaires"

Final Project Report (May 2006)

Sponsored by

Defense Advanced Research Projects Agency (DARPA/ATO)

DARPA Order P436/00

Issued by U.S. Army Aviation and Missile Command Under
Contract No. DAAH01-03-C-R157

Prepared by:
Eric Arons, Research Engineer
SRI International
333 Ravenswood Ave.
Menlo Park, CA 94025
650-859-3733

Effective Date of Contract: 04 February 2003
Contract Expiration Date: 05 February 2006
Reporting Period: 04 February 2003 – 04 February 2006

TABLE OF CONTENTS

PROJECT OVERVIEW

The goal of the HEDLight program is to develop a complete remote source lighting system for area, task, and navigational lighting on naval platforms. Within the scope of the overall program is the development of the source, distribution system, and luminaire, along with the integration of the entire system. The technical objectives of the program emphasize the attainment of high efficiency with regard to electrical, mass, and luminous output. In addition, the output of the luminaire should achieve certain spectral and spatial uniformity specifications. The program is divided into three phases, with efficiency goals increasing in each subsequent year. Figure 1 shows the expected technical milestones for the overall program. SRI is one of two contractors developing the luminaire for the system. Fiberstars, Inc., is the other luminaire contractor.

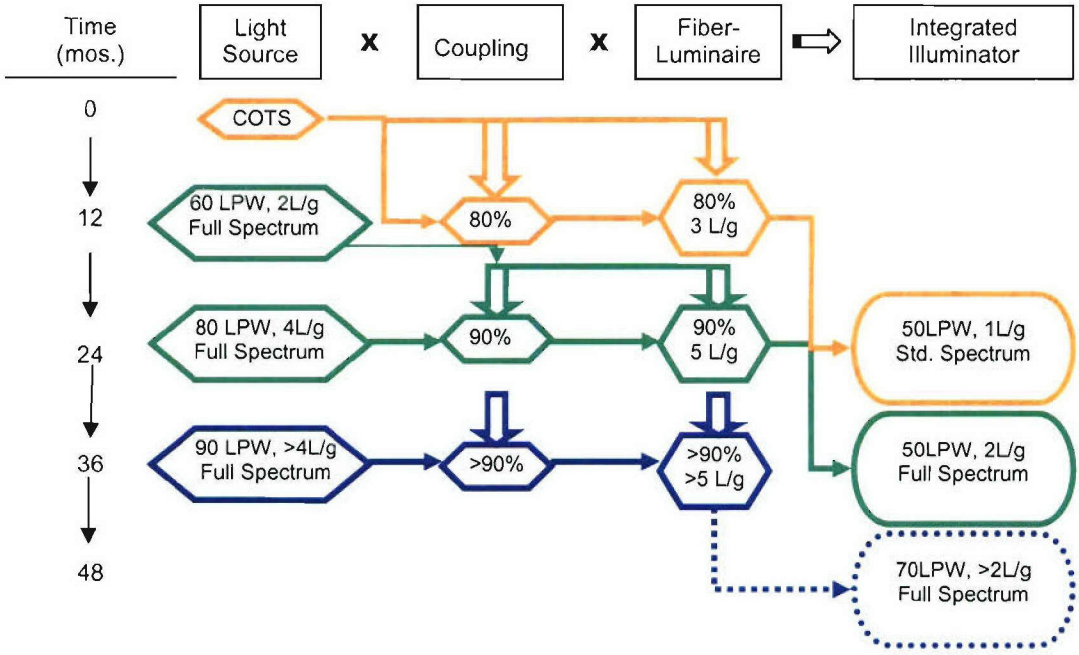

Figure 1 – Overall technical goals for the HEDLight Program.

In year 1 of the program, SRI was tasked with developing the luminaire using hollow-core waveguide technology. For a complete technical discussion of year 1 accomplishments, please refer to Appendix A. Upon completion of the first year of work, DARPA decided to refocus the effort on developing special-purpose point luminaires to be used for task lighting or as navigational beacons for naval ships. This application requires a cut-off Lambertian angular distribution (Figure 2), a compact form factor, and lightweight design. Most of year 2 was spent down-selecting designs for the compact specialty point luminaires. Appendix B contains a complete technical description and final results of the down-selection process.

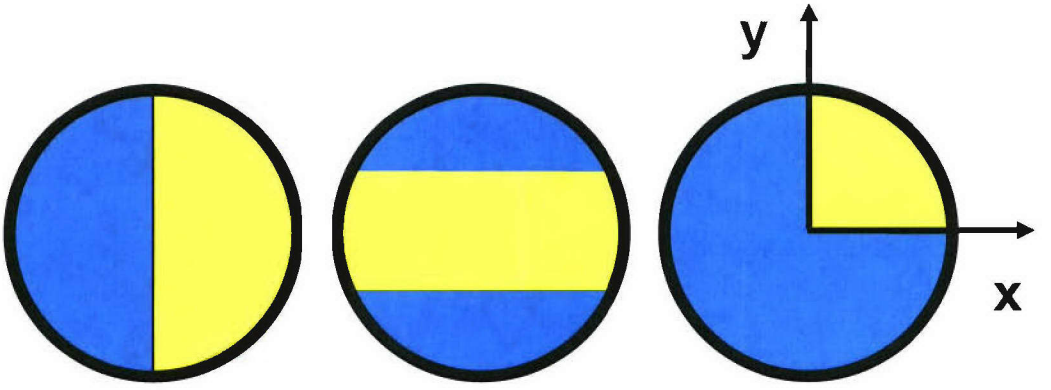

Figure 2 – Examples of cut-off Lambertian distributions represented in direction cosine space.

TECHNICAL PROGRESS

As described in Appendix B, the decision was made at the end of year 2 to optimize and build a small-scale side-fire luminaire prototype. Before the design could be finalized, we needed to further investigate several options for beam expansion and homogenization. These decisions would have a direct impact on the choice of vendors for the final product. The primary concern was that the angular spread achievable with COTS diffusers made by Physical Optics Corporation (POC) would not approximate the desired Lambertian distribution closely enough. The options we considered were as follows:

1) Develop a method for pre-expanding beam prior to entering POC diffuser

2) Use custom structured diffusers manufactured by RPC Photonics (RPC)

3) Test molded diffusers from POC to see if they had better performance than the COTS items.

Each of these will be described briefly in a separate section.

Pre-Expansion

One of the initial pre-expansion methods we considered was to use a tapered fiber to increase the angular spread of the light entering the luminaire. Figure 3 shows a CAD image of a tapered fiber model.

Figure 3 – CAD model of a tapered fiber expander at the end of the input fiber.

The model results are shown in Figure 4. The input for this model was an angular source distribution matching the sources coming out of the HEDLight program. Given the numerical aperture constraints of the input fiber and the constraints on taper length, the resulting expansion from the fiber was minimal and led us to abandon this approach.

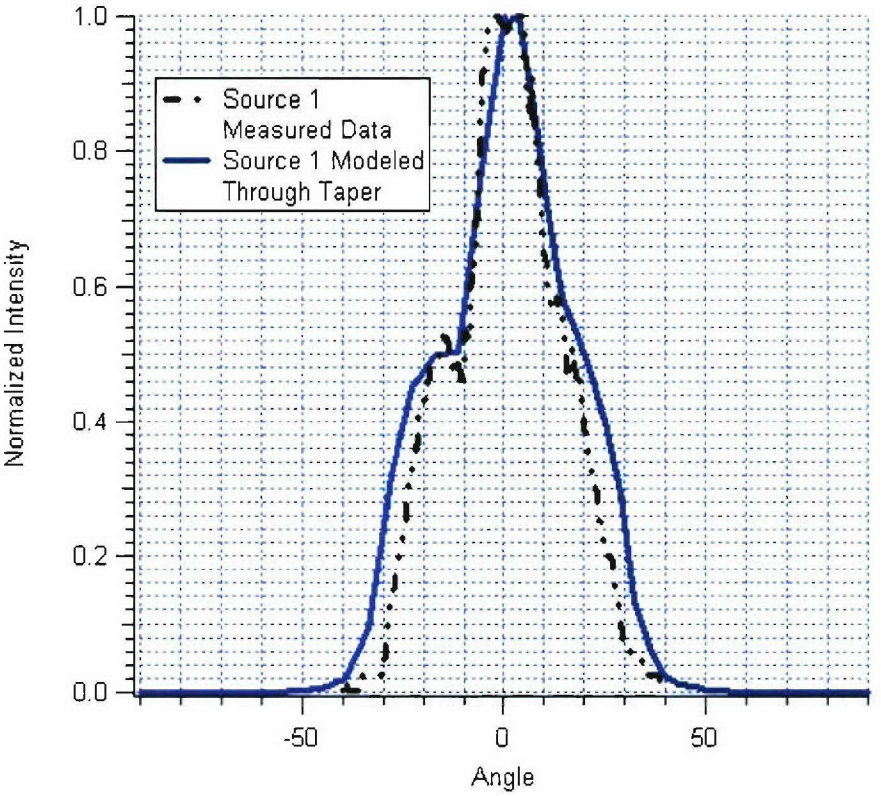

Figure 4 – HEDLight source distribution modeled through tapered fiber, showing minimal expansion of angular spread.

Structured Diffusers

RPC Photonics of Rochester, New York, has a unique approach to making diffusing elements. They pattern a refractive structure on a surface, which allows them to control the output light distribution precisely for a given input distribution. Figure 5 shows an electron micrograph of an RPC diffuser along with some of the patterns they are able to create.

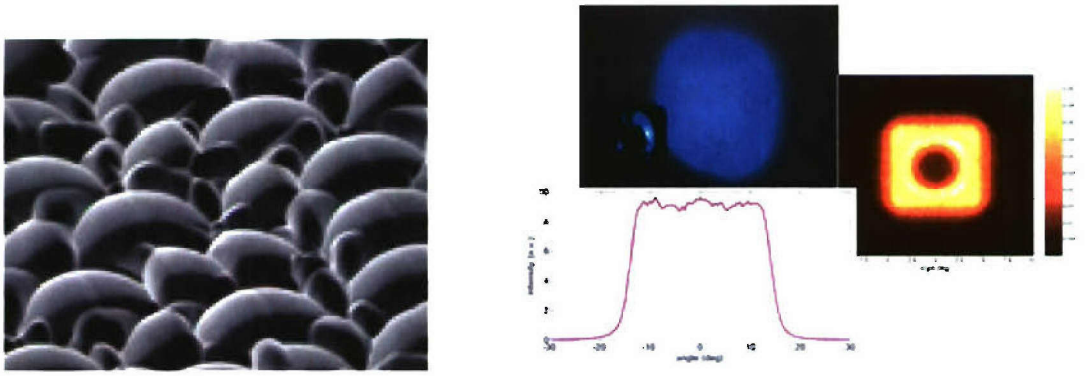

Figure 5 – Electron micrograph of an RPC structured diffuser surface along with images of sample angular distributions.

One possibility is that a properly designed structure would in fact obviate the need for taking advantage of the total internal reflection off the top surface of the side-fire prism. The structured diffuser could be designed to take the light from the fiber and directly shape it into a half-Lambertian distribution. RPC indicated in several discussions that they thought this was possible, but that it would require a significant research effort. Had this option presented itself earlier in the program, we believe it would have merited significant attention. However, given schedule and budget constraints, the decision was made to focus on our original design.

We therefore began to assess whether RPC could produce a structured diffuser pattern that would provide a full Lambertian pattern. They performed modeling to provide us with an estimate of what they thought they could achieve. Figure 6 shows a plot of an ideal Lambertian distribution, a theoretical curve sent by RPC, and the first two attempts by RPC to manufacture diffusers to meet the requirements. For these two initial attempts they had difficulty matching the theoretical curve for the high angles and the low angles simultaneously. Figure 7 shows a plot of their next two attempts at meeting the requirements. For these two samples, they moved much closer to what we needed, but as can be seen in the blue curve, asymmetry was an issue. This was because the scale of the structures was too large, leading to undersampling of the structured pattern. At this point, again due to schedule and budget constraints, the decision was made to move forward with the POC diffuser approach, as we felt this had the lowest risk.

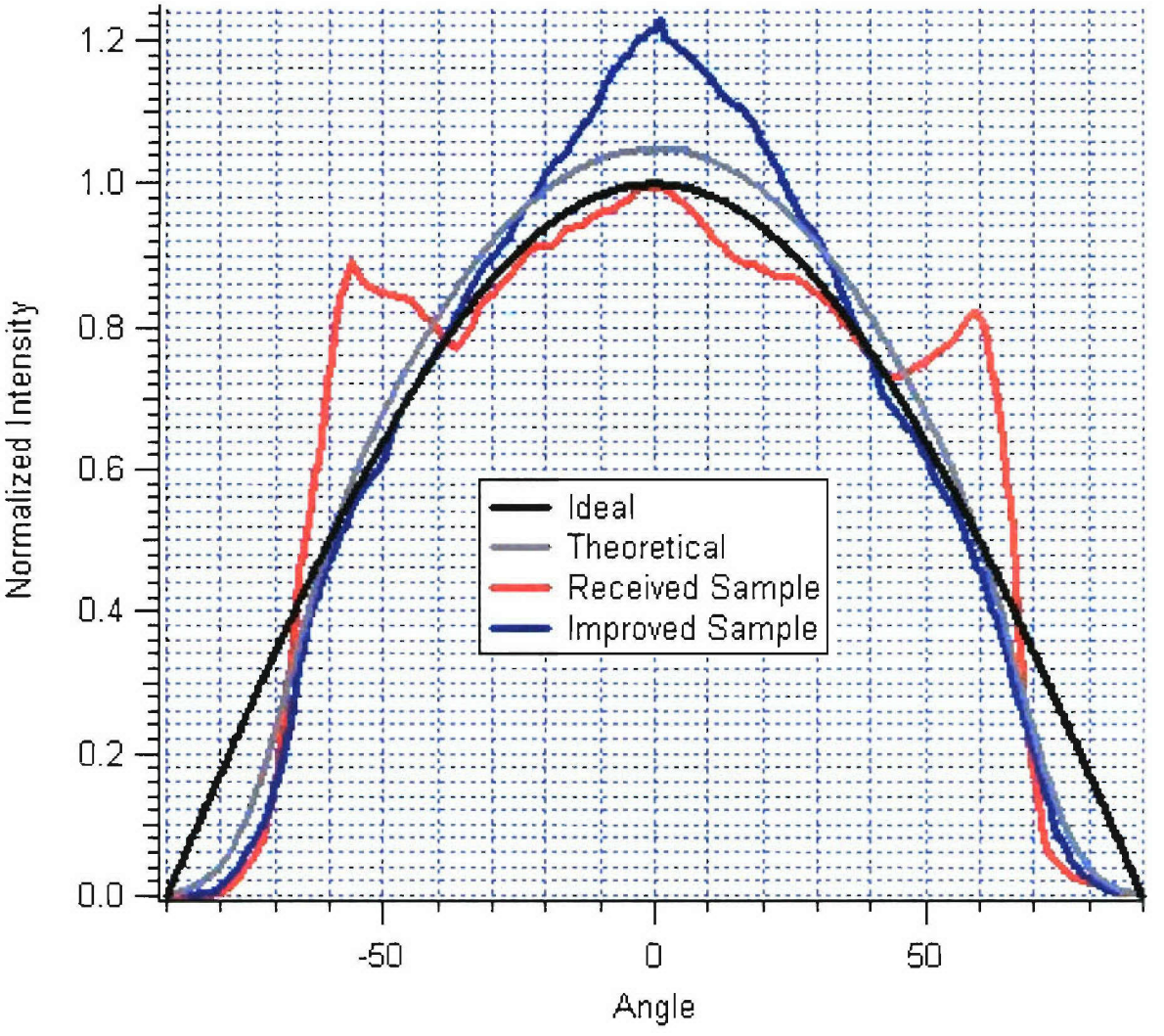

Figure 6 – Plot showing theoretical performance of RPC Lambertian diffuser with first two measured attempts.

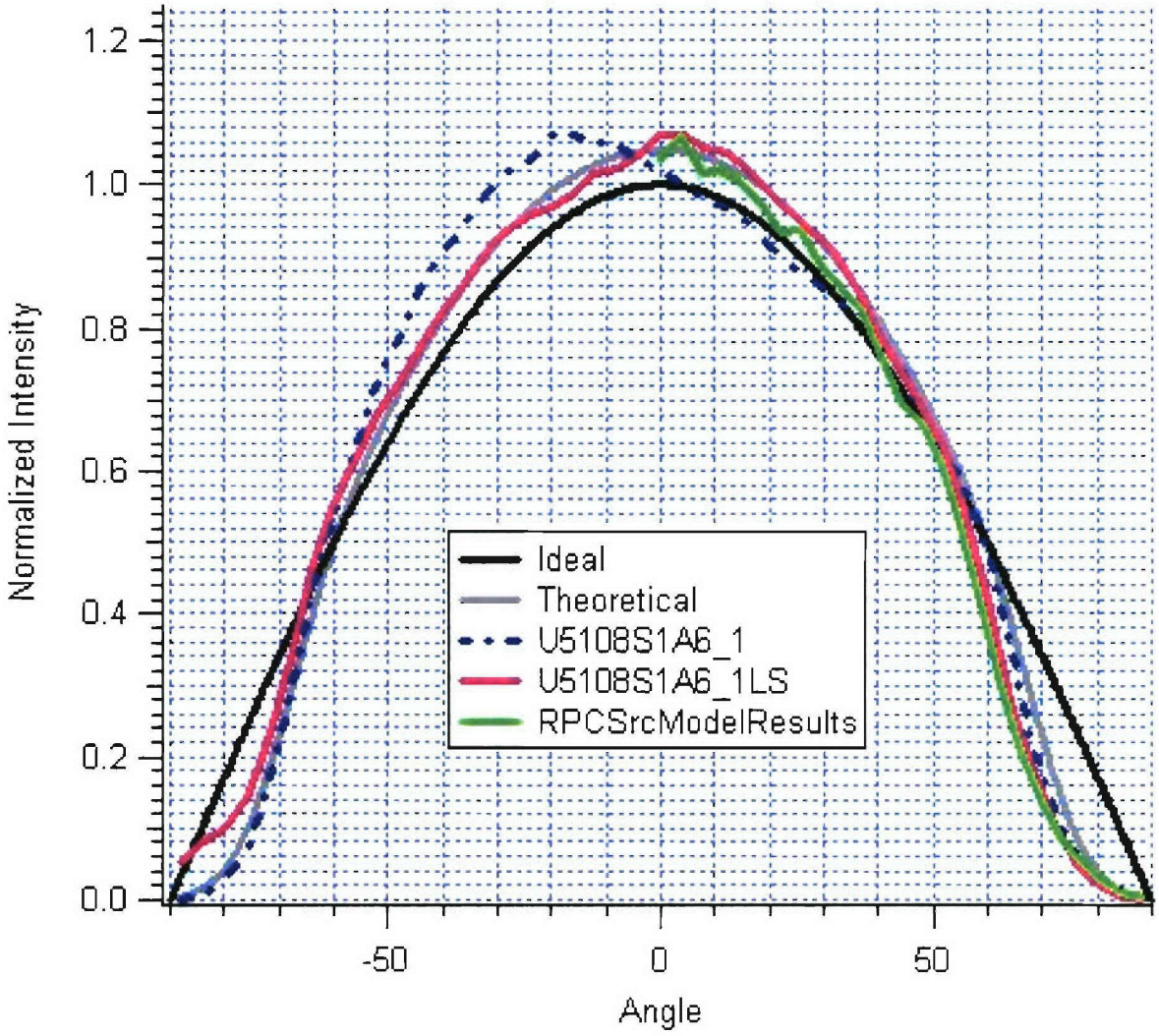

Figure 7 – Plot showing theoretical performance of RPC Lambertian diffuser along with measurements of two final samples. Sample performance improved, but out of concerns over reliability, schedule, and budget the decision was made to not continue pursuing this option.

POC Molded Diffusers

Physical Optics Corporation is a developer of holographic diffusers. They have an established track record of molding diffuser patterns into custom-molded optics. We presented them with a design for a side-fire luminaire with their diffuser molded into the input face. Because of their proprietary diffuser design, POC would accept the project only if they could act as the system integrator. Ideally we would have taken the diffuser mold insert to a plastic optics molder of our choice, but under the terms of our agreement with POC, this was not allowed.

After several iterations, we began receiving parts from POC. Figure 8 shows a couple of images of the typical POC molded parts, none of which had adequate quality to be useful. At this point they are still trying to perfect their process. They have since produced molded parts with dimensions and tolerances that are likely adequate, but they have not been able to demonstrate the ability to simultaneously mold in a diffuser and maintain overall prism quality.

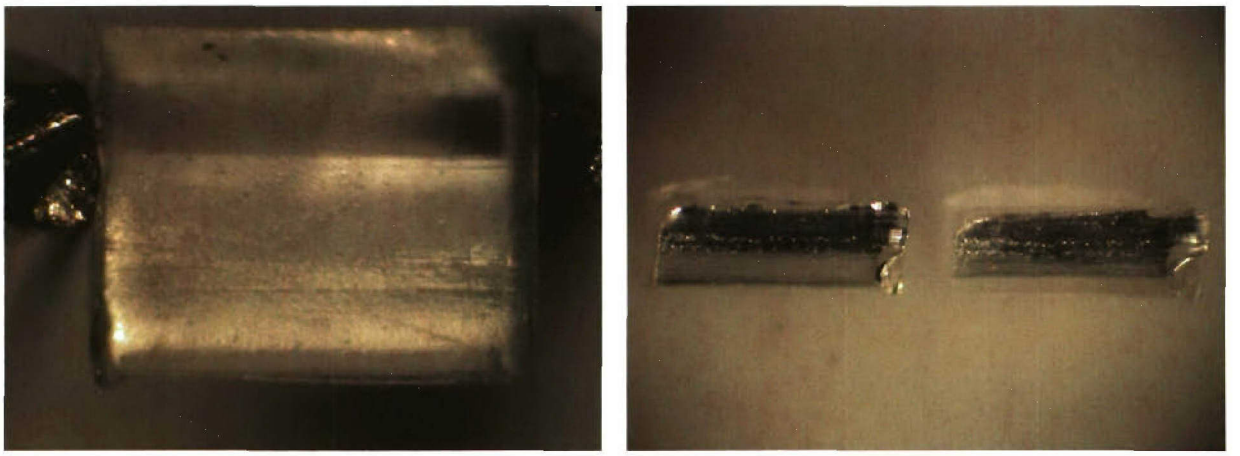

Figure 8 – Images of the typical poor quality of POC molded luminaires.

SUMMARY

The performance of the side-fire luminaire relies on a key optical element: the input diffuser. Few vendors are able to manufacture diffusers of sufficient angular range, as the market for such diffusers is small. RPC Photonics has a technology that showed promise and might have provided a path to selecting more capable molders of plastic optics than those POC produced. In addition, it would be worthwhile to investigate the possibility of using structured diffusers to directly produce the desired angular distribution without relying on features of the molded optical part.

APPENDIX A

HOLLOW-CORE LUMINAIRES

April 2004

"Hollow-Core Luminaires"

Year-End Summary Report (April 2004)

Sponsored by

Defense Advanced Research Projects Agency (DOD)
(ATO)

ARPA Order P436/00

Issued by U.S. Army Aviation and Missile Command Under
Contract No. DAAH01-03-C-R157

Prepared by:
Eric Arons, Research Engineer
SRI International
333 Ravenswood Ave.,
Menlo Park, CA 94025
650-859-3733

Effective Date of Contract: 04 February 2003
Contract Expiration Date: 05 February 2006
Reporting Period: 04 Feb 2003 - 02 Apr 2004

PROJECT OVERVIEW

The goal of the HEDLight program is to develop a complete remote source lighting system for area lighting on naval platforms. Within the scope of the overall program is the development of the source, distribution system, and luminaire, along with the integration of the entire system. The technical objectives of the program emphasize achieving high efficiency with regard to electrical, mass, and luminous output efficiencies. In addition, the output of the luminaire should achieve certain spectral and spatial uniformity specifications. The program is divided into three phases, with efficiency goals increasing in each subsequent year. Figure 1 shows the expected technical milestones for the overall program. SRI is one of two contractors developing the luminaire for the system. Fiberstars, Inc., is the other luminaire contractor.

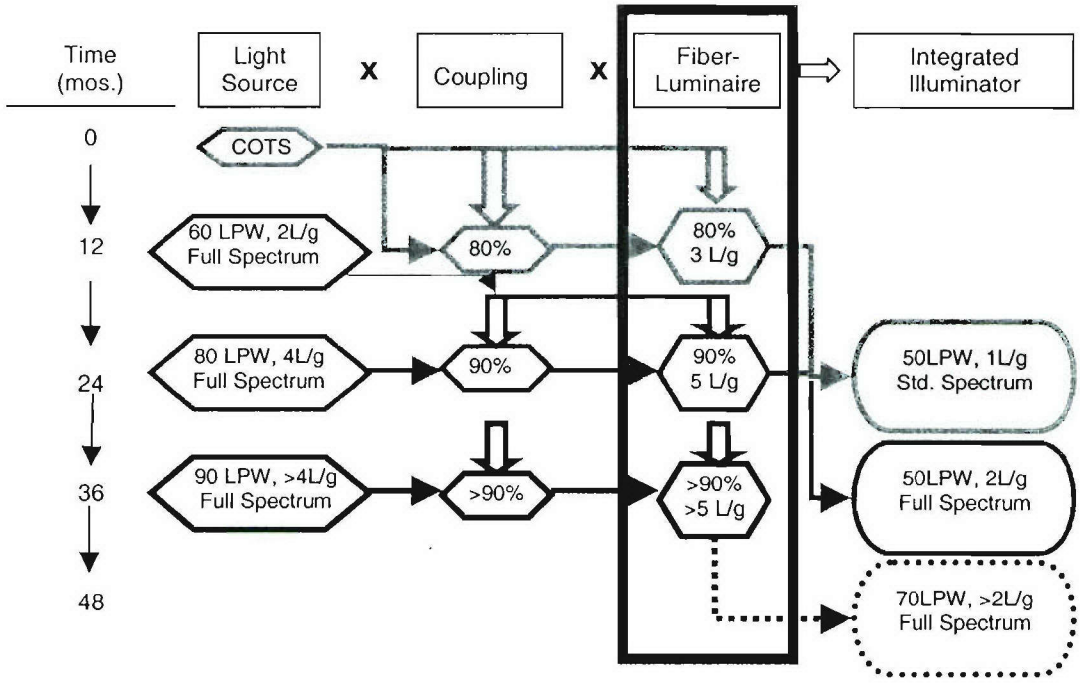

Figure 1 – Overall technical goals for the HEDLight Program with SRI's contribution highlighted in red.

The approach SRI has followed is to develop the luminaire based on hollow-core waveguide technology. These waveguides can be constructed from microstructured, prismatic polymer films such as Optical Lighting Film (OLF) developed by 3M Corporation. Such waveguides are extremely lightweight compared with solid-core fiber guides. Figure 2 shows the general concept of how prismatic film can be used for development of hollow-core waveguides. Shown are the angular distributions for the transmitted and reflected components of light incident onto the prismatic film, along with a concept for a cylindrical waveguide with a diffuse extractor running the length of the tube. Figure 3 shows several other conceptual designs for hollow-core waveguides using the prismatic film.

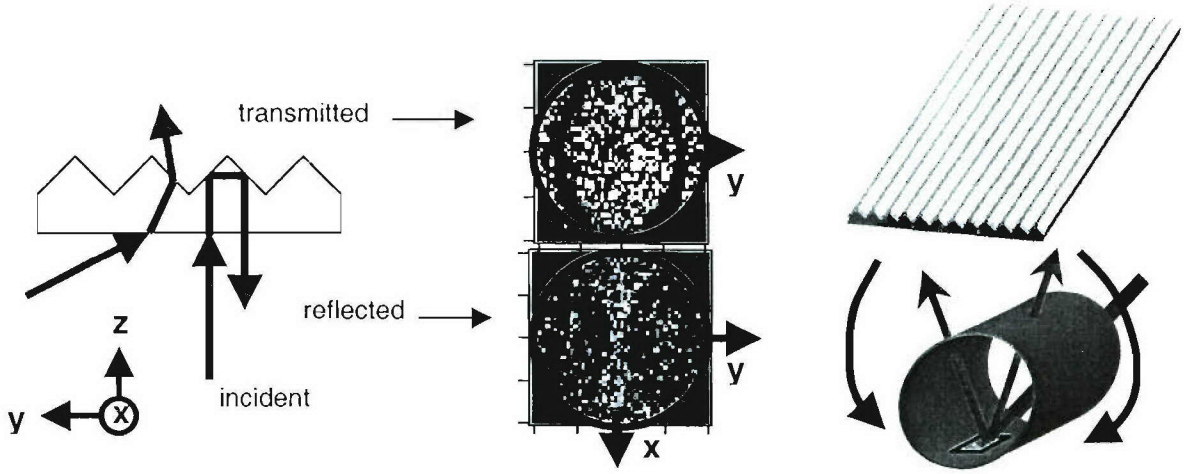

Figure 2 – Angular distributions for transmitted and reflected components of diffuse light incident on prismatic film, along with conceptual design for cylindrical hollow-core waveguide.

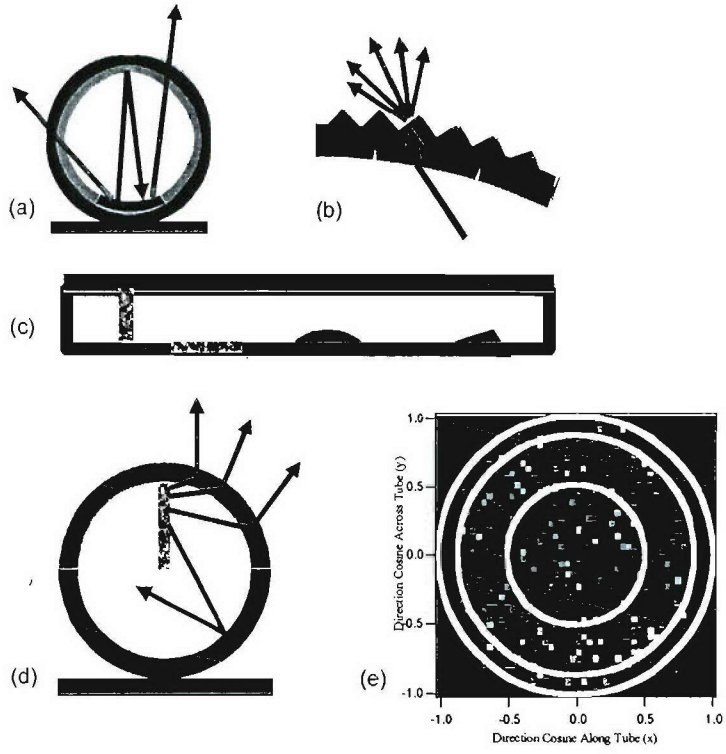

Figure 3 – Examples of extractor designs for hollow-core light guides using (a) double-wall OLF; (b) single-wall OLF with selective scattering; (c-d) single-wall OLF combined with radiant mirror film (black); (e) ray trace simulation of projected hemispherical output of design shown in (d), when end-illuminated with a source simulating the output of a typical solid-core fiber.

A commercial company, TIR Systems of Vancouver, Canada, is currently using the OLF technology to build long-distance luminaires for use in tunnels. We acquired one of the luminaires from TIR systems and characterized it to determine whether it was sufficiently close to meeting the program goals. It was not, so we continued to design and build versions of the hollow-core luminaire that would meet the program goals.

We have developed our initial prototypes using the commercially available OLF, which is made from polycarbonate. Because polycarbonate has a high bulk absorption coefficient, we have been focusing our efforts on later prototypes, which duplicate the prismatic film in acrylic using thermoforming techniques.

TECHNICAL PROGRESS

The reporting period described here covers the entirety of Phase I, from 4 February 2003 to 2 April 2004. The technical proposal divided the Phase I effort into two separate tasks, Modeling and Prototype Development. We report on these tasks separately below.

Task 1: Modeling

The modeling work was done primarily using LightTools,[1] with waveguide structures designed using SolidWorks.[2] LightTools contains material absorption data for polymethyl methacrylate (PMMA), but not for polycarbonate. Since we suspected that polycarbonate would prove to be too absorbing to reach our efficiency goals, we performed most of the modeling using PMMA as the material.

We began by modeling the basic prismatic film in a cylindrical configuration with various outcoupling methods. It became clear that for a 1-m length, outcoupling most of the light efficiently requires a cylinder of a fairly small diameter. At the kickoff meeting it was pointed out that cylinders made from OLF with diameters smaller than approximately 4 in. demonstrate markedly decreased efficiency due to bend-related stress induced in the material. This led us to examine rectangular, trapezoidal, and triangular structures. In addition, we considered inward facing as well as outward facing prismatic structures for the waveguide.

One of the initial decisions we needed to make was whether to use the prismatic film with the prismatic surface facing inward versus outward. While the film was designed to be used with the prism surface on the side opposite the guided light, the light still remains highly guided when the prismatic surface is located on the interior of the lightguide. One advantage of locating the prismatic surface interior to the waveguide is that the structure is somewhat more protected from the elements.

---

[1] LightTools is an optical ray-tracing program developed by Optical Research Associates. Descriptions of the program can be found at http://www.opticalres.com

[2] SolidWorks is a 3D mechanical design program. Descriptions of the program can be found at http://www.solidworks.com

Figure 4 shows the angular distributions for reflection and transmission of the prismatic film with diffuse light incident on both the flat surface as well as the prismatic surface. The transmitted angular distributions are most important, since they determine the angular output of light as seen exiting the luminaire. For the inward-facing facets, the transmitted distributions are primarily concentrated at higher angles. If we consider a square luminaire (Figure 5), this correlates to the light exiting the top facet being directed toward the sides, while light exiting the sides of the luminaire gets directed toward both the floor and the ceiling. For certain applications, this profile could be desirable. However, since the goal of this initial effort was to produce a Lambertian angular distribution, we decided that using outward-facing facets was the best approach.

Our design effort focused primarily on two waveguide shapes: rectangular and trapezoidal. In addition to the waveguide shape, we needed to develop an appropriate outcoupler. Our initial modeling effort focused on varying the waveguide shape while using a basic diffusing strip running along the bottom of the waveguide as the outcoupler.

Figure 6 shows a CAD model of the trapezoidal design under consideration. The trapezoid design has a height of 20 mm and a width of 60 mm, with the sides angled at 45° to the horizontal plane. Figure 7 shows the angular distribution in direction cosine space for this particular design. This distribution includes only the light propagating in the positive z hemisphere, that is to say, light directed toward the floor if the luminaire were to be placed on the ceiling. The angular distribution looks promising, as much of the light is directed away from the center and more toward the sides. This directionality is useful in minimizing glare for people walking down a hallway.

To calculate the efficiency for this design, we modeled a triangular diffusing strip along the bottom of the luminaire for the outcoupler. The strip is narrowest at the end closest to the source, and widens at the far end of the luminaire. For this model we assumed the diffusing strip was 98% reflective. The initial model showed as much as 20% of the light exiting in the negative z-direction (toward the ceiling), much of that exiting the prismatic film that surrounded the outcoupler. By surrounding the trapezoidal luminaire with a reflective tray, we were able to get the model to demonstrate approximately 85% of the light traveling in the positive z-direction. But the primary advantage of the trapezoidal approach was that it had an interesting angular distribution due to the light exiting the angularly oriented prismatic sheets. The reflective tray has the additional advantage of producing a more Lambertian distribution than the trapezoidal one. Since a rectangular luminaire would be somewhat easier to manufacture, we decided to move our modeling effort in that direction.

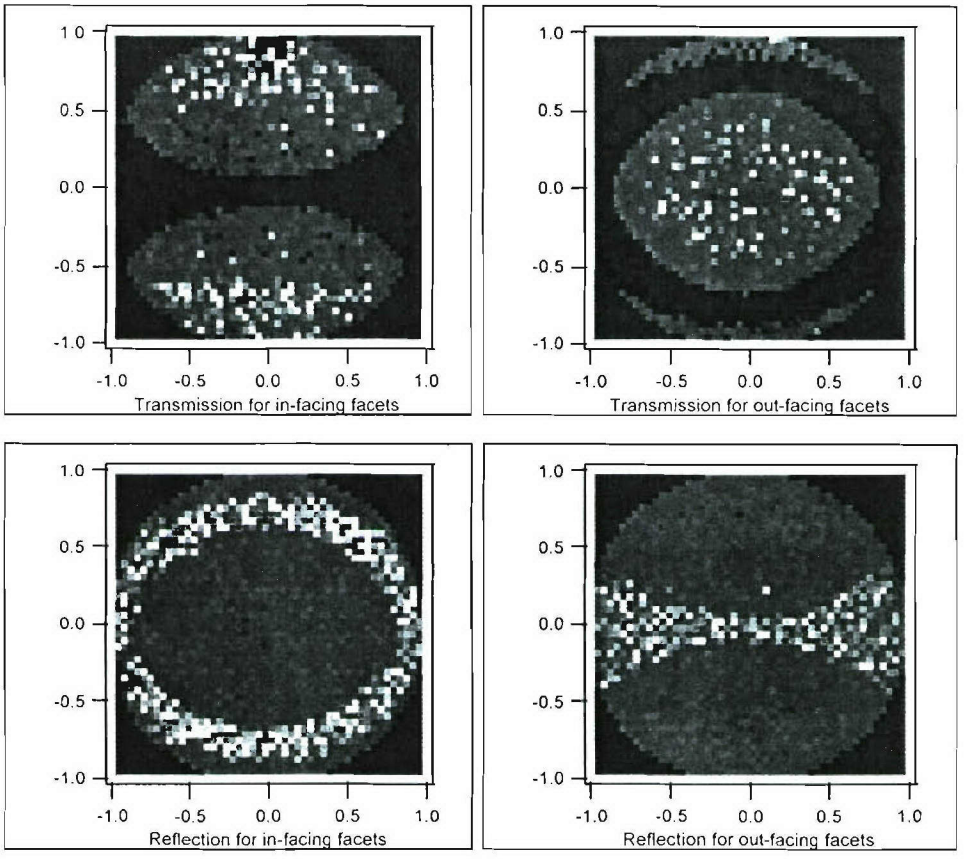

Figure 4 – Angular distributions in direction cosine space showing transmission and reflection through prismatic film for light incident on planar side of film (outward-facing) and light incident on prismatic side of film (inward-facing).

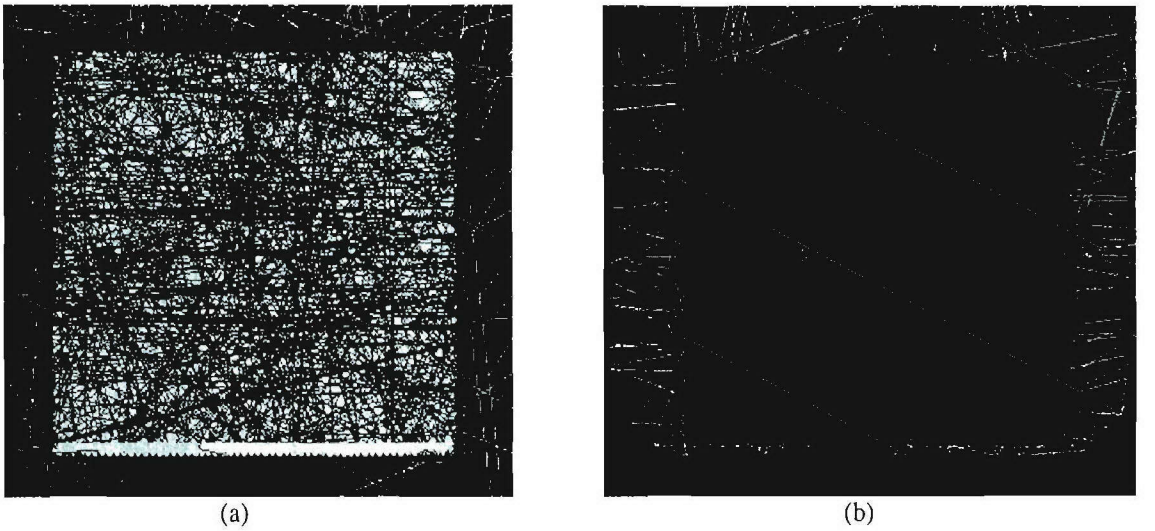

(a) (b)

Figure 5 – End views of square box luminaire waveguides with (a) inward-facing and (b) outward-facing prismatic surfaces. For the inward-facing prisms, the light is more strongly directed away from the surface normal than for the outward-facing prisms.

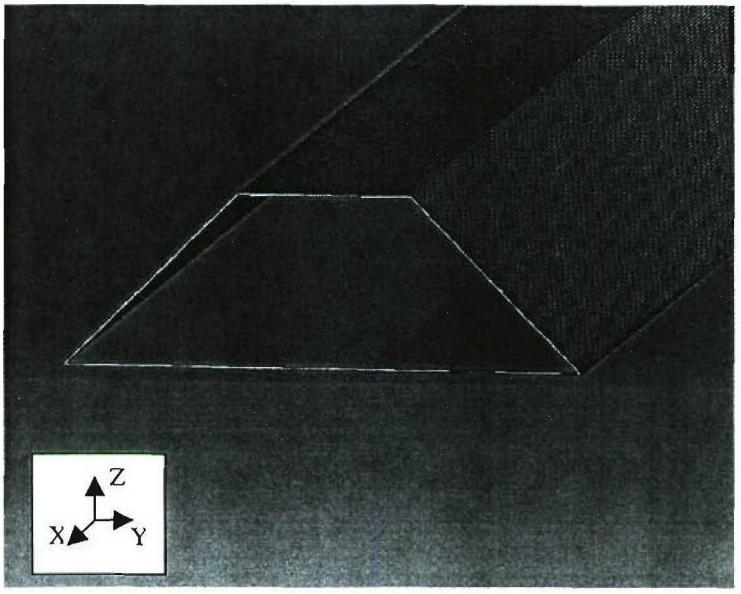

Figure 6 – CAD model of trapezoidal luminaire design with coordinate system.

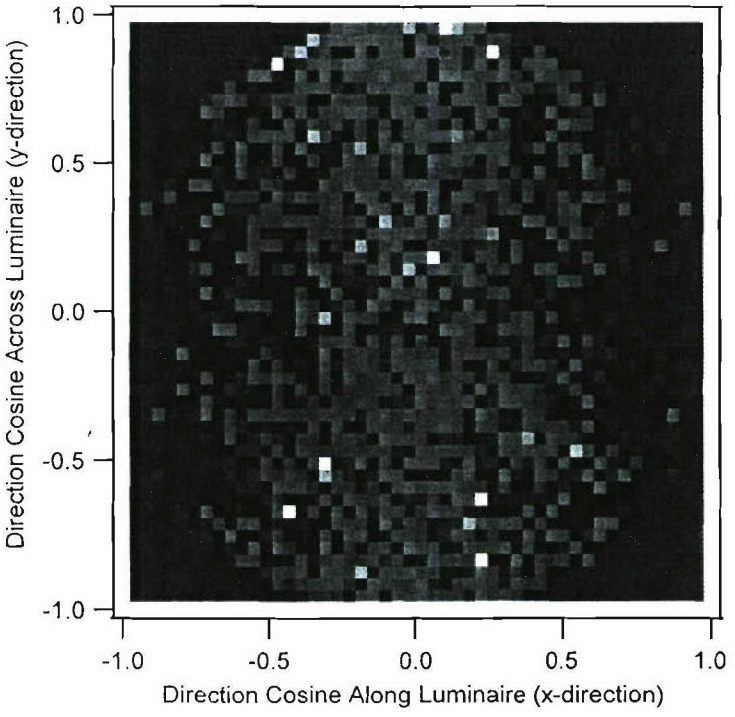

Figure 7 – Angular distribution in direction cosine space for light exiting trapezoidal luminaire in the positive z hemisphere.

Figure 8 shows a CAD model of the as-built luminaire design, including the diffuse reflective backplane and the triangular diffusing outcoupler. Not shown are the source and the two endcaps that redirect light back into the waveguide at each end. The design initially assumed 98% reflectivity for the diffusing surfaces. We also assumed the material for the OLF was PMMA. A complete absorption model is included with LightTools for PMMA, and the transmission spectrum for this model is shown in Figure 9. With these assumptions, the model indicated 85% efficiency in the desired hemisphere. If we lower the diffuse reflectivity to 95%, the modeled efficiency drops to 77%.

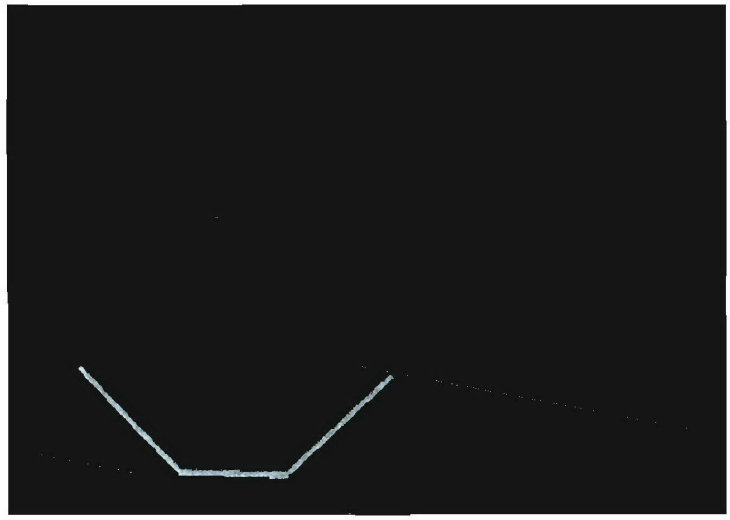

Figure 8 – CAD model of final luminaire design, including triangular diffusing outcoupler and diffusing reflector.

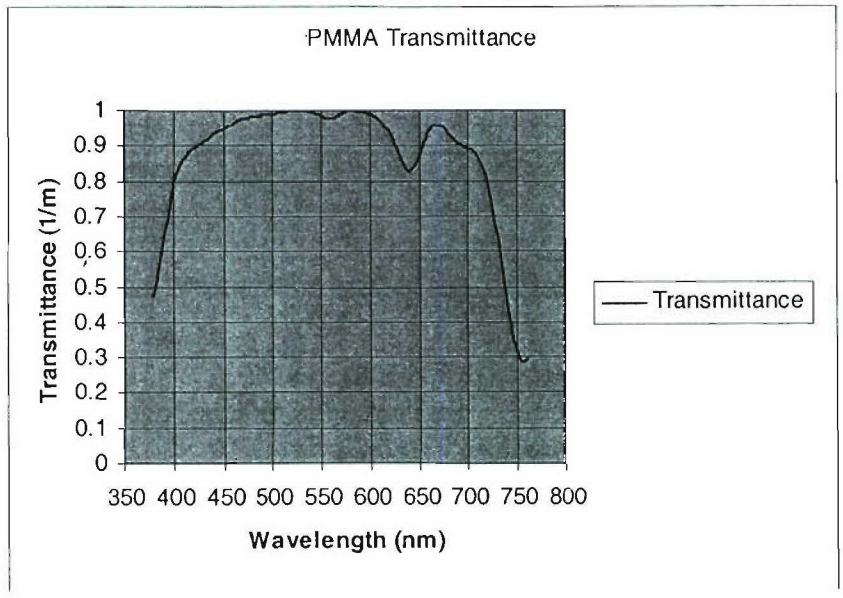

Figure 9 – Transmission model for PMMA included in LightTools.

While the modeled efficiency of the system meets the program specifications, there were some concerns about the angular and spatial uniformity of the light exiting the luminaire. One issue was that the light launched from the commercial off-the-shelf (COTS) input fiber has a broader angular extent than can be guided by the prismatic film. Figure 10 shows the angular distribution in direction cosine space for the output from the 19-mm Fiberstars fiber. The model for the fiber was generously provided to us by Fiberstars. The maximum angular extent is 45°, and much of the light is concentrated away from the central axis. The polycarbonate prismatic film can guide light with a maximum angle of approximately 30°, and PMMA would have an even lower acceptance angle. To keep light from leaking out of the waveguide prematurely and at high angles of incidence, we designed a concentrator to limit the entrance angles into the luminaire. Figure 11 shows a CAD image of the fiber with the concentrator, and Figure 12 shows the resulting angular distribution. Figure 13 (a) shows the angular distribution of the complete luminaire system without the concentrator. The strong bright region at angles near 40° corresponds to the light that is not trapped by the film and immediately leaks out of the luminaire. Figure 13 (b) shows the final angular distribution with the concentrator in place. The leaked light has largely disappeared. Further modifications to the concentrator design could be made to improve the coupling further.

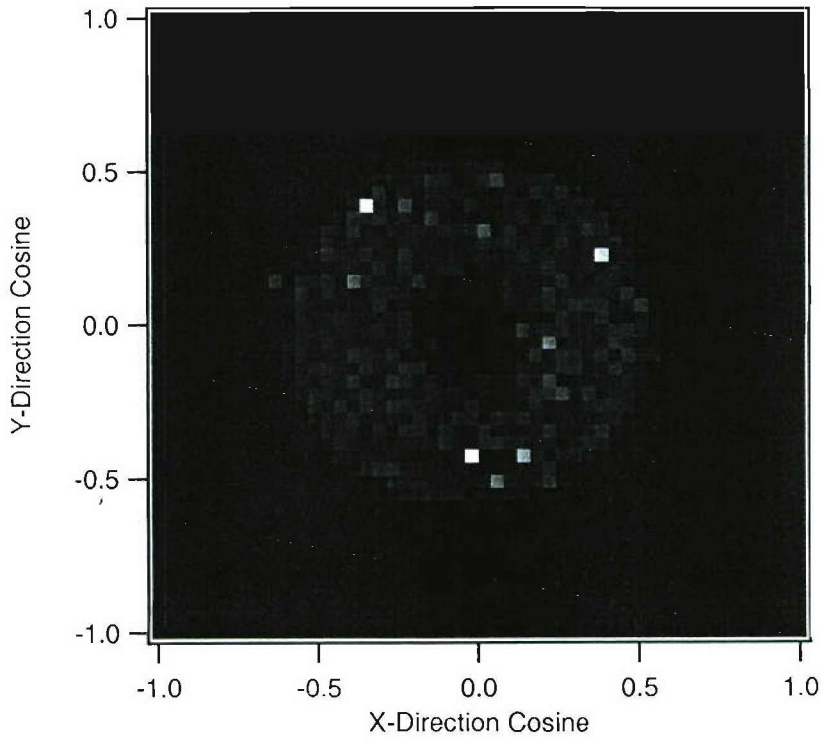

Figure 10 – Angular distribution for light exiting COTS 19-mm transport fiber. Maximum angular spread corresponds to approximately 45º.

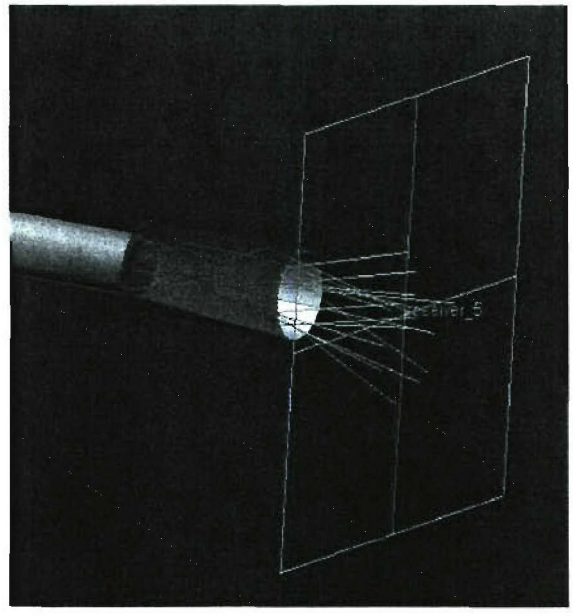

Figure 11 – CAD image of transport fiber and concentrator.

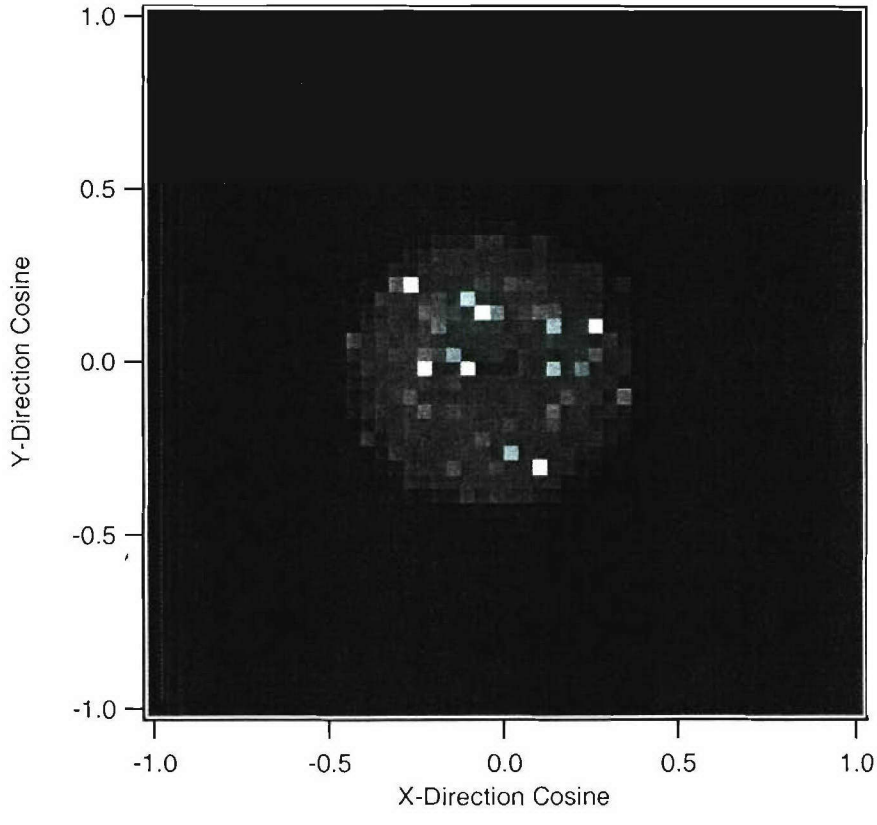

Figure 12 – Angular distribution for light exiting combination of transport fiber and concentrator. Maximum angular extent is approximately 33º.

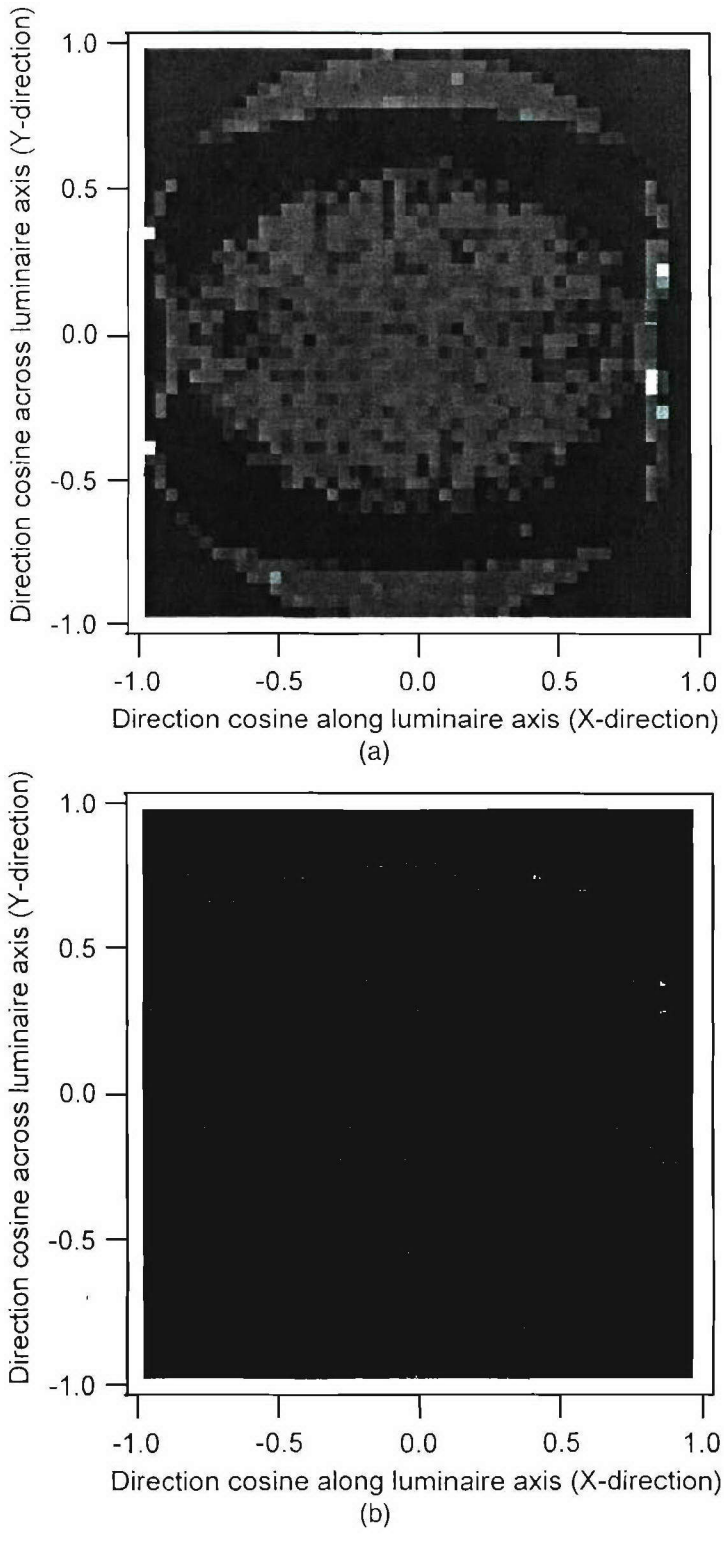

Figure 13 – Angular distributions for square waveguide luminaire (a) without concentrator and (b) with concentrator after transport fiber. Angular distribution without concentrator shows bright forward directed component of light.

In addition to the overall design modeling, there were also some materials issues we needed to investigate. One of our concerns was whether the polycarbonate prismatic film sold by 3M would have sufficient clarity to meet the efficiency goals for Phase I. LightTools does not have an accurate absorption model for polycarbonate, so we ran a series of model runs calculating the efficiency for our design versus material transmission. Figure 14 (a) shows the plot of design efficiency versus transmission. The model assumed 100% reflectance values for all diffusers and mirrors in the system. Because the light has such a short path length in the material, the material absorption has a small effect on overall system efficiency. For material transmissivity in the 1-5%/m range, design efficiency drops more rapidly. Certain types of polycarbonate have transmissivity of approximately 3%/m. Switching to acrylic could result in a 5-10% gain in overall system efficiency.

Figure 14 (b) shows the effect of reflectivity of the diffusers and mirrors in the system on the overall efficiency. It is clear from this figure that the outcoupler efficiency has a much stronger effect on overall efficiency than the material absorption of the OLF. We believe this effect is also stronger for the hollow-core design than for the solid-core design because with the hollow-core design the likelihood is greater that light will strike the outcoupler multiple times before exiting the luminaire. This is due to the reflection properties of the OLF film, which causes light at certain angles to be completely reflected back into the luminaire.

Another issue with the prismatic film from 3M is that the corners of the prisms are not perfectly square. This will mostly affect the angular distribution of the luminaire by allowing guided light to escape prematurely and in the forward direction. We modeled a square waveguide with various amounts of rounding on the corners of the prism to determine how much light would leak out given a 20° half-angle source distribution. Figure 15 shows the percentage of light leaking out of the waveguide versus modeled radius of curvature on a corner of each prism. Electron micrographs of the 3M prismatic film indicated a radius of curvature on the order of 0.5-1 μm, which can lead to a significant amount of leaked light in the forward direction. Part of our materials effort will be aimed at producing material with sharper features than those provided by 3M.

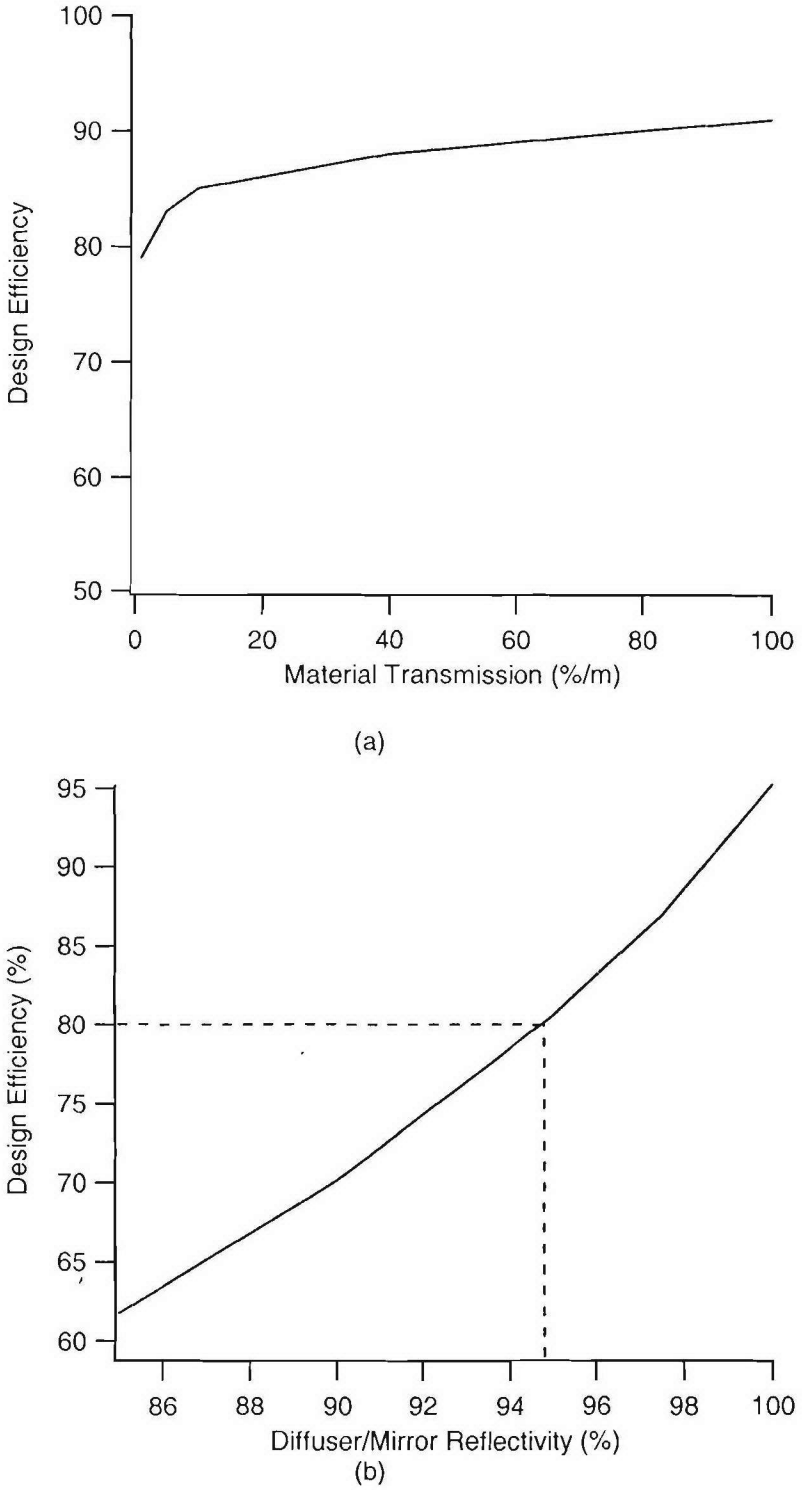

Figure 14 – (a) Overall design efficiency as a function of material transmission and (b) diffuser and mirror reflectivity. To reach the 80% goal, a minimum of 96% reflectivity on the outcoupler and end mirror is required. Note that 100% efficiency is not attainable due to some absorption by the jacket of the transport fiber and some light returning to the source.

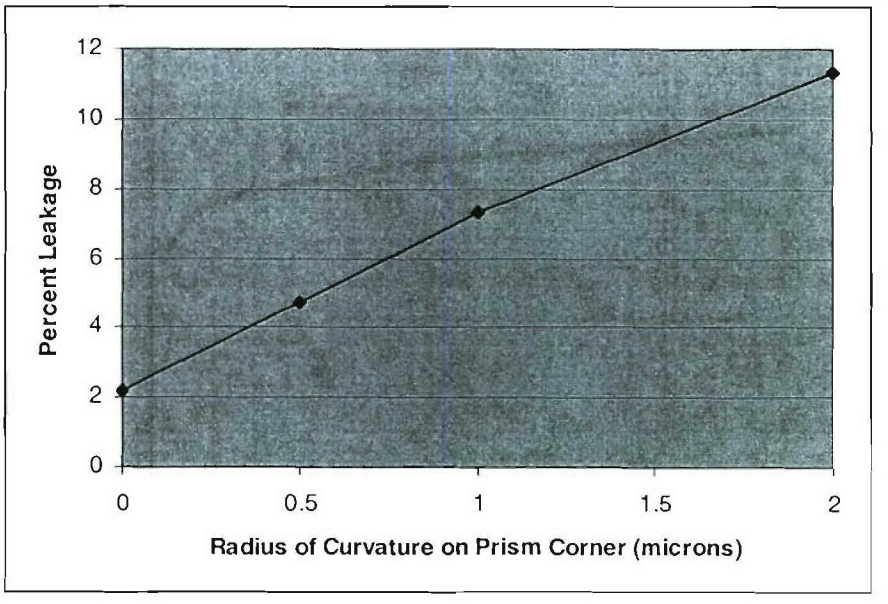

Figure 15 – Percentage of light leaked versus radius of curvature on prism corners for imperfect prismatic film.

Task 2: Prototype Development

The first activity in the prototyping task was to secure a sample of the COTS hollow-core luminaires manufactured by TIR Systems for characterization. The sample we procured was a 6-ft length, 6–in.-diameter cylindrical midfeed luminaire. A picture of the luminaire is shown in Figure 16. We chose the midfeed luminaire thinking that we would be able to make measurements more easily on a 3-ft segment of luminaire. This turned out not to be the case. To initially characterize the luminaire, we made estimates of total luminous output using a radiometric detector at a distance of 2 m unders the assumption of Lambertian emission from the luminaire. If anything, this would end up overestimating the luminous output, as the luminaire had a compressed Lambertian distribution. Our measurement estimated the total output to be approximately 2000 lumens. The input flux for our sample system was approximately 4500 lumens. This yields an efficiency of slightly under 50%, which agrees with an efficiency estimate provided to us by TIR systems. The sample system provided to us weighed approximately 7000 g, for a mass efficiency of 0.3 lm/g. However, we were provided with a 250-W source for our sample. 1000-W sources are available, and these would yield a mass efficiency closer to 1.2 lm/g. Upon seeing these numbers, we determined that the COTS solution provided by TIR Systems was not close enough to the Phase I specifications to warrant further investigation.

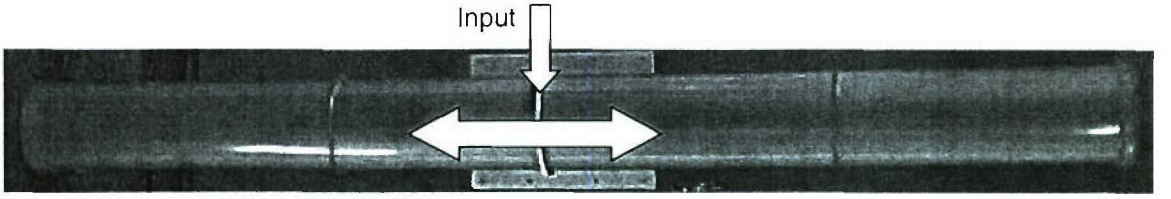

Figure 16 – COTS hollow-core luminaire from TIR Systems of Vancouver, Canada.

We began to fabricate prototypes using prismatic film manufactured by 3M. The first prototype we developed was a 20-mm-square luminaire placed inside a 1–-in.-square acrylic box. The entire luminaire was resting on a diffuse white tray. This prototype was based on the model shown in Figure 8. The diffusing tray had a reflectivity on the order of 96%, while the outcoupler had a reflectivity of only 88%. The lower reflectivity for the outcoupler was due to insufficient thickness of the paint. The luminaire was designed for use with the 13.5-mm transport fiber. Figure 17 shows an image of the initial prototype in the (a) illuminated state and (b) darkened state.

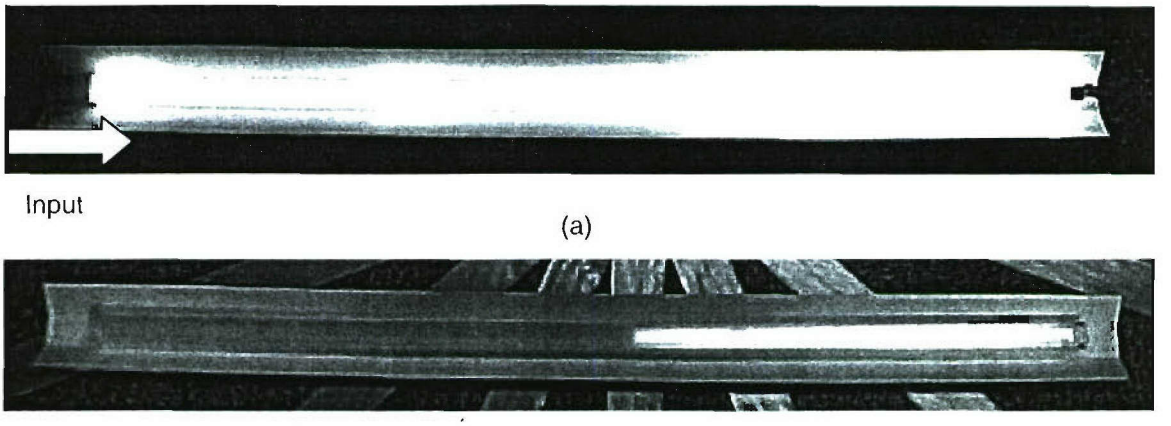

Figure 17 – Initial prototype in the (a) illuminated and (b) darkened states (bright area is reflection of room lights above).

To measure the efficiency of the prototypes, we performed manual goniometric measurements using a calibrated photometric detector. We marked off segments on the floor spaced 22.5° apart in azimuth. Along each of these segments we indexed positions corresponding to 2.5° increments in altitude, assuming a 2-m radius sphere. We also placed similar indices on a 2-m rod used to hold the detector. The measurements were made by placing the detector at the appropriate height and distance from the luminaire, pointing the detector toward the luminaire, and recording the power density. The sample values of 22.5° in azimuth and 2.5° in altitude were chosen based on the IESNA test procedure LM-76-02. Figure 18 shows an overview of the 22.5° segments along with the second prototype luminaire. Figure 19 shows a view of the system including the photometric detector and rod.

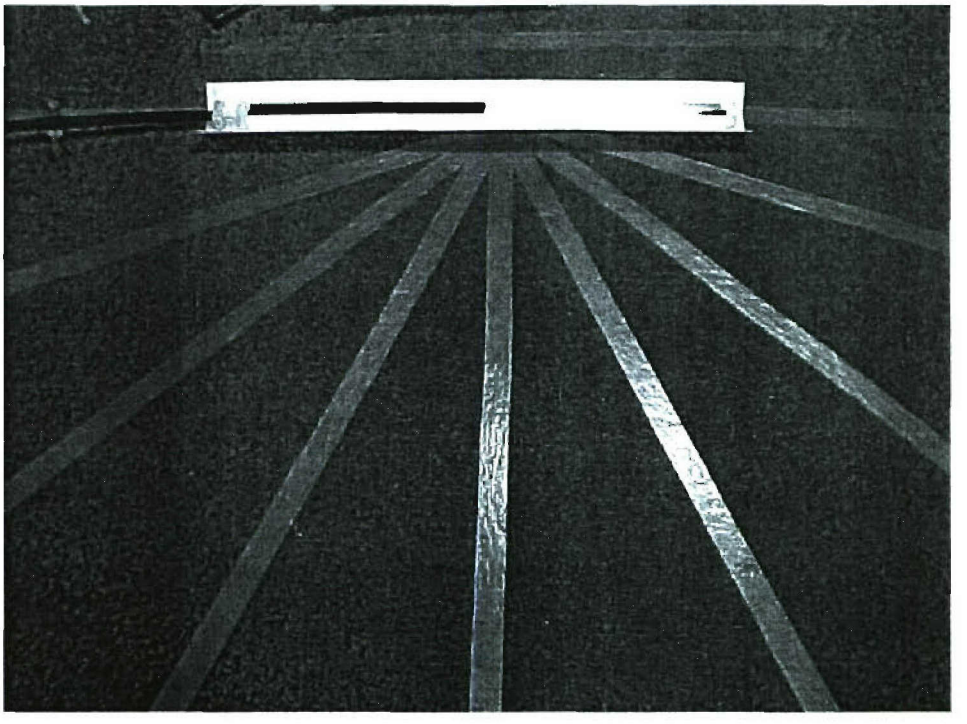

Figure 18 – Overview of goniometric setup. Planes are spaced 22.5º in azimuth. Luminaire shown is second SRI prototype (bright spot is reflection of overhead room lights).

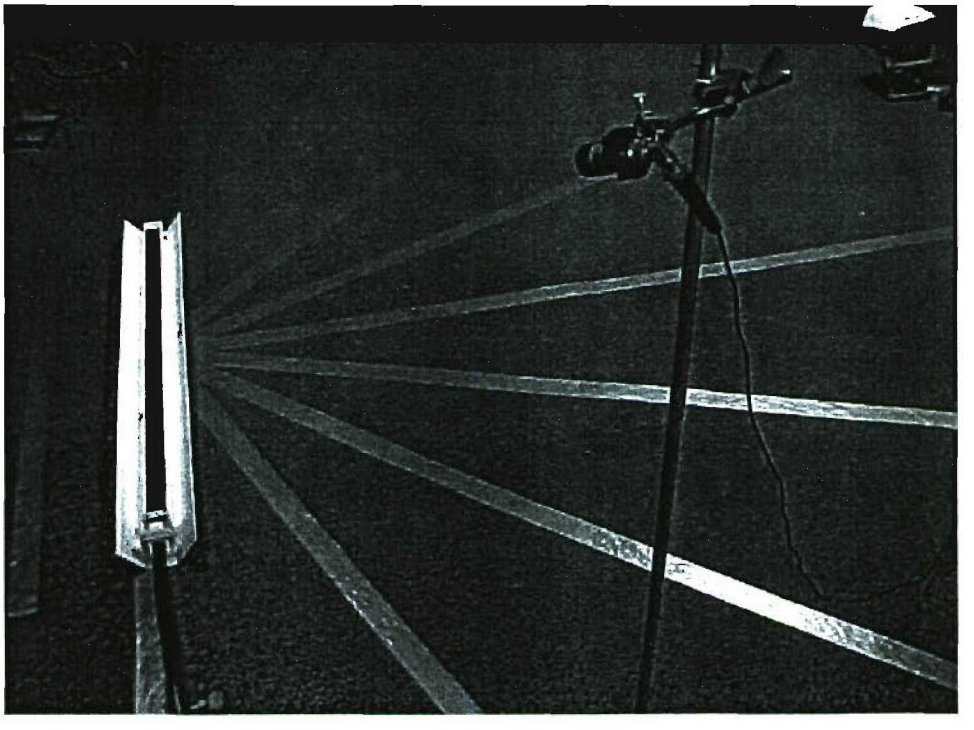

Figure 19 – Goniometric test setup with detector and rod. Luminaire shown is second SRI prototype.

Goniometric efficiency measurements on the first prototype indicated it was less than 70% efficient. However, we were concerned that for this luminaire the goniometric approach was not accurate, as there was a large amount of forward-directed light exiting the luminaire because this initial prototype did not include a concentrator at its input (and in fact provided the experimental evidence that a concentrator was needed). We were concerned that the goniometric approach might be undersampling this light. We decided to make another set of efficiency measurements, this time using a small integrating sphere and partially inserting the luminaire into the sphere, one segment at a time. Again this approach is not ideal, but we were hoping for a rough estimate of the efficiency. From this approach we calculated efficiencies in the 60%-70% range.

The efficiency of the first prototype did not reach the 80% goal for two reasons. First, the diffusing strip was only 88% reflective. Much of the light hits multiple times off this strip, which can drastically affect the efficiency. This problem can be solved by adding more layers of highly reflective paint when making the outcoupler.

Second, the initial prototype used prismatic film made from polycarbonate. Polycarbonate has much higher bulk absorption than acrylic. Modeling indicated that in order to reach the 80% efficiency goal we would need to develop a prototype based on acrylic prismatic film. This required a separate material development effort, so in parallel with our effort to develop an acrylic luminaire, we decided to make a second prototype based on the polycarbonate prismatic material from 3M. This second prototype included a conical concentrator to limit the angular spread of the light entering the luminaire. In addition, we improved the reflectivity of the diffusing strip to approximately 95%. This prototype also made use of the 19-mm transport fiber provided to us by Fiberstars. Figure 20 shows an image of the second prototype.

This prototype was sent to Fiberstars in Solon, OH, so that the efficiency could be measured in a 2-m integrating sphere. Their measurements reported an efficiency of greater than 70%. We believe the increased efficiency was largely due to the improved reflectivity of the diffusing outcoupler. We also made some uniformity measurements on the second prototype. These measurements were made by masking the luminaire in either 10- or 20-cm segments and measuring the flux from those segments using a calibrated cosine detector placed 1 m above the luminaire. Figure 21 shows a schematic of the experimental setup used to make these measurements. This method of measuring the uniformity would be accurate if the source were Lambertian in its angular distribution. As the source was not completely Lambertian, this method of measurement can only give an estimate of the uniformity of the Luminaire.

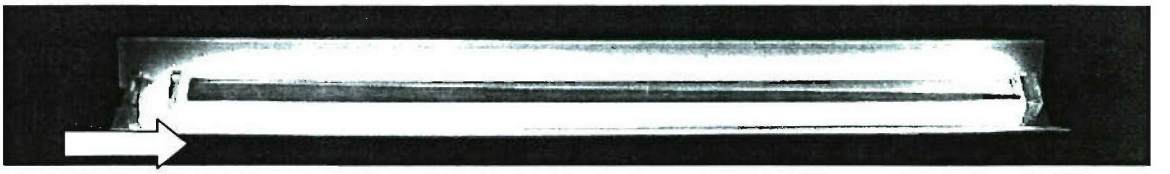

(a)

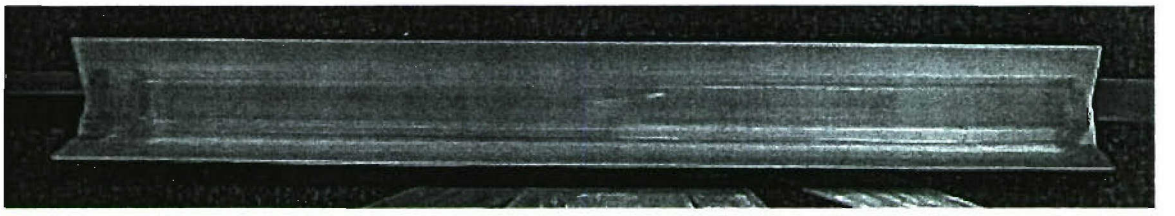

(b)

Figure 20 – Second prototype in the (a) illuminated and (b) darkened states.

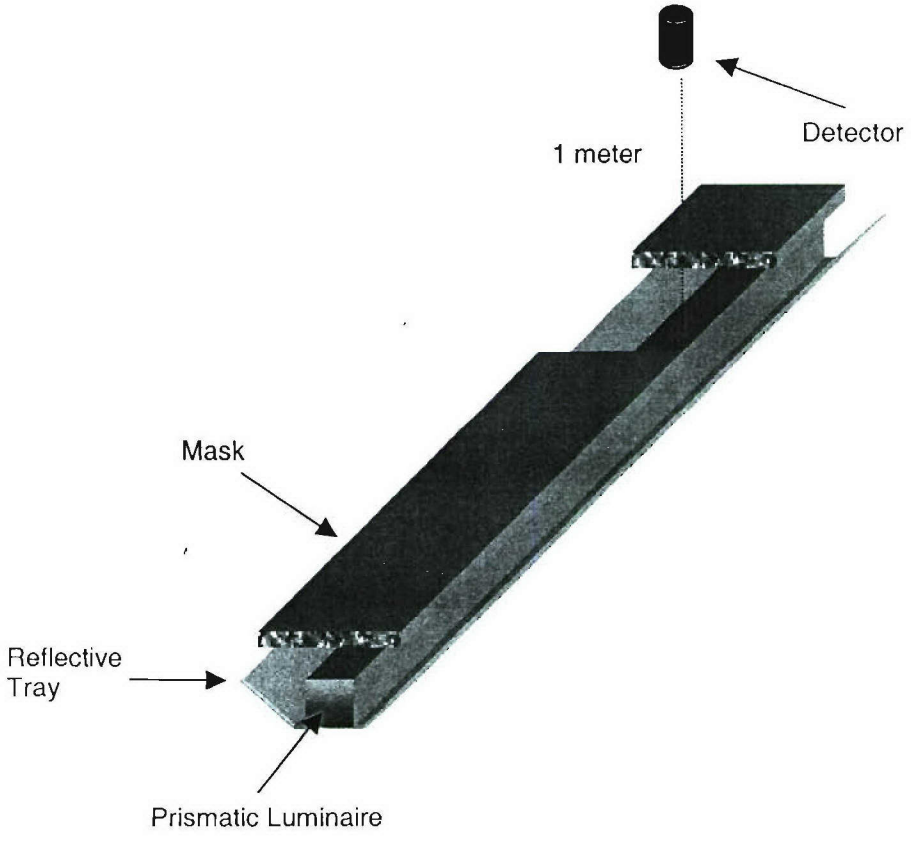

Figure 21 – Schematic for measuring uniformity by masking off 10- to 20-cm segments of luminaire.

Figure 22 shows the results of the uniformity measurement for both the 10- and 20-cm segments. Also shown are the mean values and lines indicating levels ±10% of the mean value. There are only a few regions where the uniformity deviates by more than 10% of the mean in either direction. This can be corrected by simply changing the width of the diffusing strip as a function of position along the luminaire.

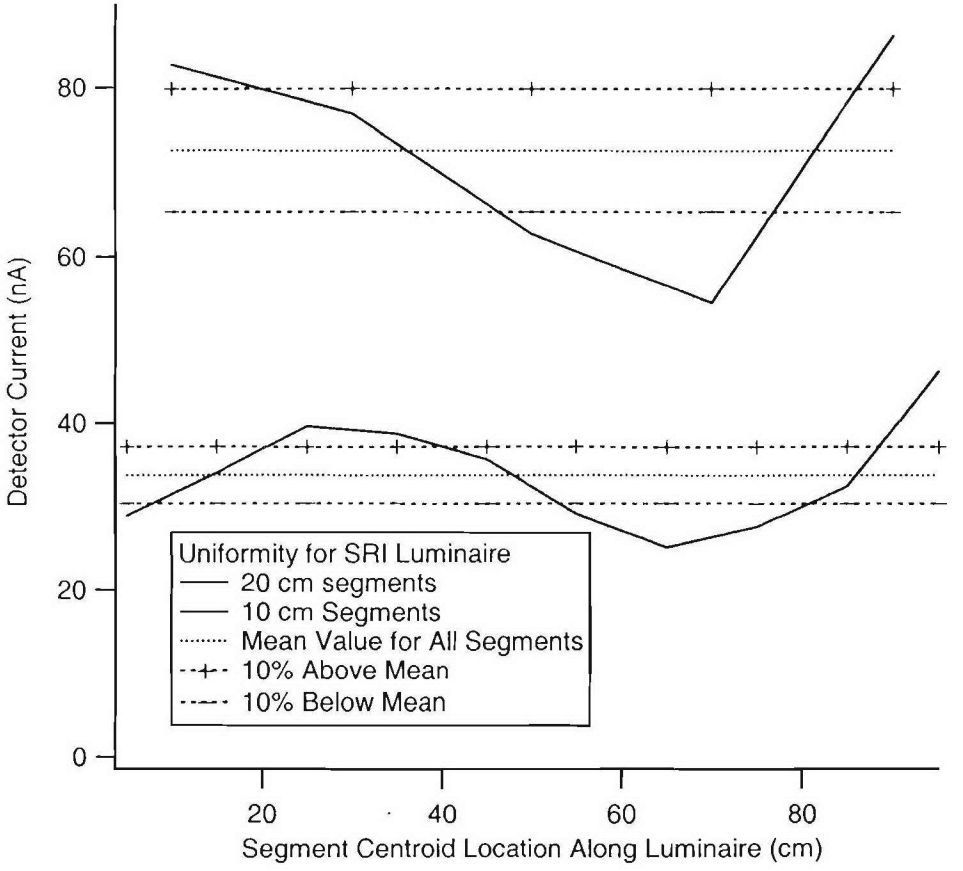

Figure 22 – Spatial uniformity measurements of luminaire for both 10- and 20-cm segments, showing the mean value as well as 10% deviations from the mean.

Our approach to developing prismatic film using acrylic involved the following steps: 1) vapor deposition of nickel onto existing OLF material; 2) electroplating a thick layer of nickel on the coated OLF to form a shim; and 3) using the shim to thermoform the prismatic pattern into optically clear acrylic sheets. Using these steps, we were able to transfer the pattern, but we had some difficulty with the transfer process because some of the polycarbonate would adhere to the shim and transfer onto the acrylic, creating a milky, scattering surface. Scattering will have a stronger effect on the uniformity of the luminaire than on the efficiency. Attempts to improve the transfer process met with some success, although some of the final pieces still had some scattering present.

We assembled the acrylic luminaire by using square acrylic rods to form a corner joint between sections of acrylic prismatic film, as shown in Figure 23. The prismatic film was

solvent bonded to the square rods using a right-angle form. The diffusing outcoupler was painted onto the bottom surface of the luminaire using LabSphere Spectraflect paint (R≈95%). The far end of the luminaire was capped with a mirror tilted at 5° and coated with 3M Radiant Mirror Film (R≈95%).

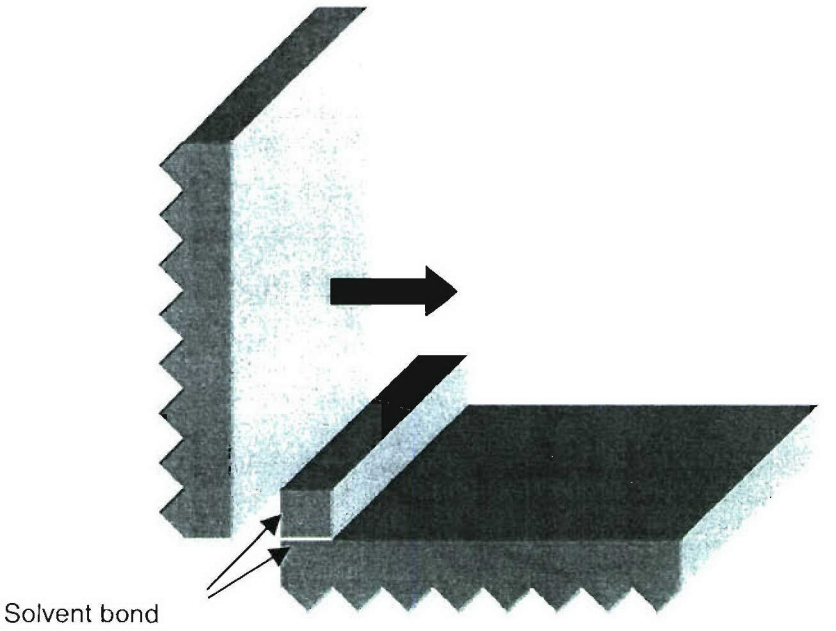

Figure 23 – Assembly of acrylic luminaire using square rods as corner supports for acrylic prismatic sheets.

Because acrylic has a lower index of refraction than polycarbonate, the numerical aperture of the luminaire is lower. This factor required us to redesign the concentrator between the output of the fiber and the input of the luminaire. To improve the performance even further, we decided to design a true parabolic concentrator instead of the conical concentrator used in the previous prototypes. Figure 24 shows a CAD image of the compound parabolic concentrator (CPC) used for the acrylic prototype. Figure 25 (a) shows the output direct from the Fiberstars 19mm fiber, while Figure 25 (b) shows the output from the fiber after passing through the CPC. The angular spread after passing through the CPC is approximately 25°.

The entire luminaire was then placed into a large acrylic box for protection from dust and damage, and was mounted in an aluminum tray also painted with Spectraflect. Figure 26 shows the final illuminated luminaire.

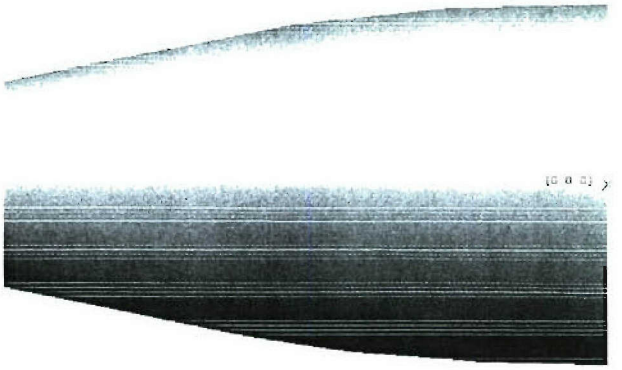

Figure 24 – CAD image of the CPC used to better collimate the light exiting the 19mm fiber.

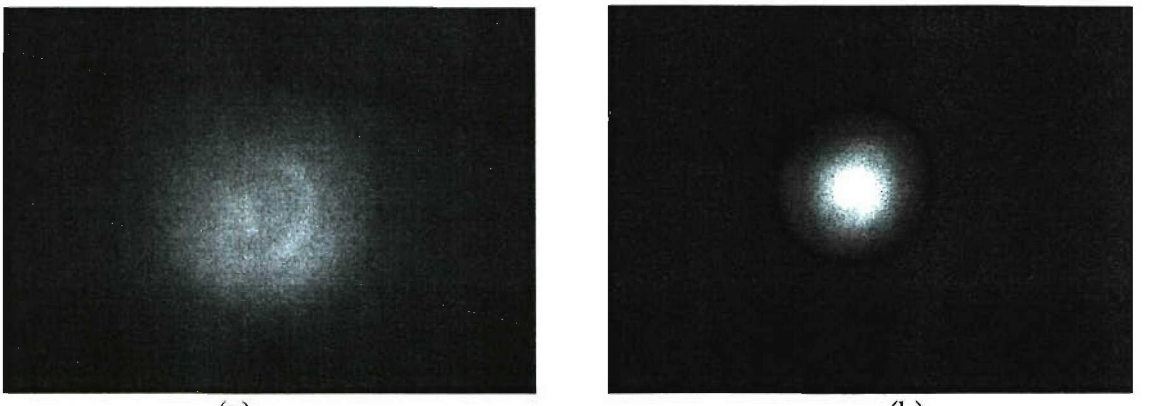

(a) (b)

Figure 25 – Image of beam pattern (a) exiting directly from 19mm fiber and (b) after passing through custom CPC.

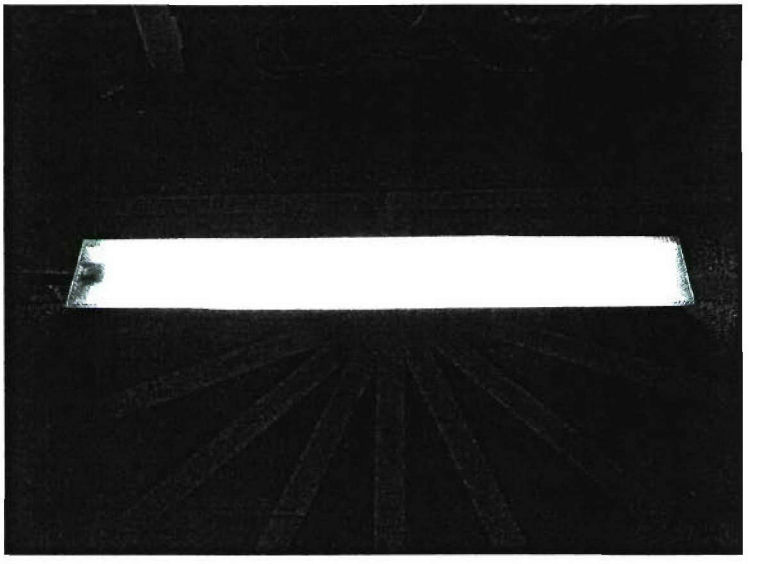

Figure 26 – Image of acrylic luminaire in illuminated state.

We conducted goniometric measurements on the acrylic prototype in the same manner as described above for the polycarbonate prototypes. Figure 27 shows the projected direction cosine distributions for the second polycarbonate and acrylic luminaires. The acrylic luminaire showed improved angular uniformity, but still demonstrated a strong forward-directed component.

We also measured spatial uniformity on the acrylic luminaire. Figure 28 shows the results of spatial uniformity measurements for both 10cm and 20cm segments. The acrylic luminaire meets the required ±10% uniformity specification with the exception of the extreme endpoints.

The luminaire was then shipped to Fiberstars in Solon, OH, for efficiency measurements in their 2-m integrating sphere. Efficiency measurements without the reflecting tray indicated an overall efficiency of 78%, just shy of the 80% requirement for the program. We believe the 80% goal could easily be reached with improvements in the manufacturing process for the acrylic prismatic pieces.

Based on the efficiency measurements from Fiberstars, and assuming a 6400 Lumen input from the source, the mass efficiency for the acrylic luminaire is approximately 3.7 L/g, well above the 3 L/g specification. Much of this weight is taken up by support structures such as the acrylic box (682 g) and the reflecting tray (654 g), both of which could have their masses reduced by 50% or more, leading to a mass efficiency of 7 L/g or more. The actual acrylic luminaire weighs only 30g.

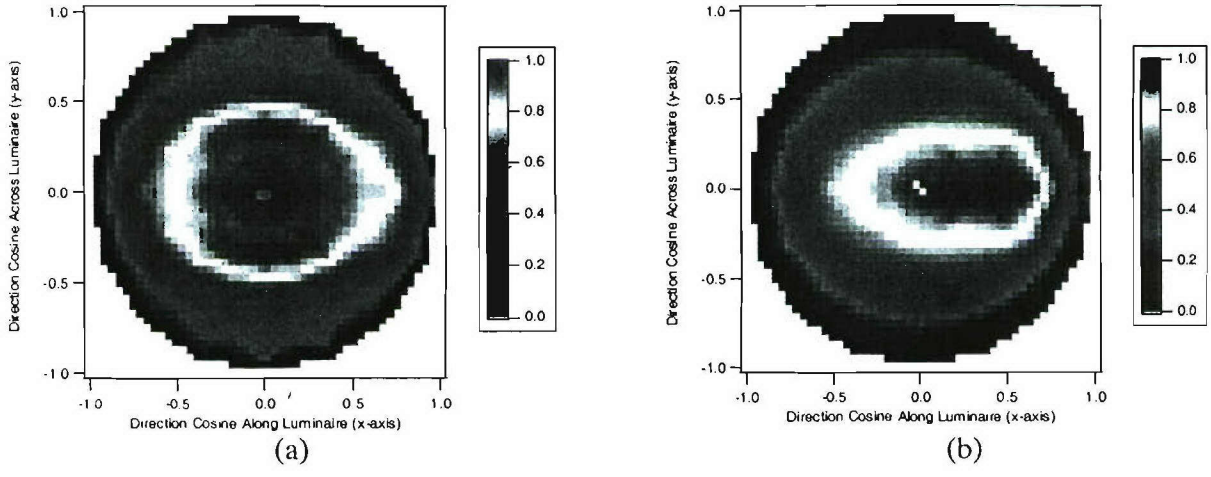

Figure 27 – Angular output distributions for (a) second polycarbonate and (b) acrylic luminaires. Angular distributions are represented as projected direction cosine plots.

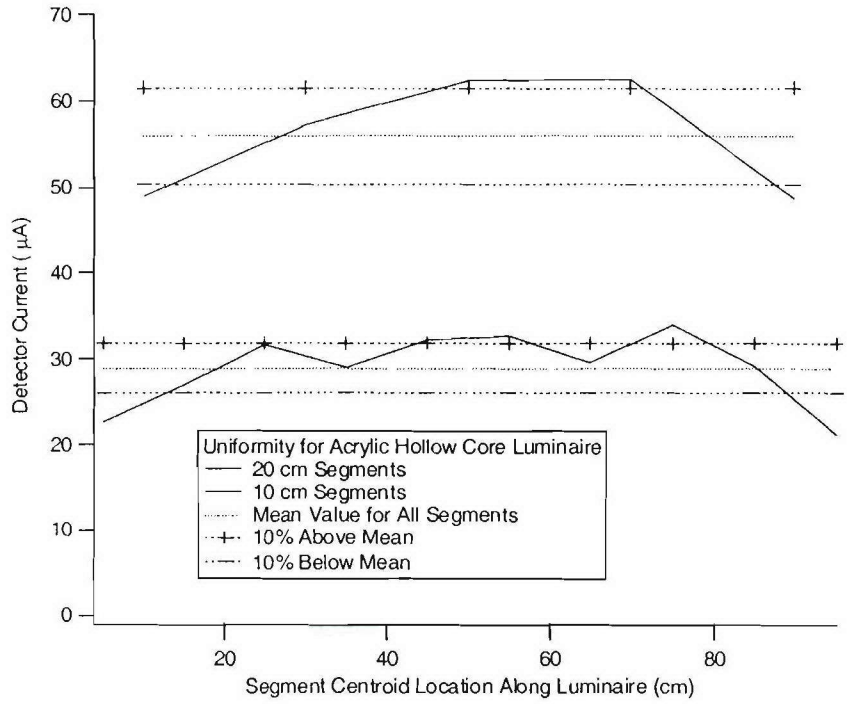

Figure 28 – Spatial uniformity measurements of acrylic luminaire for both 10- and 20-cm segments, showing the mean value as well as 10% deviations from the mean.

REMAINING WORK PLANNED

In response to client needs, we will discontinue work on the hollow-core luminaire for FY04 and redirect our effort toward special purpose point luminaires and their supporting components. Some of the desired applications for these luminaires include task lighting, runway lighting, and naval masthead lighting. These luminaires will need to be compact, efficient, and provide cutoff Lambertian angular distributions. Other system components that might be required include corner bends and beam homogenizers.

APPENDIX B

SPECIALTY POINT LUMINAIRES

February 2005

"Specialty Point Luminaires"

Year End Summary Report (February 2005)

Sponsored by

Defense Advanced Research Projects Agency (DARPA/ATO)

ARPA Order P436/00

Issued by U.S. Army Aviation and Missile Command Under
Contract No. DAAH01-03-C-R157

Prepared by:
Eric Arons, Research Engineer
SRI International
333 Ravenswood Ave.
Menlo Park, CA 94025
650-859-3733

Effective Date of Contract: 04 February 2003
Contract Expiration Date: 05 February 2006
Reporting Period: 04 February 2004 -- 04 February 2005

PROJECT OVERVIEW

The goal of the HEDLight program is to develop a complete remote source lighting system for area, task, and navigational lighting on naval platforms. Within the scope of the overall program is the development of the source, distribution system, and luminaire, along with the integration of the entire system. The technical objectives of the program emphasize the attainment of high efficiency with regard to electrical, mass, and luminous output. In addition, the output of the luminaire should achieve certain spectral and spatial uniformity specifications. The program is divided into three phases, with efficiency goals increasing in each subsequent year. Figure 1 shows the expected technical milestones for the overall program. SRI is one of two contractors developing the luminaire for the system. Fiberstars, Inc., is the other luminaire contractor.

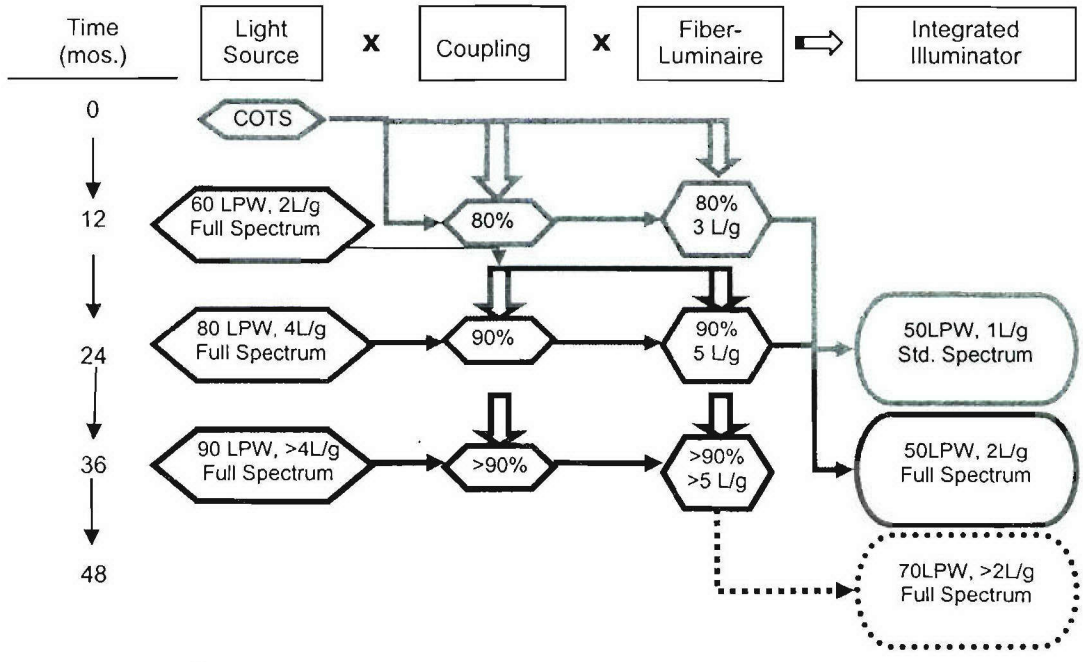

Figure 1 – Overall technical goals for the HEDLight Program.

In year 1 of the program, SRI was tasked with developing the luminaire using hollow-core waveguide technology. These waveguides were constructed from microstructured, prismatic polymer films such as Optical Lighting Film (OLF) developed by 3M Corporation. Upon completion of the first year of work, the decision was made to refocus our effort to the development of special-purpose point luminaires. These luminaires will be used for task lighting or as navigational beacons for naval ships. This requires a cut-off Lambertian angular distribution (Figure 2). The luminaires should also have a compact form factor and be lightweight.

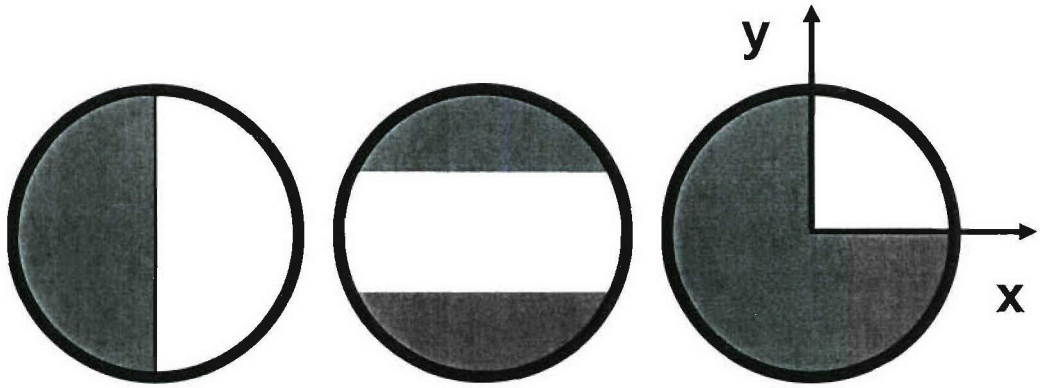

Figure 2 – Examples of cut-off Lambertian distributions represented in direction cosine space.

TECHNICAL PROGRESS

The reporting period described here covers year 2, from 4 February 2004 to 4 February 2005. The technical proposal divided the Phase II effort into two separate tasks, Modeling and Prototype Development. As these two tasks feed into each other, we will report on progress in both tasks together.

We performed the modeling work primarily using LightTools,[1] with some CAD designs developed using SolidWorks.[2] We started by investigating several different candidate designs that produced half-Lambertian distributions. Some of these designs could not be directly modeled, so we made assessments on the basis of discussions with various vendors. The candidate designs under consideration included:

1. Structured diffusing outcoupler
2. Diffusing box
3. Prism pairs
4. Holographic diffusing outcoupler
5. Mirror baffle

We evaluated the designs for several criteria including angular distribution, efficiency, size and weight, manufacturability, and ease of system integration. Through this selection process, it was determined that the mirror baffle design was the best candidate with which to move forward. Below we discuss each of the candidate designs, describing their relative advantages and disadvantages.

---

[1] LightTools is an optical ray-tracing program developed by Optical Research Associates. Descriptions of the program can be found at http://www.opticalres.com

[2] SolidWorks is a 3D mechanical design program. Descriptions of the program can be found at http://www.solidworks.com

1. Structured Diffusing Outcoupler

The structured diffusing outcoupler (SDO) design is a direct extension of the work done in Phase I of the HEDLight program. The solid core luminaire design from Phase I consists of a diffusing outcoupler on the back surface of a cylindrical waveguide. The cylindrical surface of the waveguide acts like a lens, compressing the distribution angularly in the direction perpendicular to the waveguide axis (Figure 3). The angular distribution can be further controlled by changing the width and orientation of the diffusing outcoupler. Figure 4 shows modeled angular distributions for diffusing strips oriented at 45° and 25°. Optimization of these parameters has the potential to produce arbitrary angular distributions.

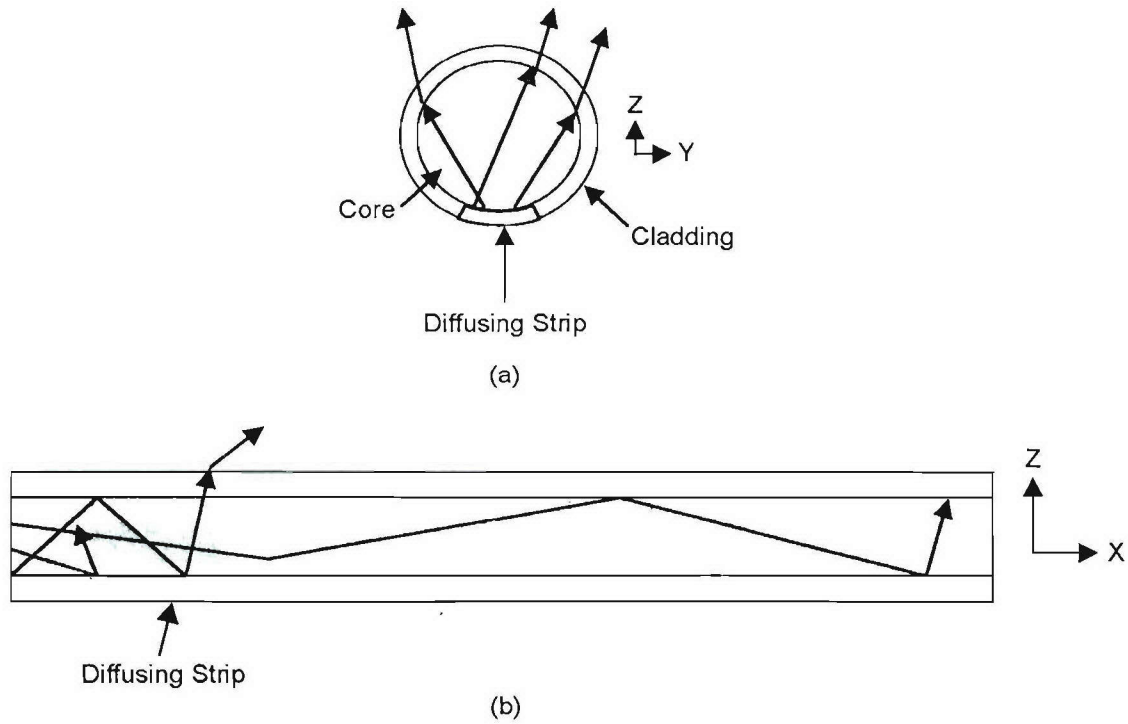

Figure 3 – (a) End and (b) side views of the **structured diffusing outcoupler luminaire.**

The primary advantage of the SDO design is that the output angular distribution is relatively insensitive to the angular distribution of the input source. However, because the scattering outcoupler is Lambertian, the design is also relatively inefficient. When this design is implemented as a smaller specialty luminaire, the area of the outcoupling region becomes much smaller relative to the area of the source input. Thus, more of the light is scattered back toward the source and lost. In addition, models show that only about 1/3 of the light is scattered out of the luminaire after a single bounce. Multiple bounces off the diffusing outcoupler further decrease the efficiency of the design. Finally, the SDO design behaves like a retroreflector for ambient illumination. This can be problematic if the luminaire is to be used as a navigational beacon on a naval ship.

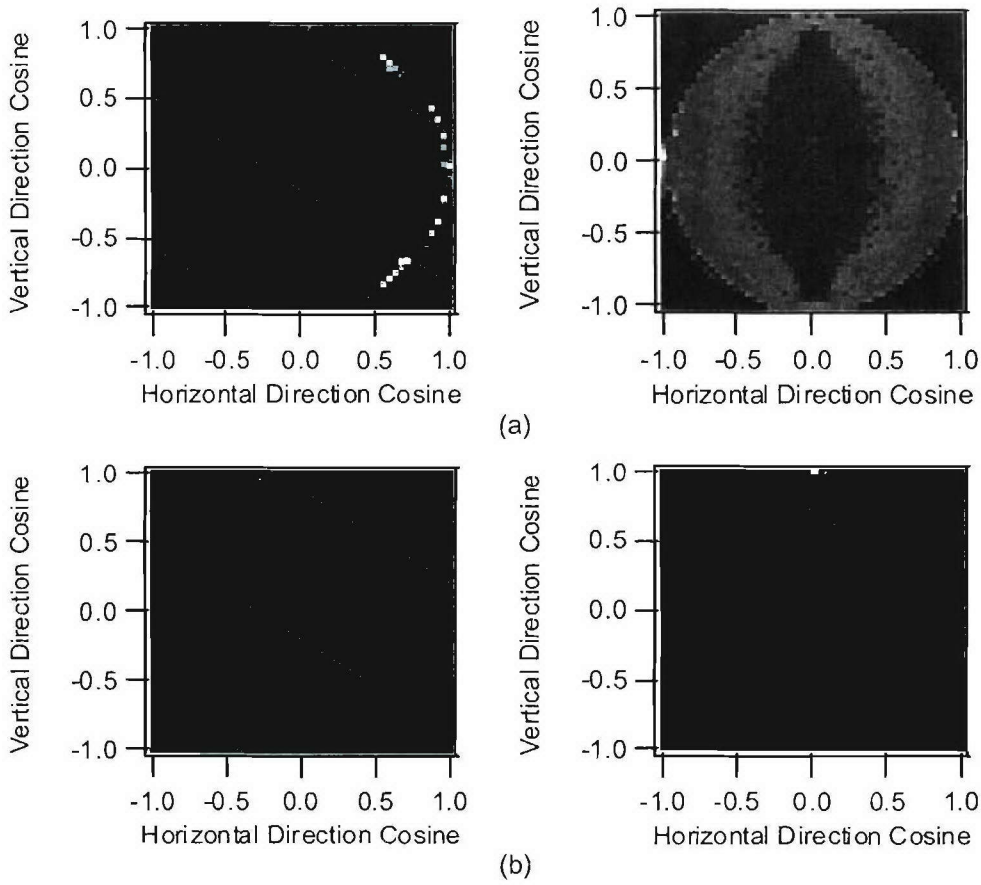

Figure 4 – Half- and full-field angular distributions for structured diffusing outcoupler luminaire for diffusing strip orientations of (a) 45° and (b) 25°.

2. Diffusing Box

The diffusing box design is a set of designs conceived to provide the required output angular distribution with little or no dependence on the angular distribution of the input source. One example of these designs is shown in Figure 5. The luminaire is a single molded plastic piece with diffuse coatings on the sides, bottom, and back of the box, and mirrored coatings on the vertical and angled surfaces of the roof structures. The top surface remains uncoated. Light is randomized by scattering off the walls of the diffusing box. Light with angles less than the total internal reflection (TIR) angle is coupled out through the uncoated slats and redirected by the vertical mirrors toward one-half of the upper angular hemisphere. The resulting angular distribution is shown in Figure 6.

The advantage of this design, as with the SDO design described above, is that it is completely insensitive to the angular distribution of the source. However, as with the SDO design, the diffusing box design can be extremely inefficient depending on the reflectivity values of the various diffuse and metal coatings. With reflectivities of 98%, this particular design is 80% efficient. However, if the reflectivities drop to 96%, the efficiency of the design drops precipitously to 60%.

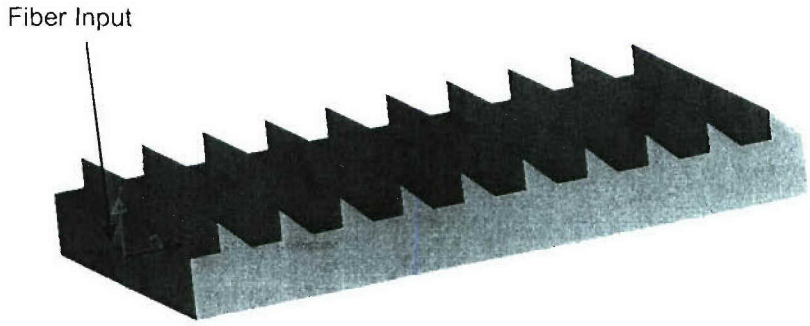

Figure 5 – One example of a diffusing box luminaire. Light from fiber enters diffusing box and is scattered out the transparent slats at top of luminaire (blue). Vertical mirrored surfaces (gray) constrain light to a single half-hemisphere.

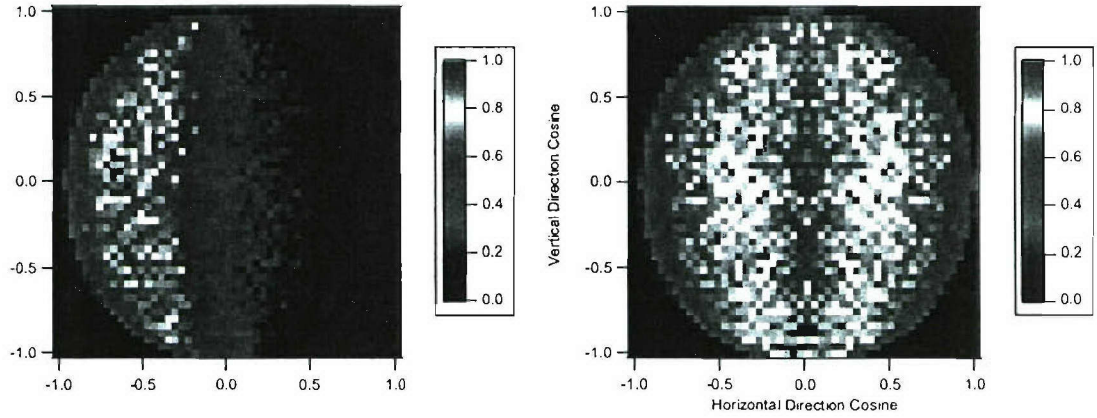

Figure 6 – (a) Half- and (b) full-field angular distributions from the diffusing box luminaire shown in Figure 5.

3. Prism Pairs

The prism pair design resulted from the discovery that light reflected from an angled mirror embedded in a square waveguide produces an angular distribution with a linear radiance output distribution along the direction of the propagation axis. The addition of two such distributions oriented in opposite directions produces a uniform Lambertian distribution (Figure 7). The prism pair luminaire design uses two waveguides with mirrors angled at approximately 35° and 55° to the optical axis, as shown in Figure 8. The exact angle depends on the index of retraction of the waveguide. The angles are selected so that rays propagating at the extreme angles in the waveguide are reflected out of the guide at a near 90° exit angle. Figure 9 shows the resulting angular distribution.

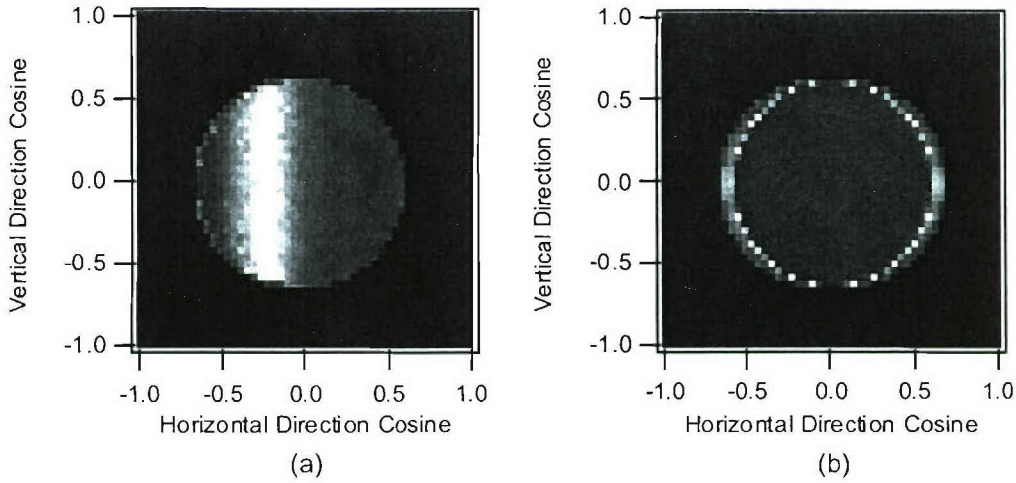

Figure 7 – The angular distribution resulting from a 45° mirror embedded in a square waveguide showing (a) a linear radiance output distribution for a single mirror, and (b) a uniform Lambertian distribution resulting from the addition of two linear distributions oriented in opposite directions.

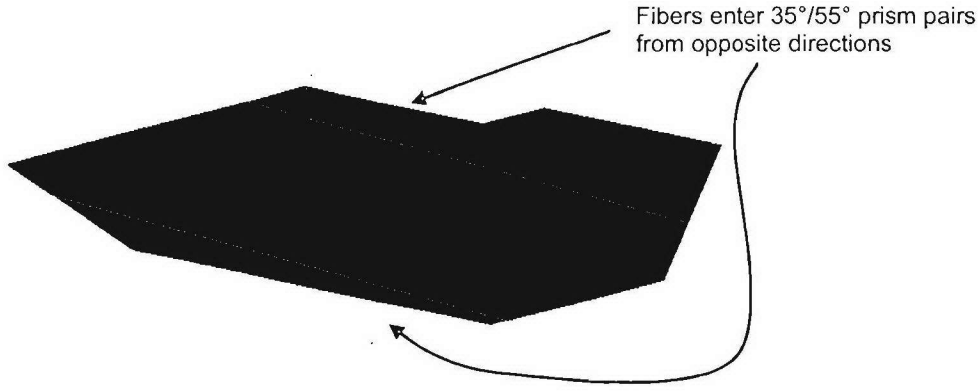

Figure 8 – Prism pair luminaire. Prisms oriented at approximately 35° and 55° direct light into a single half-hemisphere.

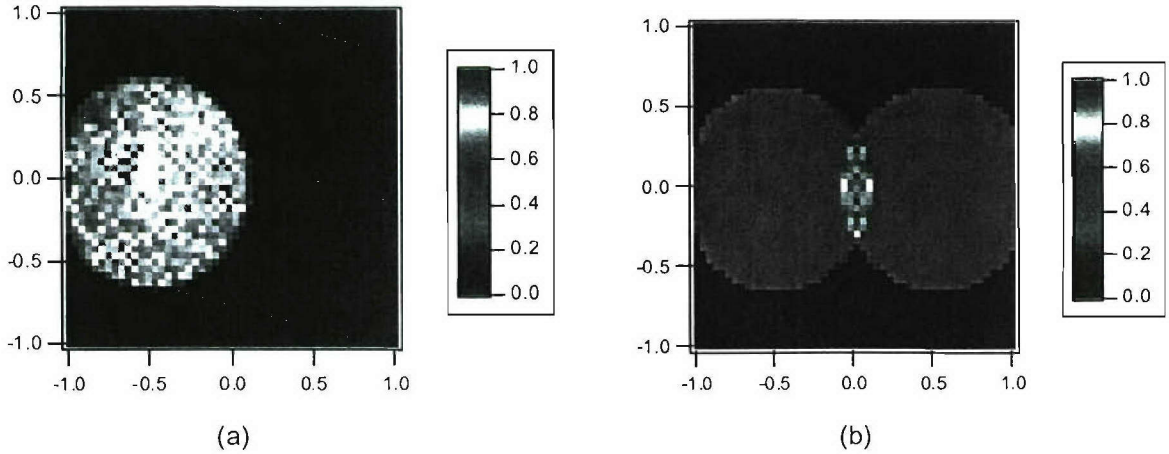

Figure 9 – Modeled angular distributions for prism pair luminaire showing (a) half-field and (b) full field distributions.

One advantage of the prism pair design is its potential for very high efficiency. The guided light is trapped by total internal reflection, and only strikes the outcoupling mirror once before exiting. In addition, the luminaire can be made extremely lightweight and compact.

The reliance of the prism pair design on specular outcoupling results in several disadvantages. Unlike the designs that use diffuse outcoupling methods, the prism pair design is very sensitive to the angular distribution of the source. This can be mitigated if a homogenizer is placed between the source fiber and the luminaire. However, if the input fiber diameter is less than the size of the luminaire, the resulting angular distribution is highly sensitive to fiber position, as shown in Figure 10.

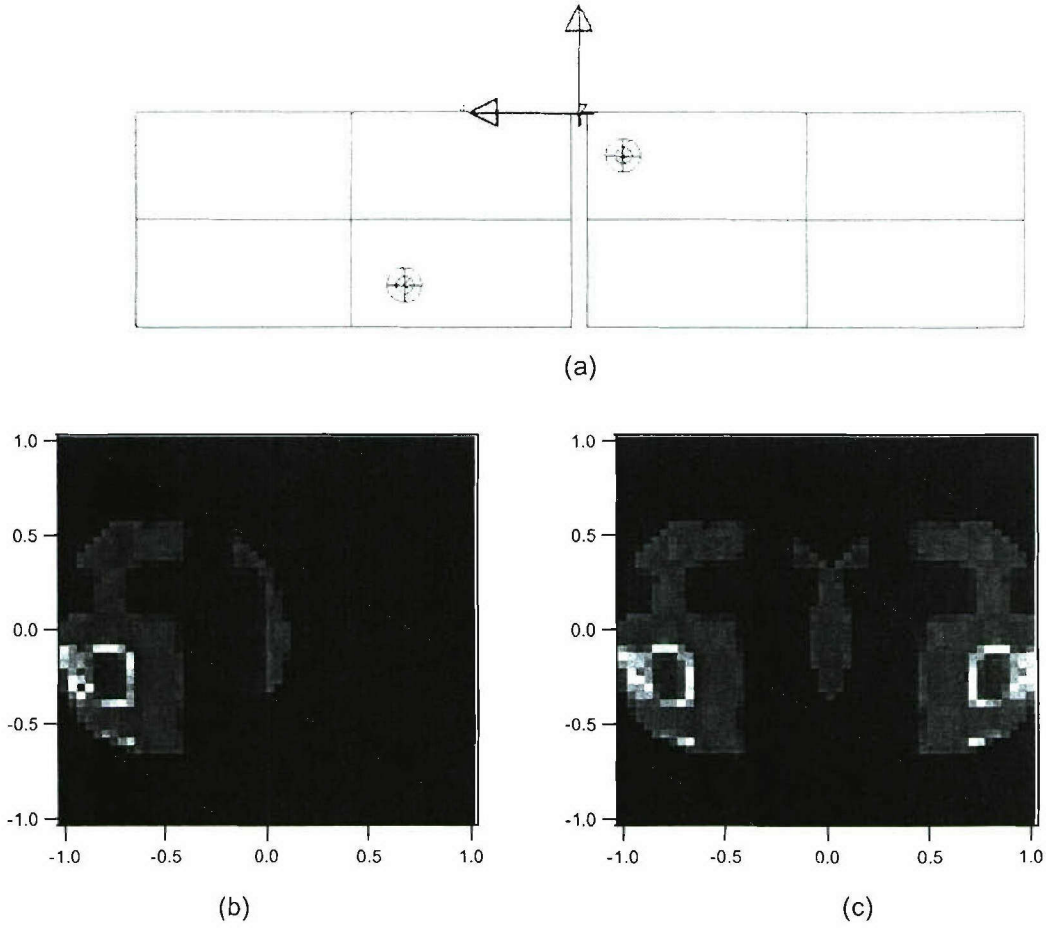

Figure 10 – Illustration of sensitivity of prism pair design to fiber misalignment, showing (a) modeled fiber input positions and the resulting angular distributions for (b) half-field and (c) full-field.

The other disadvantage to the prism pair design is that two fiber inputs are required to produce a single half-Lambertian output distribution. One way around this constraint is to integrate the prism pairs into a single luminaire with a beam splitter, as shown in Figure 11. The key to this design is a corner-bend that preserves the system etendue. This can be accomplished by placing a region of low index of refraction between the input and output waveguides and the actual corner bend, as illustrated in Figure 12. We constructed a prototype of this "T-bone" luminaire out of acrylic, using thin sheets of fluoropolymer for the low index regions. The modeled angular distribution for the "T-bone" luminaire is shown in Figure 13, and the measured angular distribution for the prototype is shown in Figure 14.

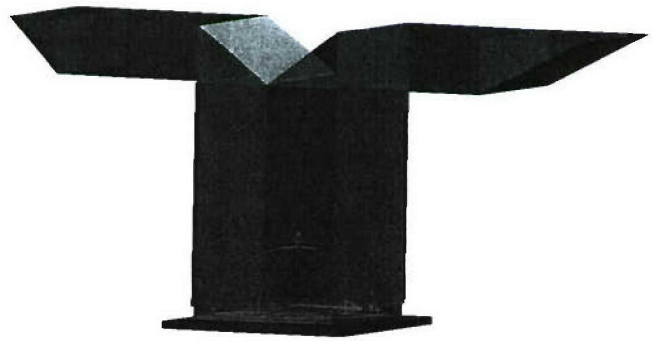

Figure 11 – Prism pair "T-bone" luminaire design with integrated 50/50 beam splitter allowing for single fiber input.

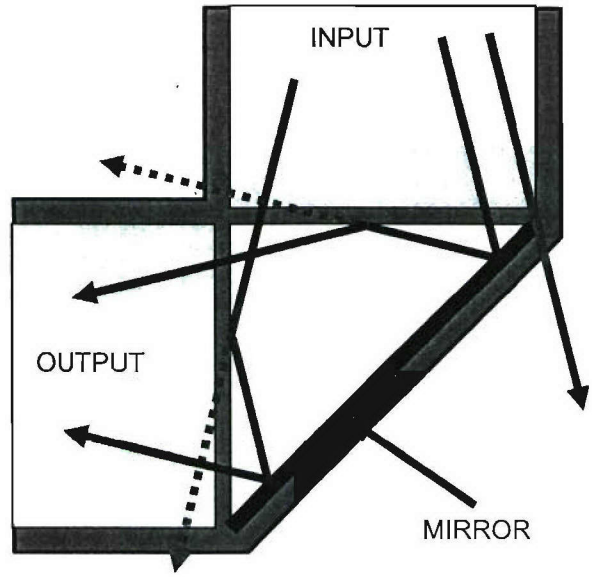

Figure 12 – Illustration of an etendue-conserving corner bend needed for the "T-bone" luminaire. Gaps of lower index of refraction invoke TIR conditions that prevent skew rays from escaping the waveguide (gray arrows). A small fraction of rays will still escape the waveguide at the low index gap (red arrow).

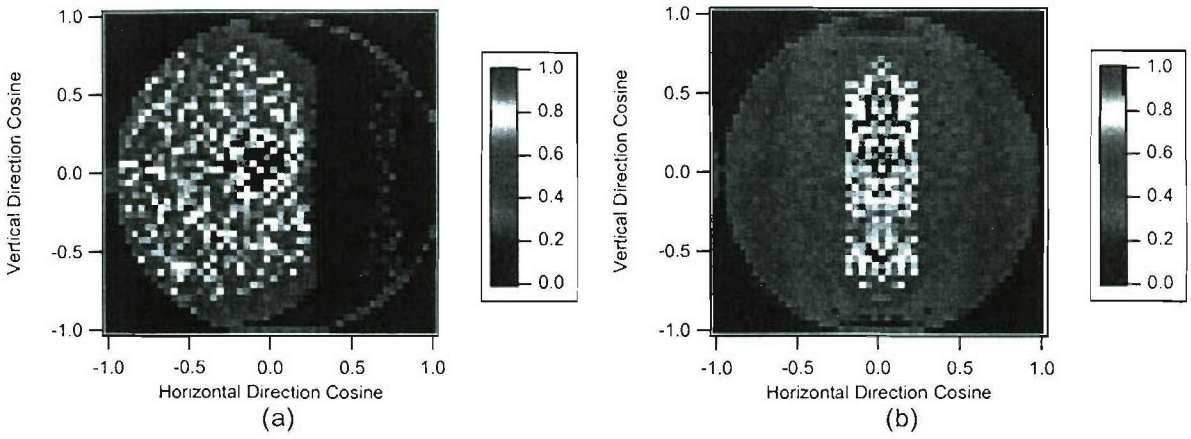

Figure 13 – Modeled angular distribution for "T-bone" luminaire showing (a) half-field and (b) full-field.

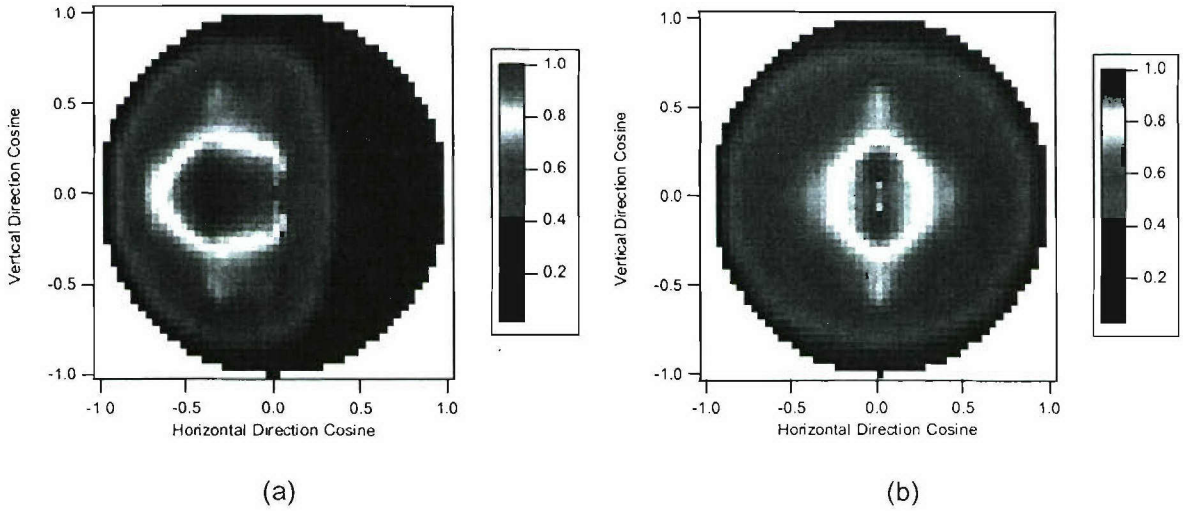

Figure 14 – Measured angular distributions for "T-bone" luminaire prototype showing (a) half-field and (b) full-field. Hot spots result from non-uniform input distribution from fiber.

4. Holographic Diffusing Outcoupler

Several companies produce custom holographic diffusers. We were involved in discussions with two of these companies, Wavefront Technologies of Hawthorne, CA, and Physical Optics Corporation of Torrance, CA, to see if they could create a custom holographic diffuser that could produce the desired angular distribution on its own. The concept is illustrated in Figure 15 both in reflection and transmission. The advantages of this approach include the potential for extremely high efficiency, as well as ease of manufacturing. All of the functionality is contained in one single molded piece. The risk comes in the difficulty with manufacturing a holographic diffuser that can produce a sharp cutoff at a specific angle while maintaining a

Lambertian distribution everywhere else. Both companies indicated their willingness to try to produce the diffuser, but neither was very confident that they could adequately meet the specifications. To determine whether the reflective design would meet our efficiency goals, we asked Wavefront Technologies to coat one of their standard transmissive diffusers with aluminum. We then glued the diffuser to the hypotenuse of a 45° prism and measured the light reflected off the diffuser using a 12.5 mm Fiberstars light-pipe as the input. The resulting angular distribution is shown in Figure 16. The efficiency of the reflective diffuser was less than 50%, with most of the light being lost to absorption. The efficiency of similar holographic diffusers in transmission is typically greater than 80%.

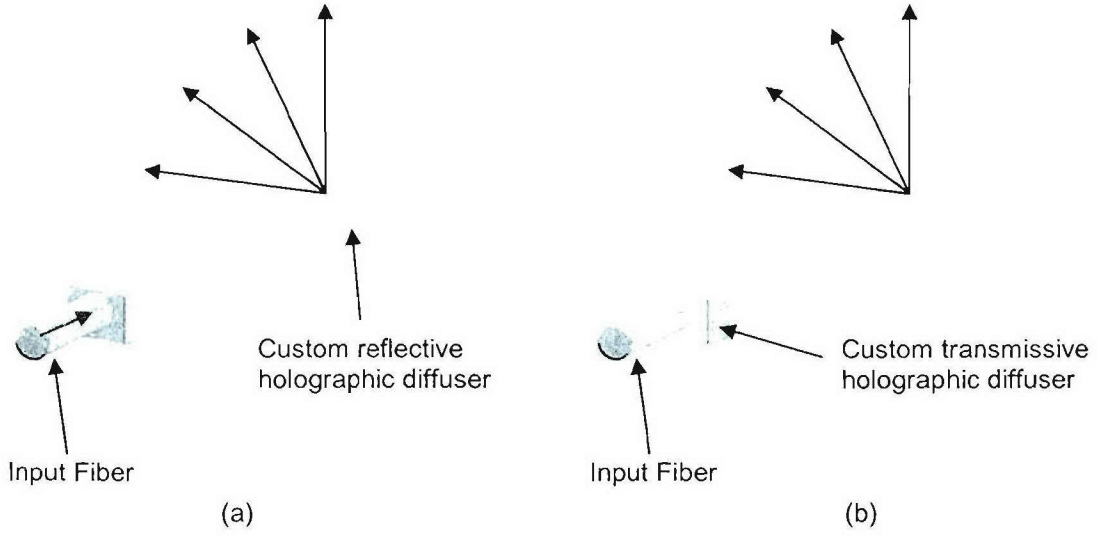

Figure 15 – Holographic diffusing outcoupler luminaire shown both in (a) reflection and (b) transmission.

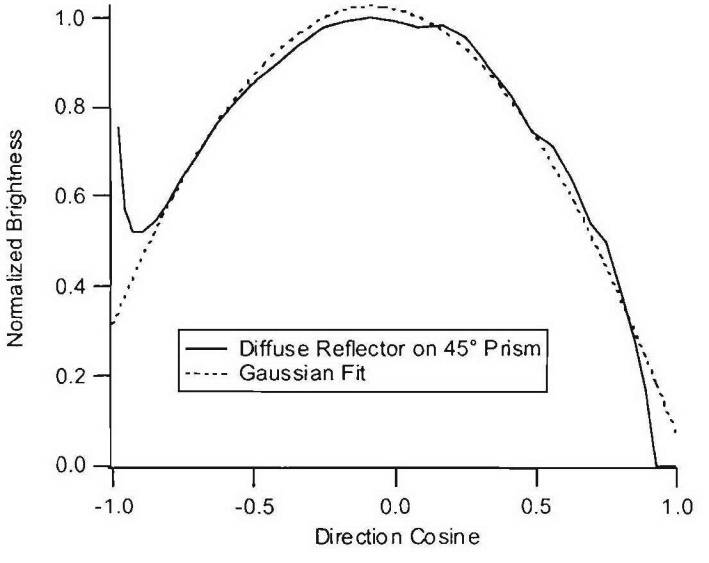

Figure 16 – Angular distribution in direction cosine space of a metal-coated diffuser glued to a 45° prism face.

5. Mirror Baffle

The simplest method for producing a half-Lambertian distribution is to start with a full Lambertian distribution and baffle the light with a mirror to constrain it to half of a hemisphere. The mirror baffle concept is illustrated in Figure 17, and the resulting angular distribution is shown in Figure 18. As a specular outcoupling solution, the mirror baffle shares many of the same advantages and disadvantages as the prism pair design. It has the potential to be very efficient and can produce a very accurate half-Lambertian angular distribution. However, it is still very sensitive to the angular distribution of the input source. An additional disadvantage is that having a vertical mirror sticking out into free space can be problematic in certain circumstances.

The latter problem is solved by injecting the light into a solid piece of plastic or glass and using one of the external surfaces as a TIR mirror. This basic approach is illustrated in Figure 19. Besides being a more robust and compact solution, with this design there are only two "optically involved" surfaces, the TIR mirror and the exiting surface. This allows for more flexibility in manufacturing and mounting.

To validate this design concept, we developed a pre-prototype from acrylic and measured the angular distribution. The experimental setup is illustrated in Figure 20. Because the output is highly dependent on having a Lambertian input, we used the output from an integrating sphere as our input. The resulting angular distribution from this pre-prototype is show in Figure 21.

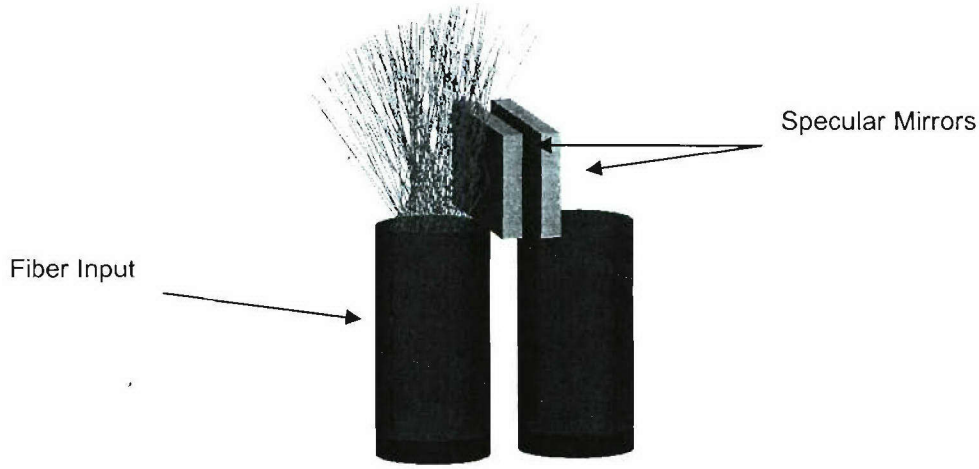

Figure 17 – Basic mirror baffle luminaire.

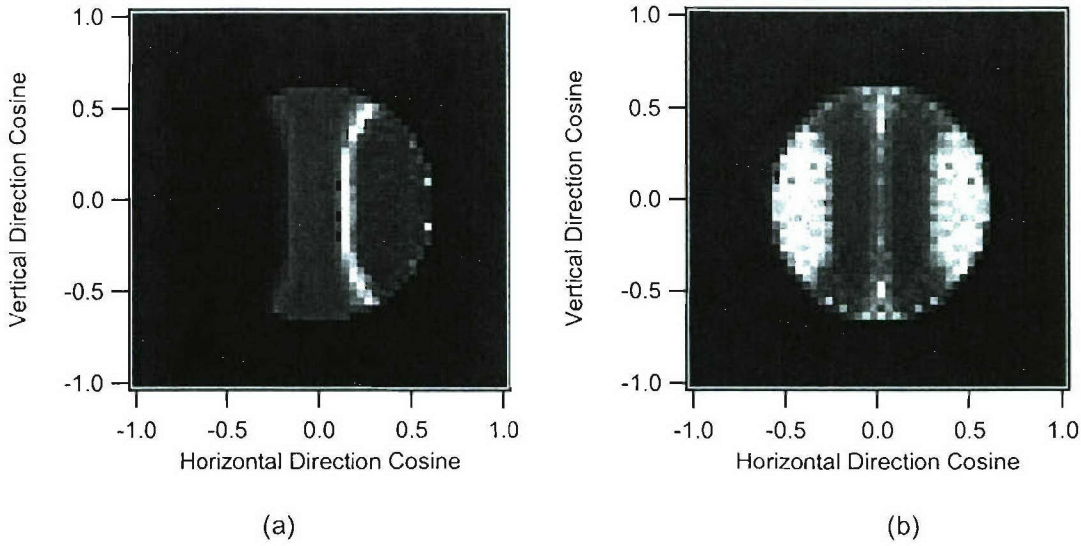

Figure 18 – (a) Half-field and (b) full-field angular distributions for basic mirror baffle luminaire with input direct from a fiber (no beam expansion).

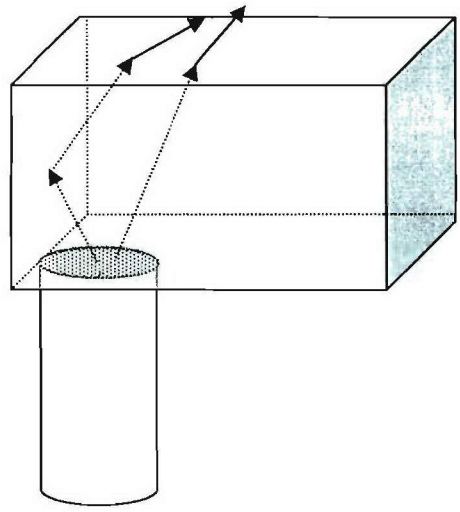

Figure 19 – Embedded mirror baffle luminaire using TIR vertical mirror.

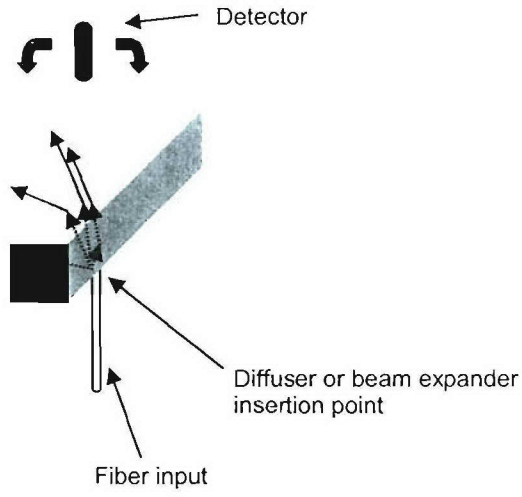

Figure 20 – Mirror baffle proof of concept experiment using a piece of acrylic painted black on three sides, with a small aperture at the bottom for source input.

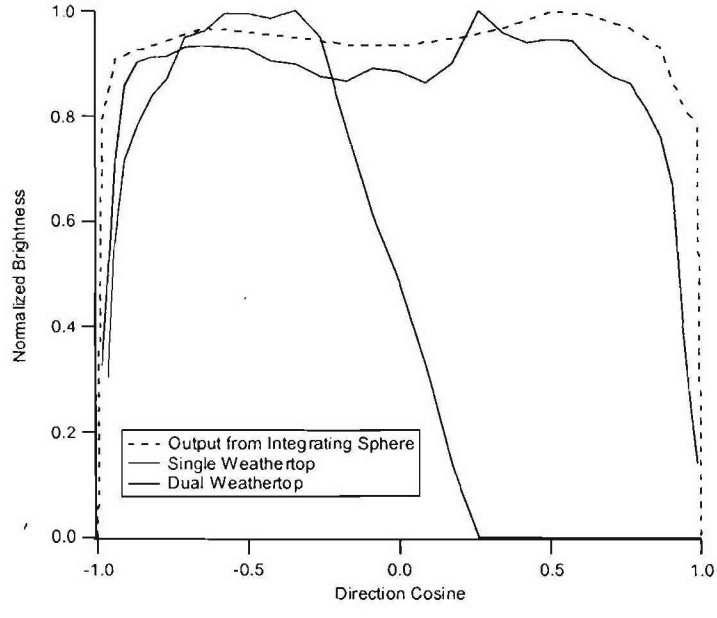

Figure 21 – Resulting angular distribution from mirror baffle pre-prototype. Input source was the output from an integrating sphere. Distributions shown are from a single luminaire (half-field) and two luminaires oriented opposite to one another (full-field). Also shown is the distribution from the integrating sphere for comparison.

5.1 Expanders and Homogenizers

One of the keys to success for the mirror baffle design is a viable method for beam expansion and homogenization. For the design to be resistant to changes in the input angular distribution, some method for randomizing the beam is essential. In addition, to achieve a Lambertian distribution out to the most extreme angles, a method for expanding the beam from the input fiber is also required. Among the possibilities are non-imaging optics, statistically random refractive structures, holographic diffusers, and other diffusers such as ground glass.

Perhaps the best-known example of a beam expander is the compound parabolic concentrator (CPC). However, as shown in Figure 22, the CPC is very sensitive to proper filling of the input aperture. This could cause significant problems in a device where tolerances cannot be kept extremely tight. In addition, the CPC provides only beam expansion; it does not provide any beam homogenization.

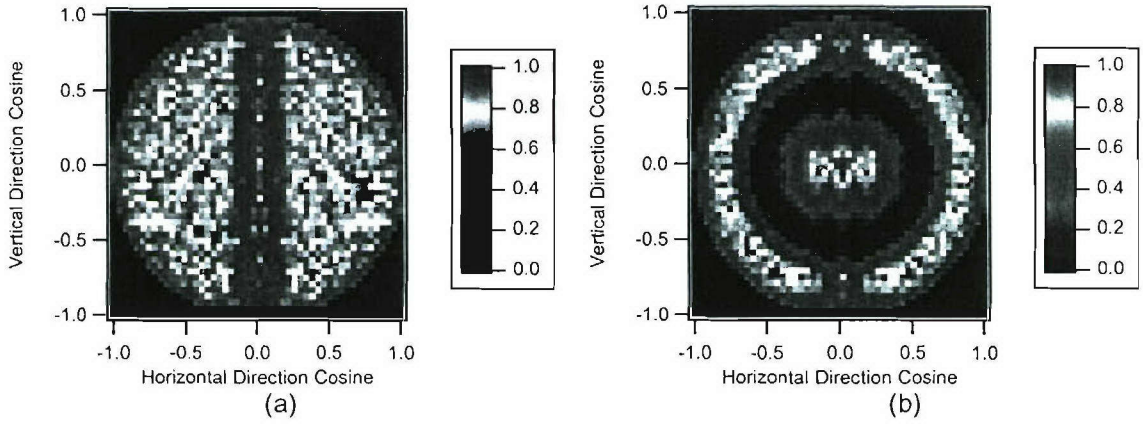

Figure 22 – Illustration of the sensitivity of CPC beam expansion to filling of the CPC input aperture. Shown are the full-field modeled angular distributions for a mirror baffle luminaire with CPC input for (a) 100% and (b) 70% filling of the CPC input aperture.

Another simple beam expansion method would be to use a simple negative ball lens molded into plastic, as shown in Figure 23. This design would be simple to implement and align, and would also allow for expansion in one dimension only by using a cylindrical lens. Figure 24 shows the angular distribution from a ball lens beam expander and fiber combination. In this case, the fiber had a numerical aperture of 0.5, and the ball lens had a diameter the size of the fiber. Also shown for comparison is the angular distribution from an integrating sphere. For this particular example, the expansion from the ball lens alone is not sufficient to meet our requirements.

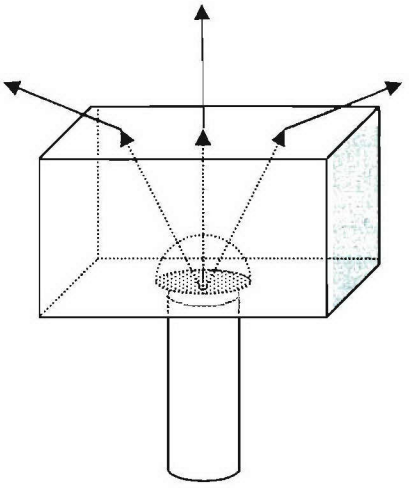

Figure 23 – Illustration of ball lens beam expander.

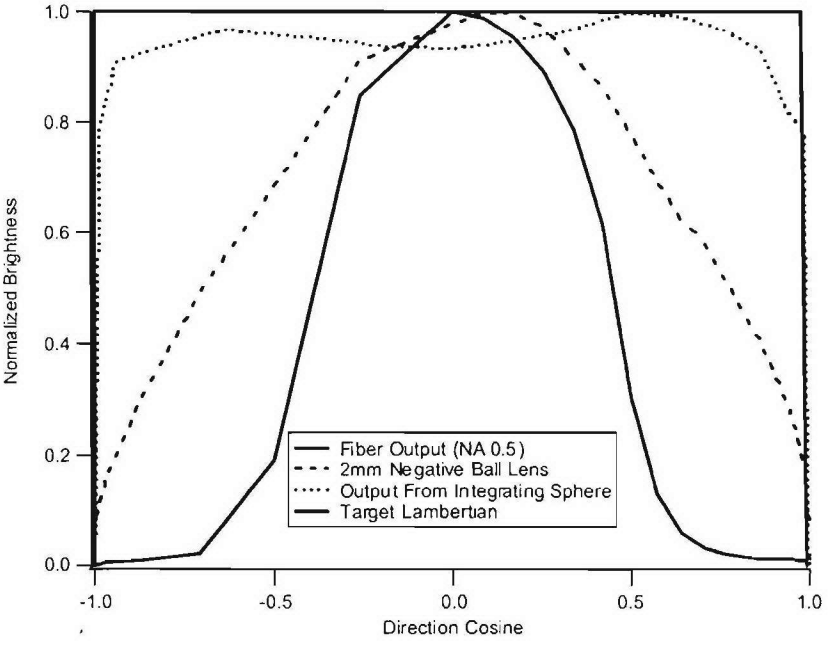

Figure 24 – Angular distribution for a ball lens beam expander with fiber input. Also shown for comparison is the angular distribution from an integrating sphere.

We also examined several types of diffuser, including holographic diffusers from Physical Optics Corporation as well as regular ground glass diffusers. Figure 25 shows the angular distributions of the best of these candidates, an 80° POC diffuser and a piece of ground frosted glass. The frosted glass exhibited the best performance, but its efficiency was around 40%. The POC diffuser also had excellent performance, and demonstrated efficiency in excess of 80%.

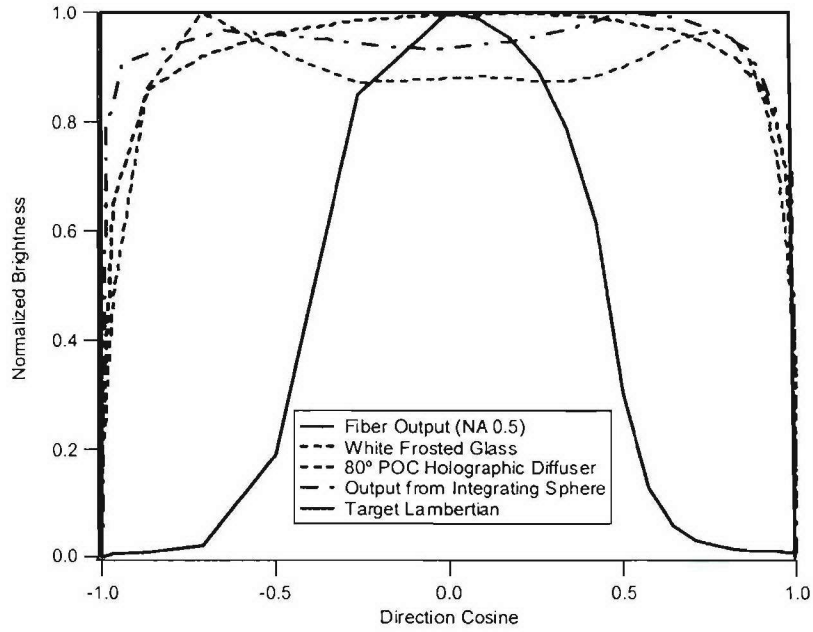

Figure 25 – Measured angular distributions for several transmissive diffusers fed by a fiber. Frosted glass efficiency is near 40%; holographic diffuser efficiency is near 80%.

Although the POC diffuser performs well, it still falls short of producing a Lambertian distribution at the extreme angles. In an attempt to improve the beam expansion further, we looked at the possibility of "pre-expansion" of the beam by a different method before passing through the POC diffuser. To test the effectiveness of this approach, we measured the angular distribution of light passing through the diffuser from two fibers, each with different numerical apertures. Figure 26 shows the resulting distributions, both from the bare fibers as well as after the beam passes through the POC diffuser. The results indicate that "pre-expansion" of the beam can indeed improve the overall angular extent.

There are several methods to expand the beam before it hits the diffuser. Modifications to the luminaire include adding a lens (such as the ball lens discussed previously), or adding an extra holographic diffuser. One can also modify the fiber by adding a taper to the fiber end, molding a lens into the fiber, or introducing a scattering surface at the end of the fiber. We examined the effect of adding an extra holographic diffuser to the end of the fiber to improve the angular distribution.

Figure 27 shows the angular distribution for two POC 80° diffusers, along with the angular distribution for a single diffuser and the integrating sphere for comparison. The angular extent with pre-expansion of the beam is much improved from the original case. However, the efficiency of the system suffers with pre-expansion. With a single 80° diffuser, the efficiency is around 80%, but with two 80° diffusers, the efficiency drops to around 50%. It may be possible to use a lower-angle diffuser for pre-expansion and still obtain similar performance improvements without such an extreme loss in efficiency.

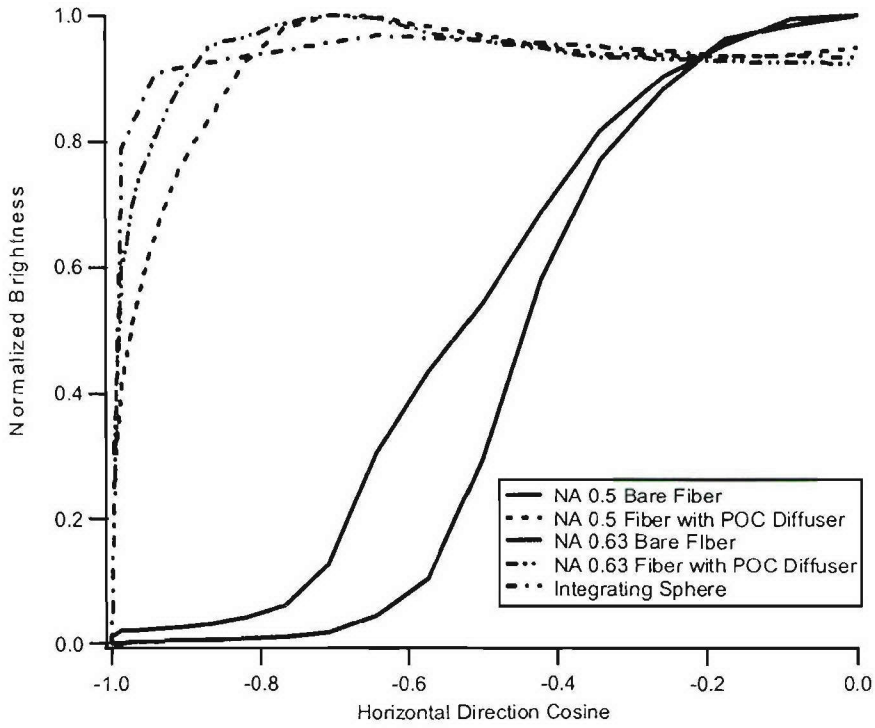

Figure 26 – Demonstration of effectiveness of pre-expansion.

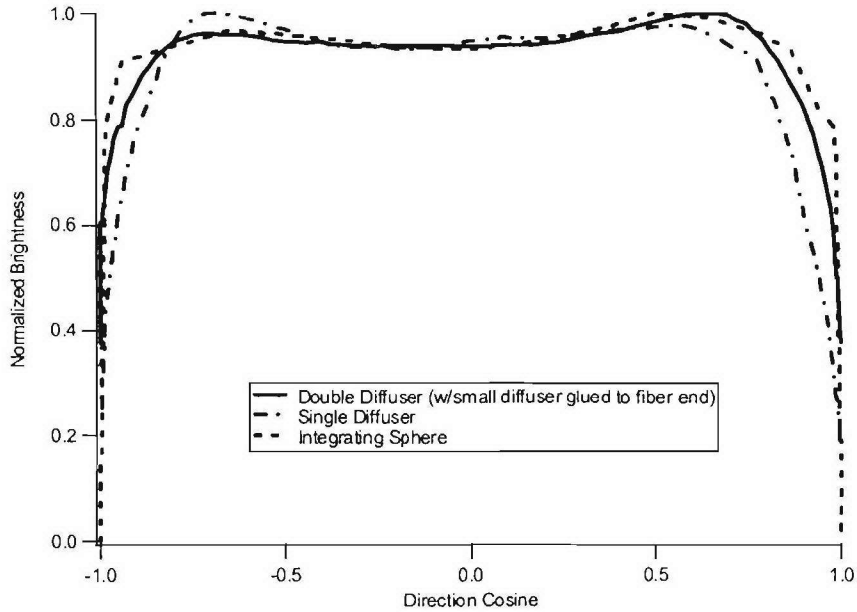

Figure 27 – Measured angular distribution showing effect of double holographic diffuser on overall angular extent. The double diffuser efficiency is only 50%, compared with 80% for the single diffuser.

Another method for pre-expansion is to place a taper on the fiber tip, as shown in Figure 28. The taper acts somewhat like a CPC in that it expands the angular extent of the exiting light. However, in this case, the light will then be entering a diffuser, making the angular uniformity of the taper output less important. Figure 29 shows model results for the expansion of light from a fiber with numerical aperture (NA) of 0.4 using a 2 mm taper whose diameter varies from 400 μm down to 300 μm. Also shown is the resulting distribution if the input aperture is only partially filled by a 200 μm fiber. The ripples are similar to the nonuniformities seen in the underfilled CPC. Without an accurate model of the holographic diffuser, it is difficult to predict how much of this variation is tolerable.

One of the concerns with the holographic diffuser is that there might be significant dispersion when illumination is with white light. This would manifest as a difference in brightness for different colors as a function of angle. Figure 30 shows measurements of the POC 80° diffuser for three different wavelength bands of 20 nm width. The bands were centered on 445 nm (blue), 530 nm (green) and 665 nm (red). The angular data was normalized to the source spectrum and then expressed as a percentage of the green band. The data indicate that the spectral performance of the POC diffuser versus angle is relatively flat.

Other HEDLight team members recommended an alternate vendor of structured diffusers. RPC Photonics of Rochester, NY, makes custom structured diffusers that differ from holographic diffusers in that the diffusing surface is specifically engineered to match a particular output distribution. Typically they design the diffusers to provide constant irradiance onto a surface, which results in an angular distribution that is relatively flat in angle space. This is a more difficult distribution to create than the Lambertian distribution we desire. Figure 31 shows measurements made of a quad sample provided by RPC Photonics showing their off-the-shelf capabilities. Even the best diffuser falls short of the desired Lambertian distribution (here the x-axis shows angle space, and therefore the ideal Lambertian appears as a cosine function). However, their engineers indicated that approaching a Lambertian distribution from a narrow fiber input would not be difficult. Figure 32 shows model results developed at RPC Photonics, showing their expectation for angular performance compared to an ideal Lambertian. We are currently ordering a custom sample from them to test.

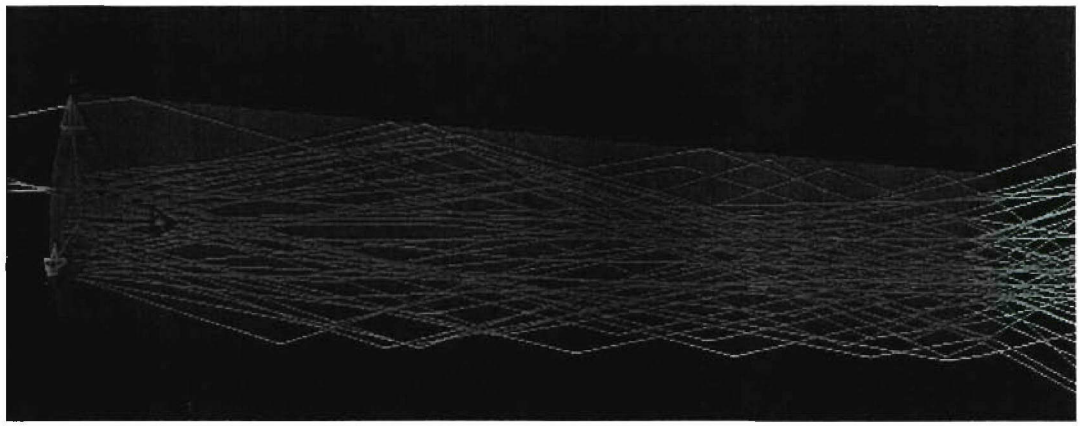

Figure 28 – CAD image of tapered fiber tip.

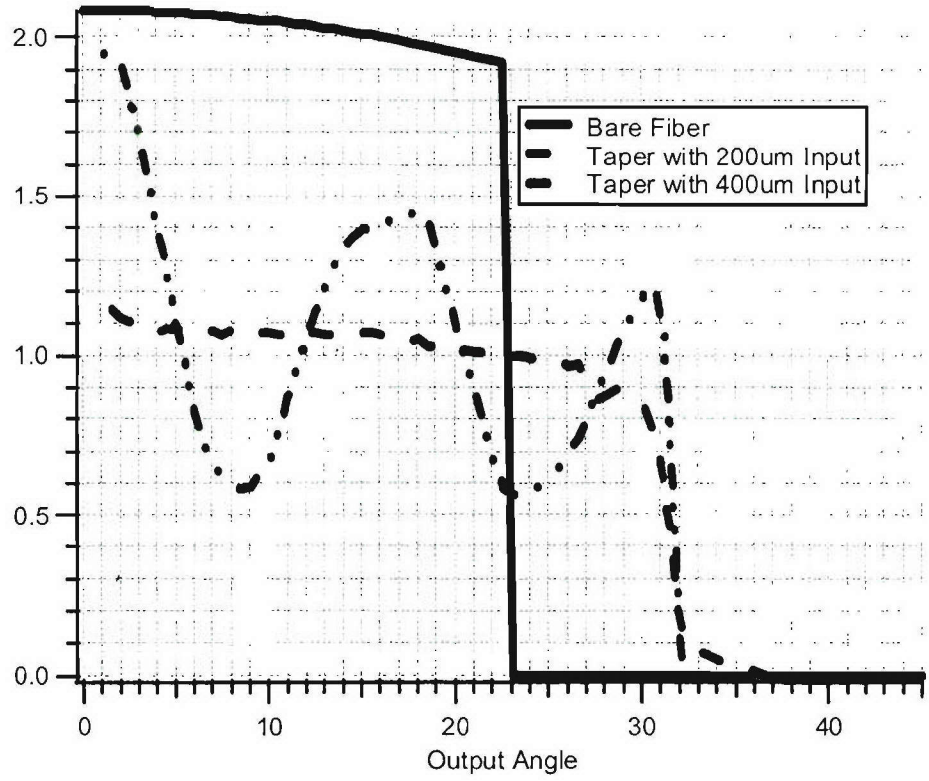

Figure 29 – Modeled angular distribution for NA=0.4 fiber, output from taper, and output from taper with underfilled aperture. Taper is 2 mm long with input diameter 400 µm and output diameter 300 µm.

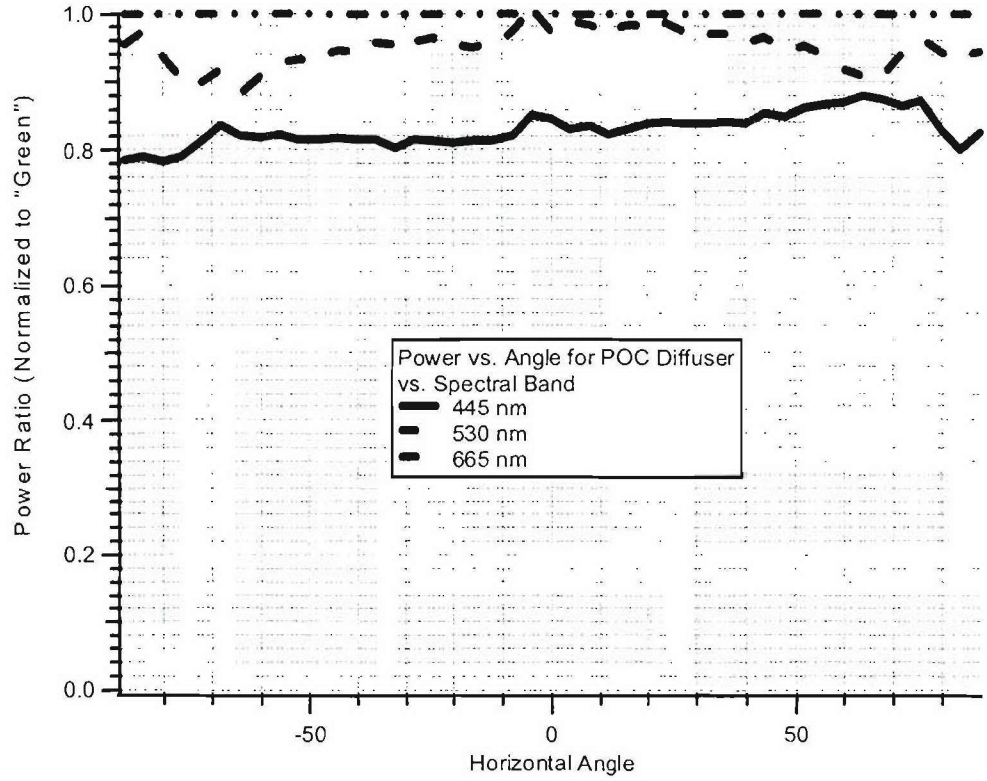

Figure 30 – Spectral performance of POC 80° diffuser vs. angle.

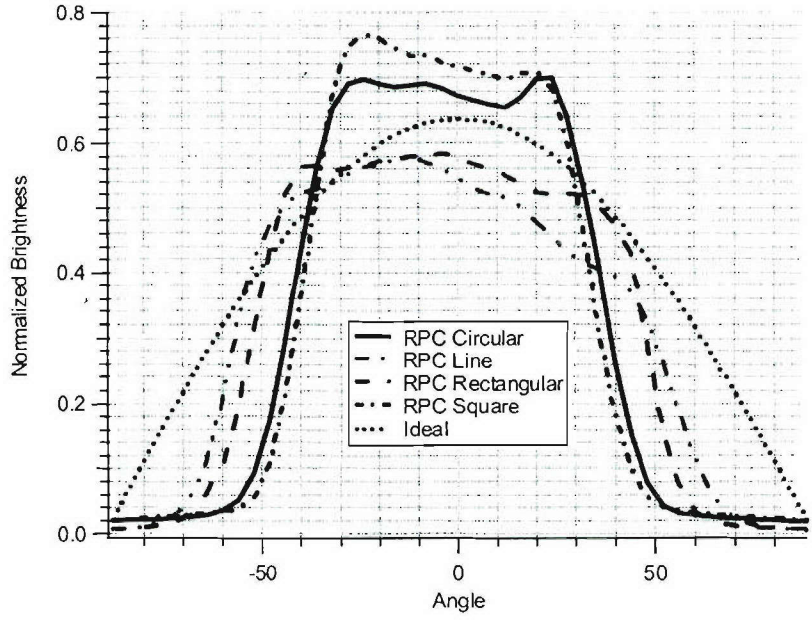

Figure 31 – Angular performance of commercial RPC structured diffusers.

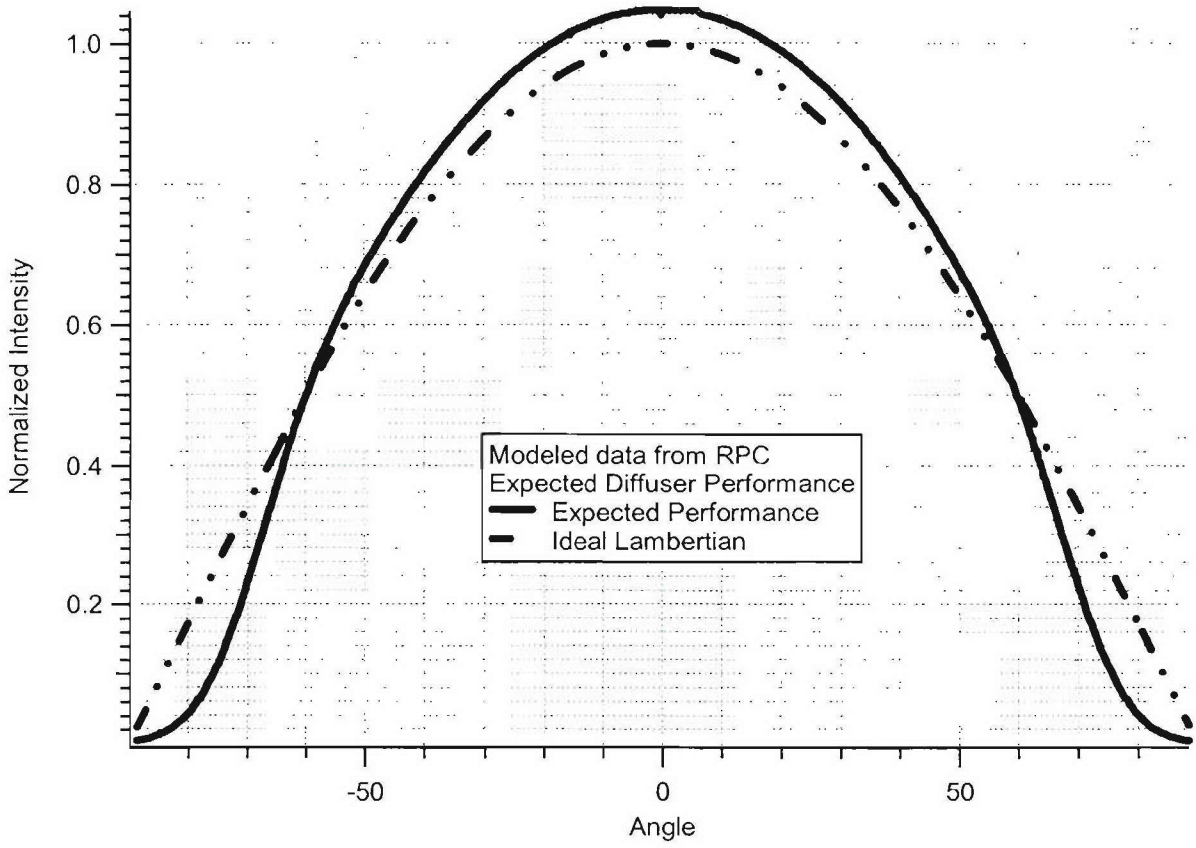

Figure 32 – Modeled expected diffuser performance for custom RPC structured diffuser.

5.2 End-fire Prototypes

In considering all of the design options, it was determined that the mirror baffle design was the candidate most likely to meet all the requirements. We therefore began designing a more complete two-zone end-fire mirror baffle luminaire that could easily be manufactured by a qualified plastic optical mold shop. We held several discussions with Physical Optics Corporation as well as Polymer Optics of Santa Rosa, CA, to get a feel for the achievable tolerances and manufacturability requirements for the design. The design we finally settled upon is shown in Figures 33 and 34. The design is made up of two parts: an optical part that provides the TIR mirror surfaces, and a mechanical part that holds the fibers in proper alignment and provides an absorbing surface for stray scattered light. Ultimately, a diffusing surface would be molded into the bottom surface of the optical part, providing beam expansion and homogenization. However, for initial prototypes, commercial holographic diffusers can be glued to the input surface of the optical part.

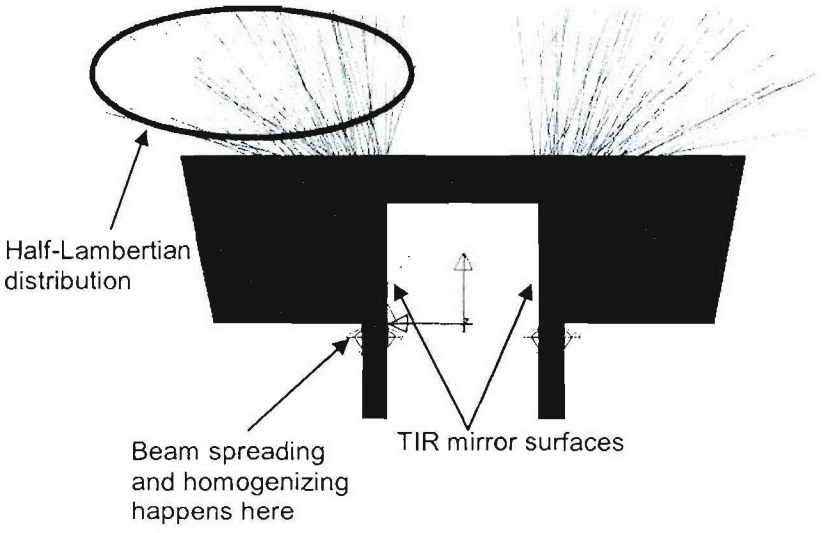

Figure 33 – CAD image of prototype mirror baffle luminaire.

In considering the manufacturability of the design, we modeled the effect of manufacturing tolerances on optical performance. In conversations with the molders it was mentioned that a draft angle might be required on the slot defining the TIR mirrors in order to facilitate mold release. This draft angle could be as high as 2°. In addition, the positioning of the fiber holes relative to the slot could be maintained only to within 25-50 μm. Figure 35 shows the geometries associated with these tolerances on the mirror baffle design.

In modeling the draft angle, we looked at both symmetric and asymmetric cases involving draft angles of 0°, 1°, and 2°. Figure 36 shows the associated angular distributions. The results indicate that to attain full-field uniformity within ±10% of the mean requires a draft angle of no more than 1°. A draft angle of 2° is the maximum allowable to achieve a full-field uniformity within ±20% of the mean.

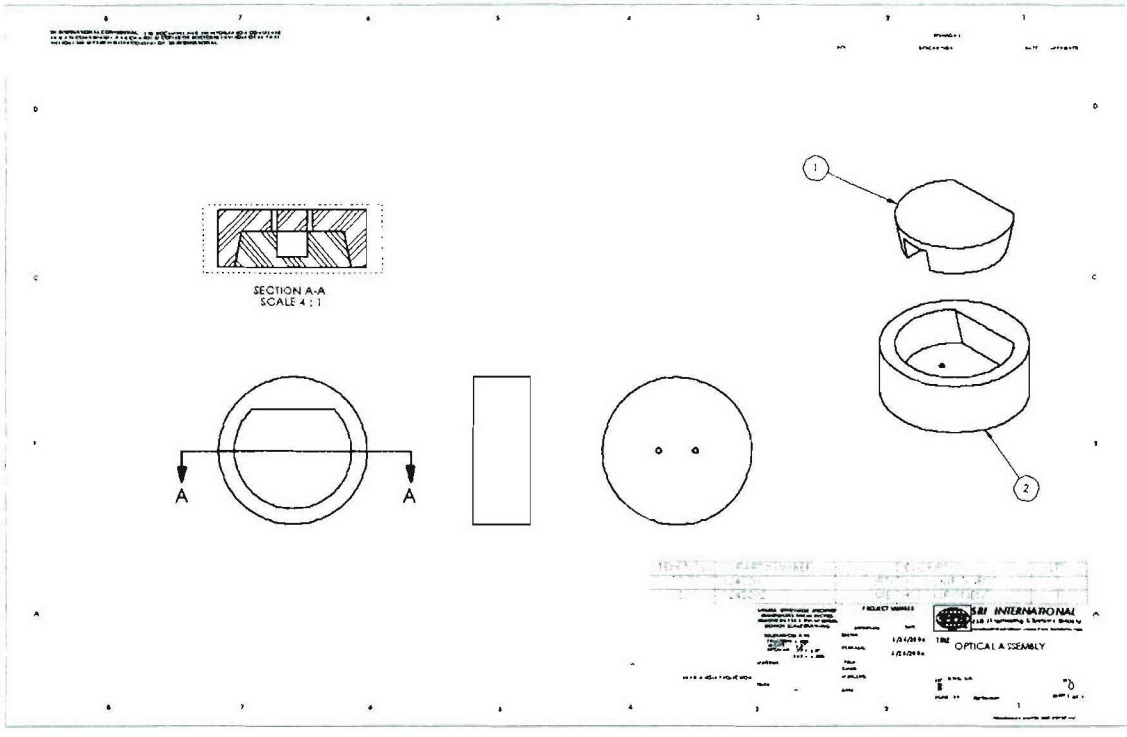

Figure 34 – Mechanical drawing of prototype mirror baffle luminaire.

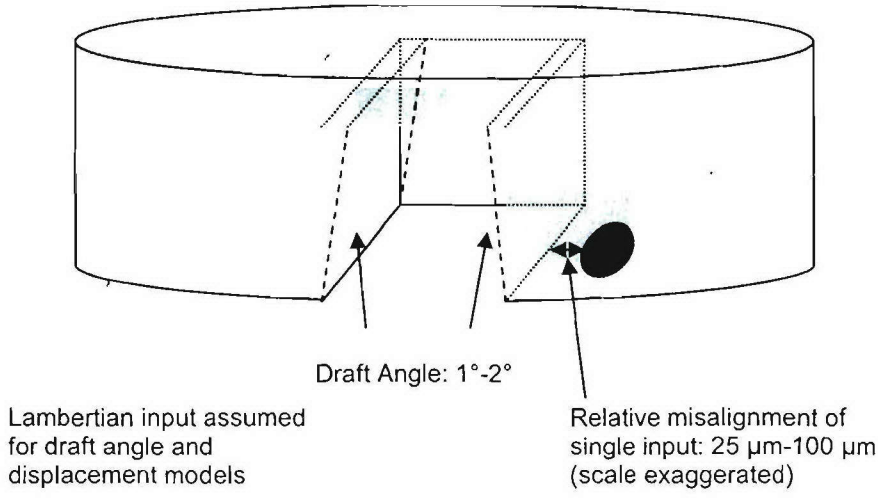

Figure 35 – Illustration of geometry used to model tolerances for mirror baffle luminaire.

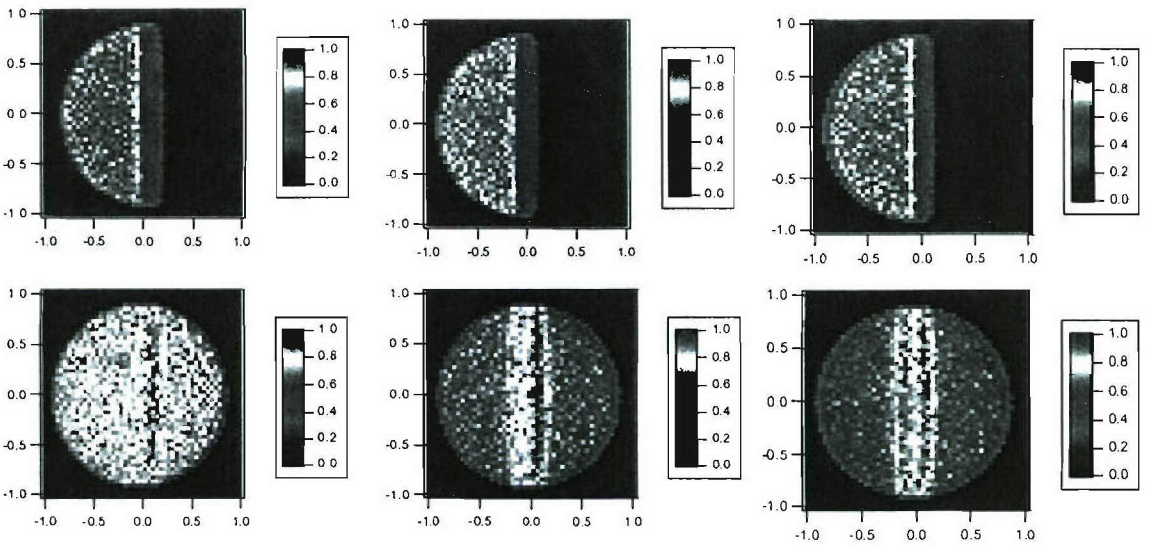

Figure 36 – Effect of TIR mirror draft angle on mirror baffle angular distribution. Top row shows half-field distributions and bottom row shows full-field distributions.

For fiber alignment, we examined the effect of moving one fiber independently of the other. When both fibers are symmetrically aligned with respect to the center of the luminaire, the full-field distribution remains uniform. Nonuniformities arise when the fibers are positioned asymmetrically with respect to the center of the luminaire. We examined the effect of misalignments of one fiber at distances of 25 μm, 50 μm, and 100 μm from the TIR mirror edge. Figure 37 shows the resulting angular distributions. Full-field uniformity within ±10% is achieved for misalignments up to 50 μm, and within ±20% for misalignments up to 100 μm.

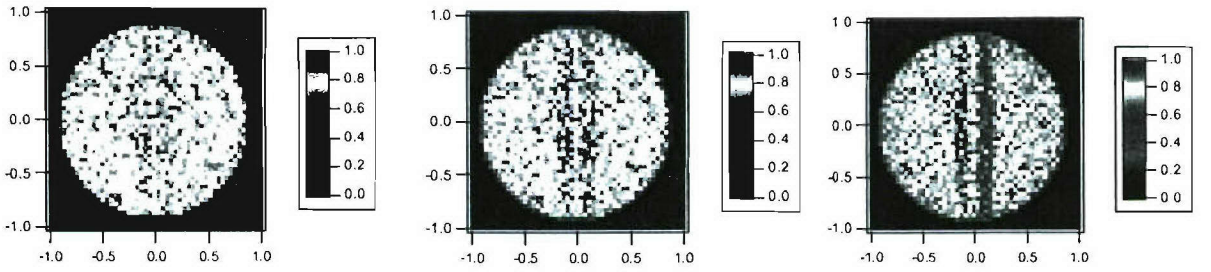

Figure 37 – Effect of fiber misalignment on angular distribution for mirror baffle luminaire showing relative displacements of (a) 25 μm, (b) 50 μm, and (c) 100 μm from the TIR mirror surface.

Using finite element analysis, we also examined the effect of temperature extremes on the optical performance of the design. The temperature range we considered varied from -40° C to +50° C. Figure 38 shows magnified images of the resulting distortion to the optical piece of the luminaire. The distortion was much more pronounced for the low-temperature case, and so for that case we ray-traced the resulting distorted optical piece. Figure 39 shows the resulting angular distribution. Essentially the angular distribution remains unchanged from the undistorted case, with the exception of two bright spots at the extreme angles.

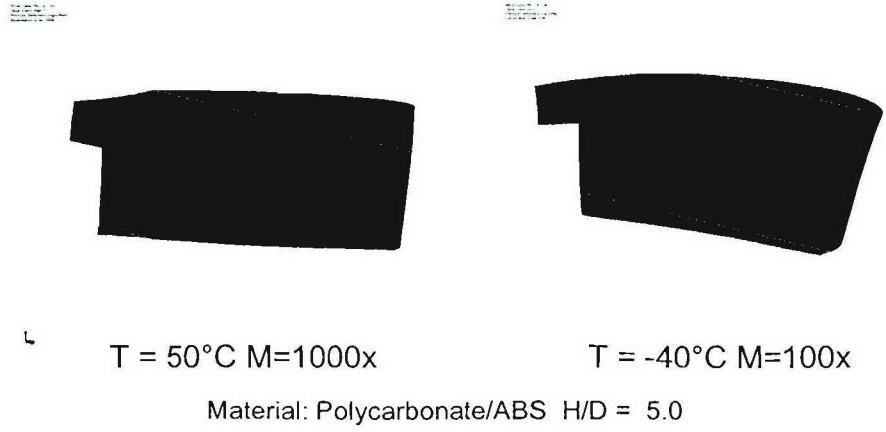

Figure 38 – Magnified CAD images of the distortion to the optical piece of the mirror baffle luminaire when exposed to temperature extremes of +50°C down to -40°C.

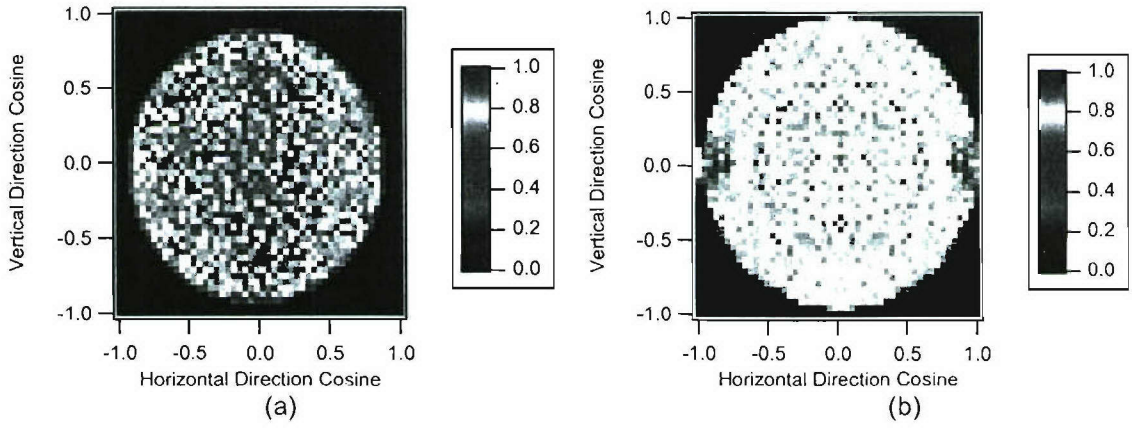

Figure 39 – Comparison of the mirror baffle angular distributions for (a) T = 25°C and (b) T = -40°C.

We then constructed a large-scale prototype model of the mirror baffle design out of acrylic and acrylonitrile butadiene styrene (ABS). We used 80° diffusers backed with pressure-sensitive adhesive from Physical Optics Corporation as a combination beam expander/homogenizer. Figure 40 shows an image of the optical and mechanical pieces of the final prototype. Figure 41 shows a single cut from the angular distribution of the device, with the original pre-prototype data as well as data from an integrating sphere (Lambertian source) for comparison. The angular distribution from the mirror baffle design falls short of Lambertian at the extreme angles. This can be improved by taking advantage of the double diffuser approach discussed previously.

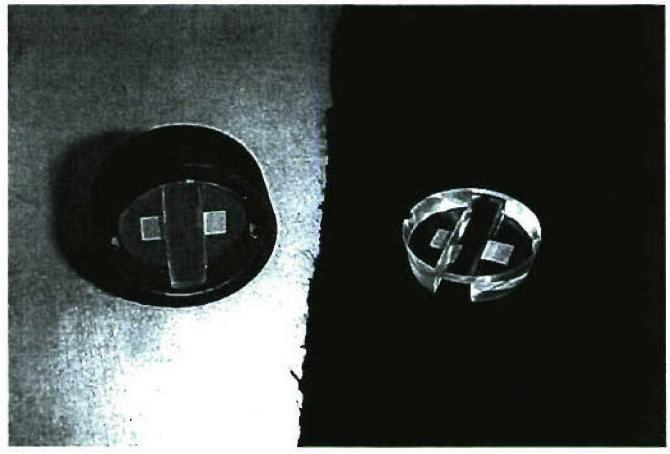

Figure 40 – Image of large-scale mirror baffle prototype. Shown are assembled prototype (left) and separate optical part (right).

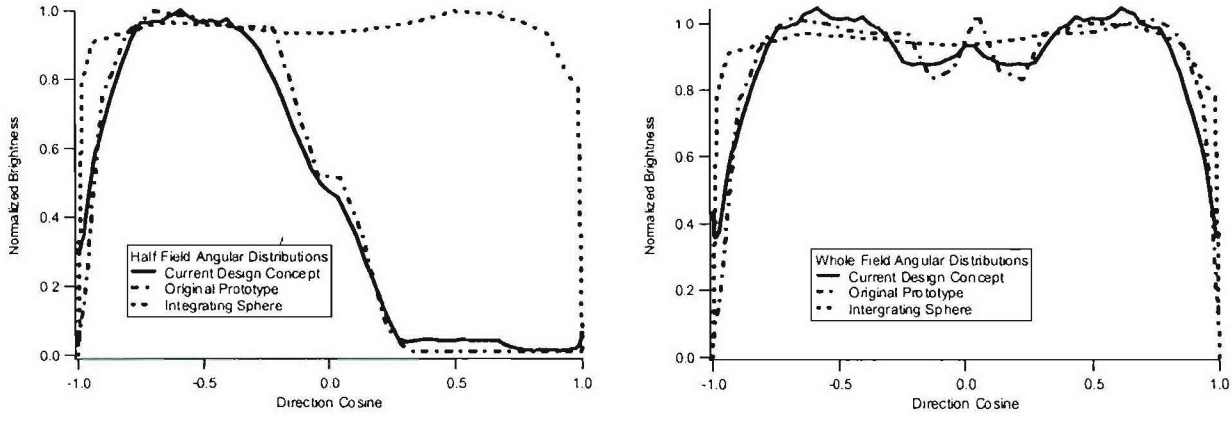

(a) (b)

Figure 41 – (a) Half-field and (b) full-field angular distributions measured from mirror baffle prototype. Shown for comparison are the distributions from the mirror baffle pre-prototype as well as the integrating sphere.

Ideally an injection-molded version of the luminaire would have the diffuser molded directly into the input surface. We therefore contracted with Physical Optics Corporation to produce a limited number of small-scale prototypes of the luminaire. Figure 42 shows the angular distribution measured from these luminaires. The luminaire was fed by a 300 μm glass core fiber with NA=0.47. The significantly lower NA results in an output distribution that falls short of the Lambertian requirement. There were also other issues with the injection-molded part. The efficiency of the optical piece alone was greater than 70%. However, the efficiency of the fully assembled luminaire dropped to 55%. The discrepancy can be explained by two factors. First, if the fiber is inserted too far into the holder, it can scrape the diffuser surface, rendering it useless. Therefore when the fiber was inserted, a small distance was left to ensure the integrity of the fiber. However, some of the spreading light exiting the fiber is absorbed by the walls of the alignment hole, lowering the efficiency. In addition, the tolerance of the fiber insertion hole was so tight that as the fiber is inserted, some plastic scrapes off the sides of the hole, partially obscuring the aperture.

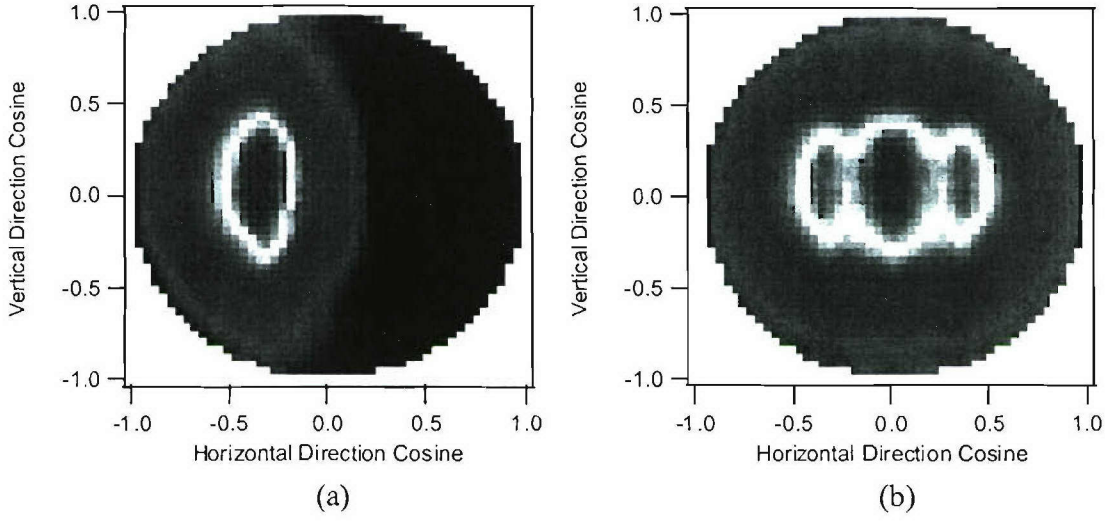

Figure 42 – Measured angular distributions for small-scale end-fire luminaire showing (a) half-field and (b) full-field.

5.3 Side-fire Prototypes

The geometry of the previous design is inherently "end-fire" in that the fibers enter the luminaire along the same axis as the light exits. In certain applications a side-fire geometry would be more appropriate. In a side-fire design, the fibers enter the luminaire perpendicular to the axis of the luminaire. A mirror angled at 45° in a block of plastic provides a plane of symmetry that allows for the creation of a side-fire mirror baffle design. Figure 43 illustrates the equivalence between the side-fire and end-fire mirror baffle concepts. The primary advantage of the side-fire mirror baffle design is that it can be much shorter than the end-fire design, as the

TIR mirror is now oriented horizontally. The main disadvantage is that the exit surface also plays the role of the TIR mirror, and therefore scratches and dirt on that surface might have a more significant detrimental effect. This design also uses a metal mirror, which introduces an additional 5-10% loss. Figure 44 shows a CAD image of a side-fire mirror baffle design; the modeled angular distribution is shown in Figure 45.

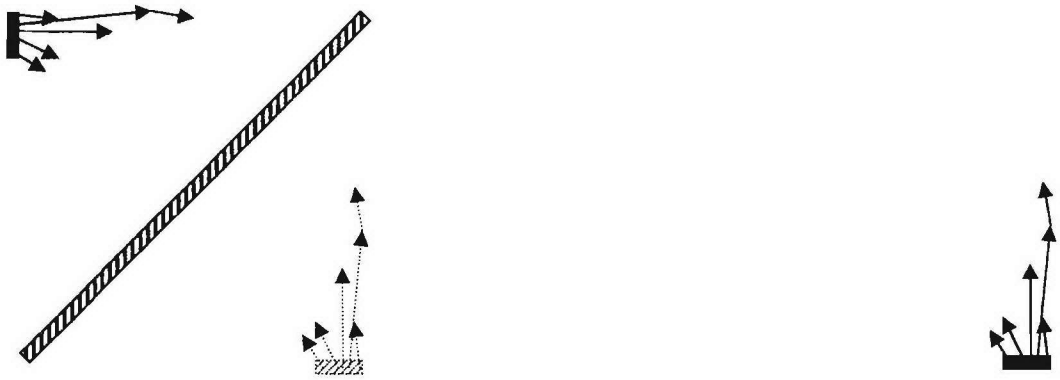

Figure 43 – Illustration of the equivalence between the end-fire mirror baffle and a side-fire version that uses an angled mirror. The mirror in (a) provides a plane of symmetry, making that design functionally equivalent to the design in (b).

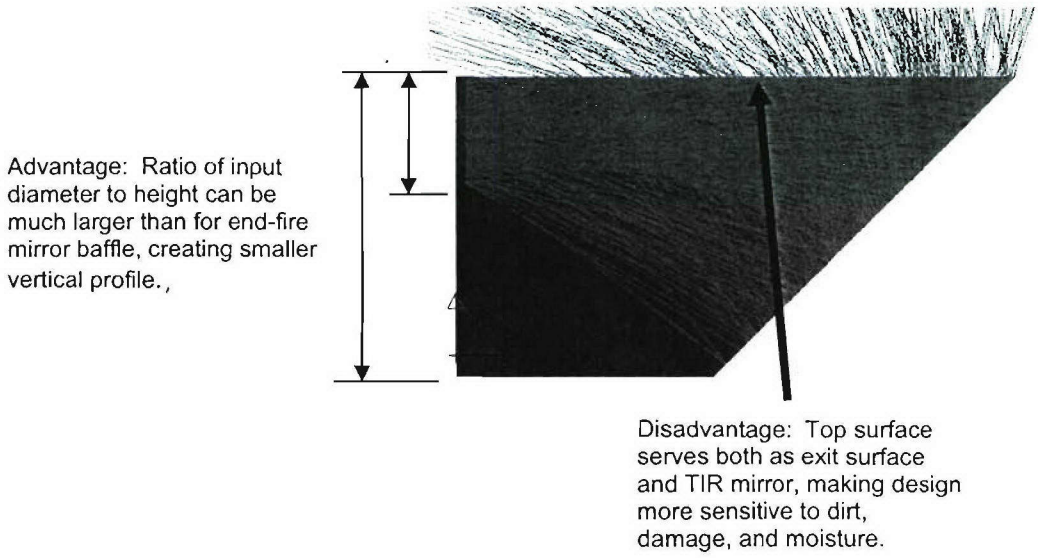

Figure 44 – CAD image of side-fire mirror baffle design.

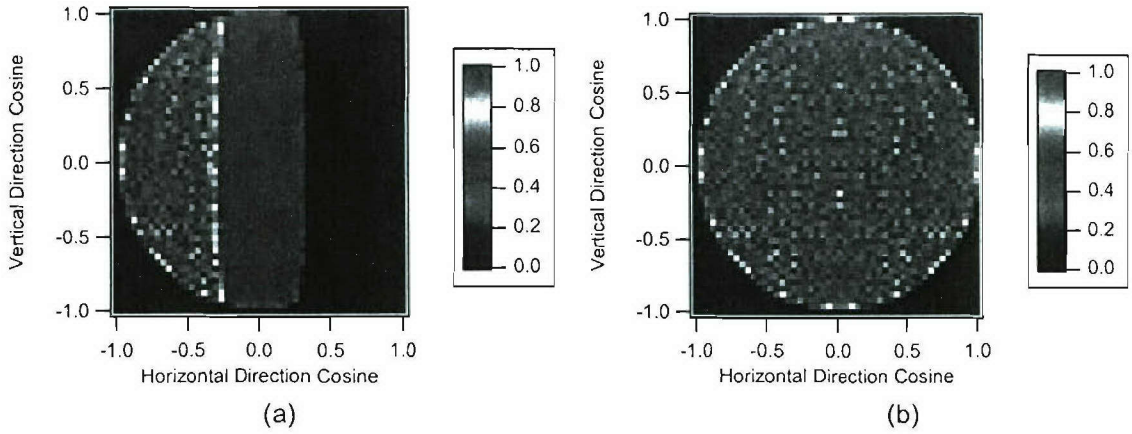

Figure 45 – Modeled angular distributions for side-fire mirror baffle showing (a) half-field and (b) full-field distributions.

As with the end-fire design, we constructed a large-scale prototype of the side-fire design in the SRI model shop. The optical piece was constructed from polycarbonate to ensure better chemical resistance, while the mechanical piece was again made from ABS. We formed the mirrored surface by gluing a thin sheet of aluminized ultem to the angled surface, and the diffuser surface was a piece of commercial POC 80° diffuser stuck to the input face of the prism. The fiber was a 1.5 mm plastic fiber with NA=0.6 and was offset 2 mm from the top surface of the luminaire to protect the junction between the fiber and the diffuser from the exterior environment. Figure 46 shows the modeled and measured angular distributions for the large-scale side-fire luminaire. The flat "shelf" within the transition region of the half-field distribution is a direct result of the fiber offset from the top surface of the luminaire. For certain applications, this shelf might be unacceptable. The efficiency of the large-scale luminaire is only 51%. The low efficiency is primarily due to the large bulk absorption of polycarbonate. Using acrylic for the optical piece would improve the efficiency by 20% at the expense of increased size and decreased chemical resistance.

One method for allowing the fiber to be positioned closer to the top surface of the luminaire while simultaneously protecting the fiber/diffuser junction would be to employ a thin protective window over the top of the luminaire, as shown in Figure 47. Figure 48 shows the (a) modeled and (b) measured angular distributions for the large-scale side-fire luminaire with a 100-μm-thick PET window. In this case the fiber was located flush with the top surface of the luminaire.

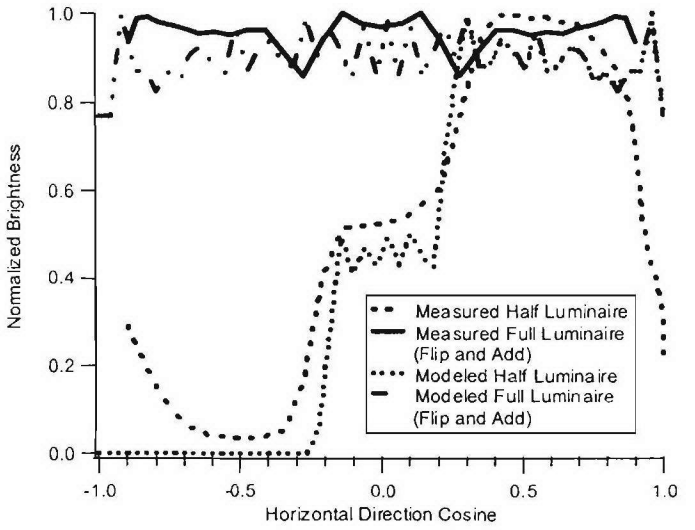

Figure 46 – Modeled and measured data for large-scale side-fire luminaire.

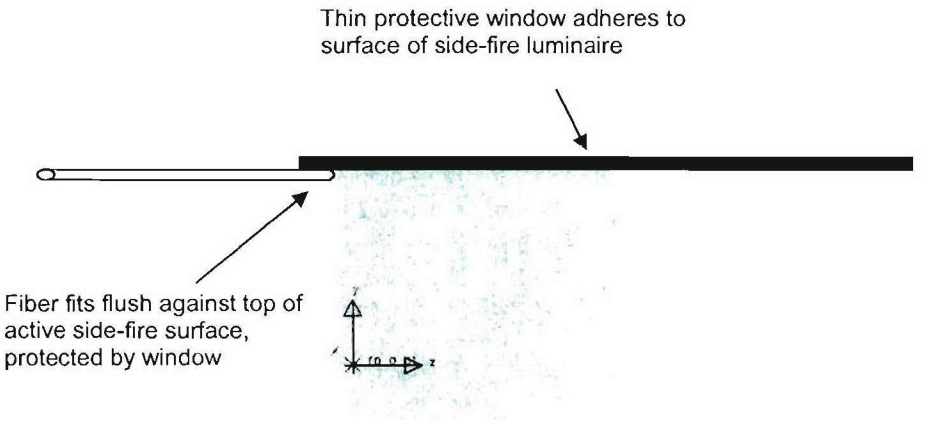

Figure 47 – Schematic of side-fire luminaire with protective window adhered to top surface.

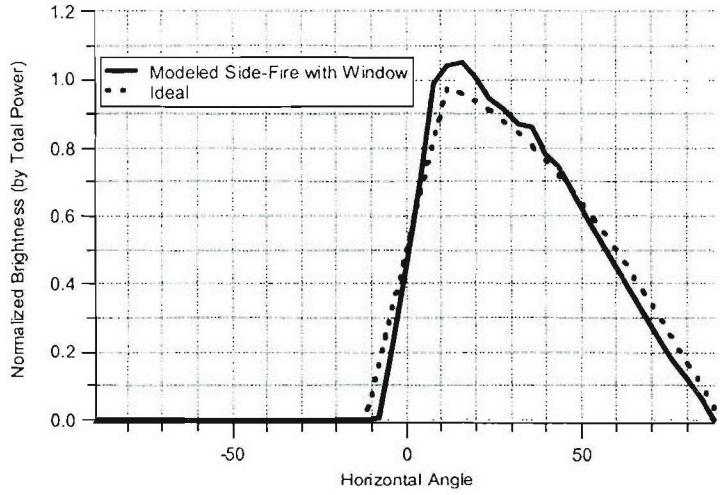

(a)

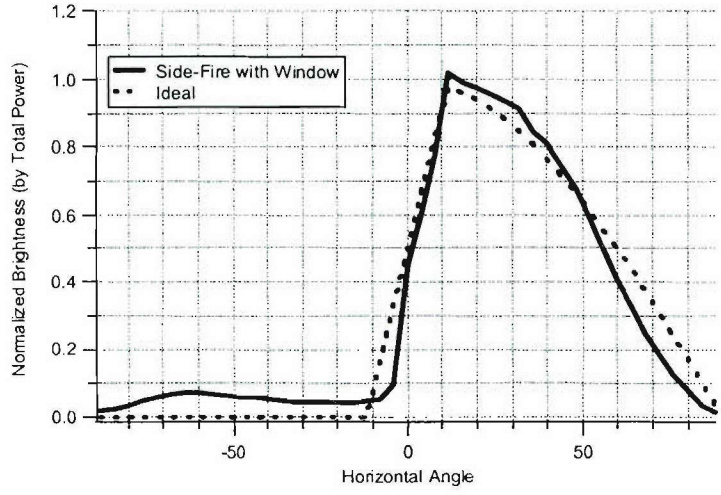

(b)

Figure 48 – Angular distributions for large-scale side-fire luminaire with protective window showing (a) results from LightTools model and (b) results from prototype measurements. Note the absence of a flat shelf in the linear transition region. Data is shown in angle space to emphasize grazing angles.

When considering a small-scale luminaire, the thickness of the window becomes significant relative to the luminaire size. One concern is that the fiber is now displaced further relative to the fiber diameter from the top surface of the luminaire, resulting in reintroduction of the flat shelf in the transition region. However, as shown in Figure 49, if the adhesive layer has a sufficiently low index, the light at grazing incidence will reflect off the polycarbonate/adhesive junction, practically eliminating the effect of the window thickness.

There is still one potentially negative consequence of using the protective window on the small-scale luminaire. As shown in Figure 50, it is possible for some of the light to enter the protective window and miss the 45° window, leading to a slight banding in the resulting angular

distribution. Figure 51 (a) shows modeled results demonstrating this banding for a polymethylmethacrylate (PMMA) window, while Figure 51 (b) shows the results for a window made of polyethylene terephthalate (PET). The banding effect is slight, and can be mitigated by appropriate material selection for the protective window.

Figure 52 shows a CAD model for a small-scale side-fire luminaire prototype with a protective window. To predict the behavior of the luminaire, we needed to develop a method for modeling the holographic diffuser. LightTools does not have the capability of modeling something as complex as a holographic diffuser on its own. Instead we decided to measure the angular output distribution of the 80° diffuser fed with a glass fiber of NA=0.47. We then used this data as the source/diffuser input to the luminaire model in LightTools. The resulting predicted performance for the small-scale side-fire luminaire is shown in Figure 53. The modeled angular performance falls short of the desired Lambertian distribution because the diffuser is now being fed with a fiber of much lower NA. We created a second model using data from a double diffuser input. These results are shown in Figure 54. The double diffuser closely matches the Lambertian distribution, but as described early, suffers from a low transmission efficiency.

We also examined modifications to the side-fire design to decrease its size. One possibility to decrease the size would be to shrink the width of the luminaire. The side surfaces can create additional mirror symmetry if they are mirrored or protected to allow TIR. Figure 55 shows a model of a narrow side-fire luminaire with mirrored sides of reflectivity 85%. The resulting angular distribution is shown in Figure 56. Because of the absorption of the mirrors, there is slight banding in the vertical angular distribution. Using TIR would eliminate this banding, but would require maintaining an air gap on both sides of the luminaire. Another issue with using the sides of the luminaire to produce lateral symmetry is that the luminaire becomes more sensitive to fiber position. Figure 57 shows the resulting angular distribution for fiber misalignment of 1% and 10% of the fiber diameter.

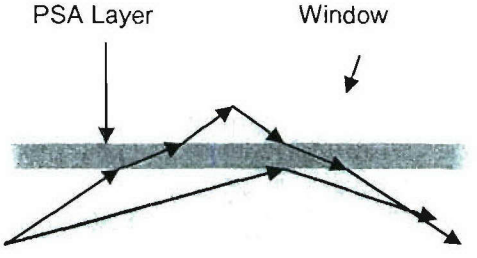

Figure 49 – Schematic of the effect of a low index adhesive layer in preventing grazing light from entering protective window.

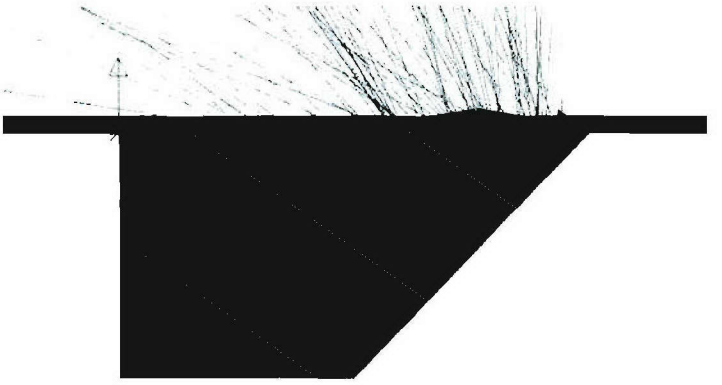

Figure 50 – Illustration of light entering protective window and missing mirrored surface. This leads to banding in the angular distribution.

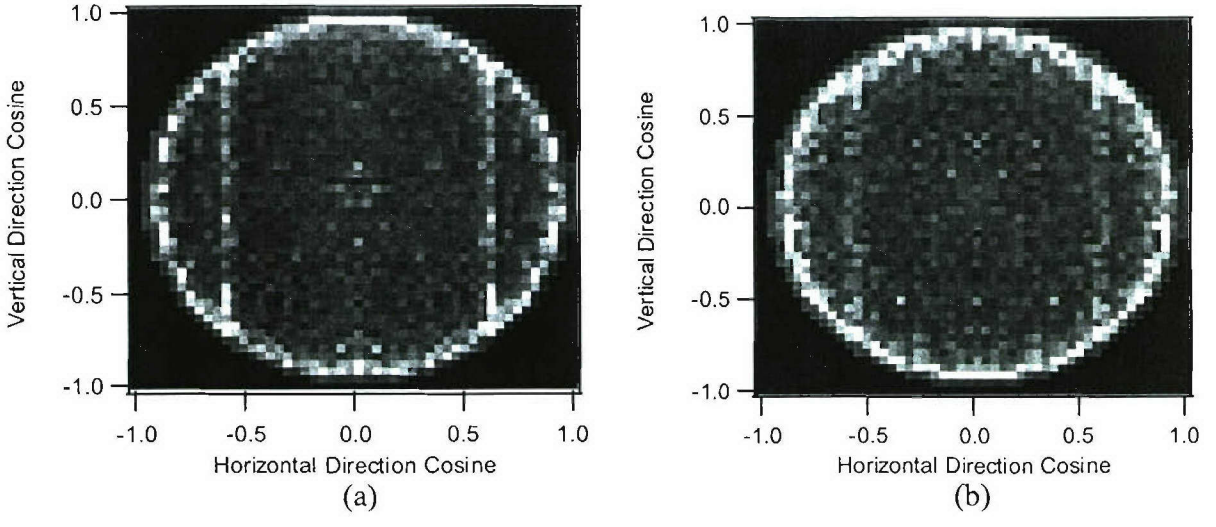

Figure 51 – Banding in the angular distributions for a luminaire with a protective window made of (a) PMMA and (b) PET.

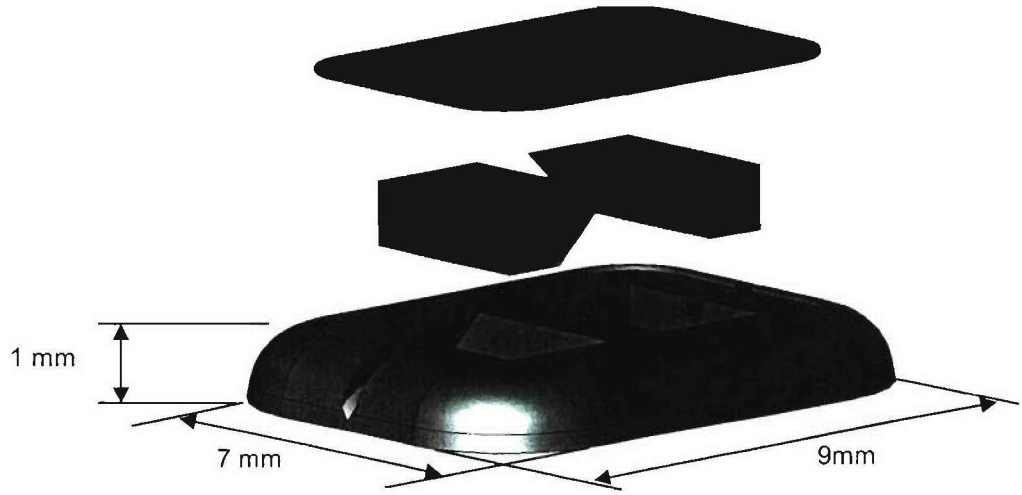

Figure 52 – CAD image of a small-scale side-fire luminaire with protective window.

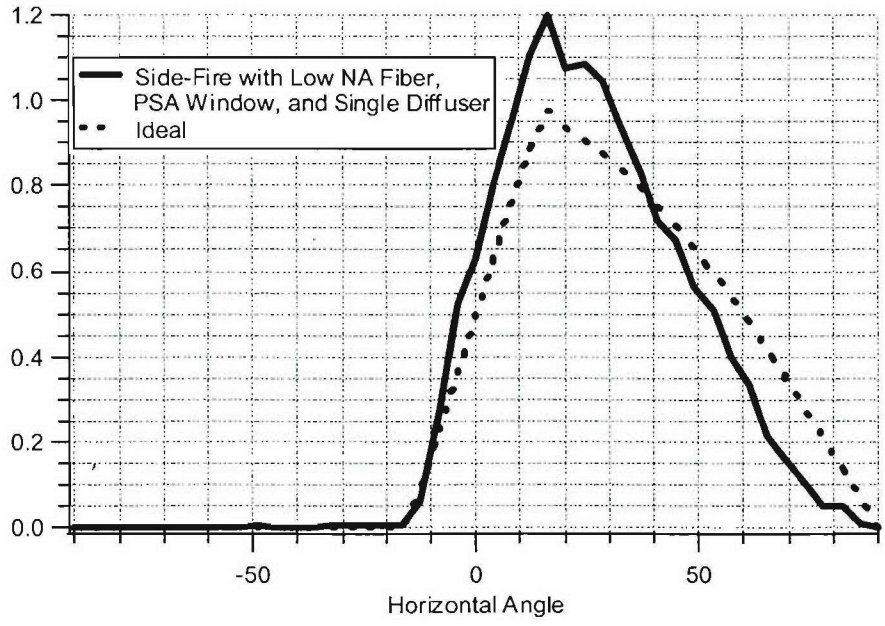

Figure 53 – Modeled angular performance for small-scale side-fire luminaire with protective window and single POC 80° diffuser.

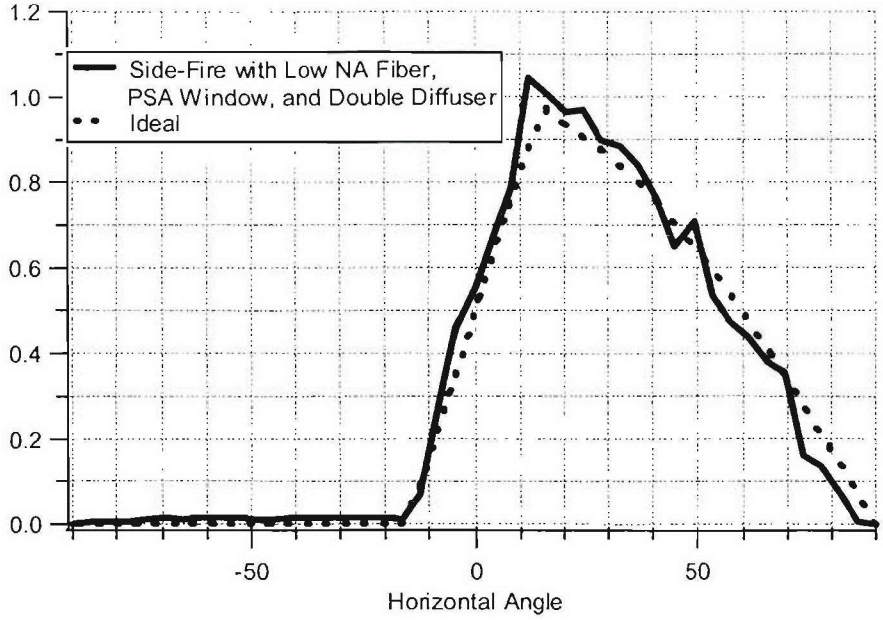

Figure 54 – Modeled angular performance for small-scale side-fire luminaire with protective window and double POC 80° diffuser.

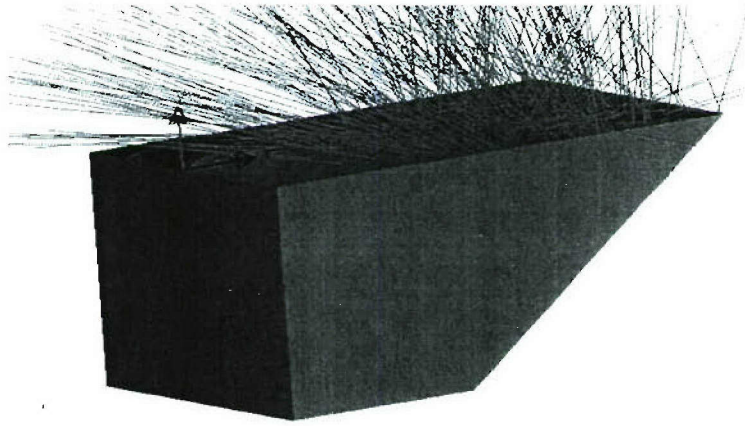

Figure 55 – CAD image of a narrow side-fire luminaire with mirrored sides.

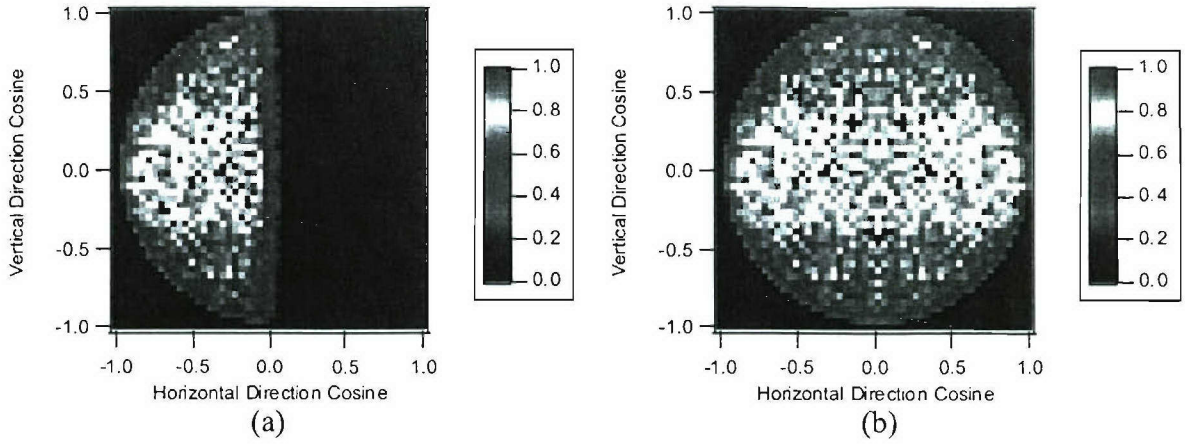

Figure 56 – Narrow side-fire luminaire angular distributions showing (a) half-field and (b) full-field. The absorption of the mirrors leads to banding in the vertical direction. This could be eliminated if TIR mirrors were used instead.

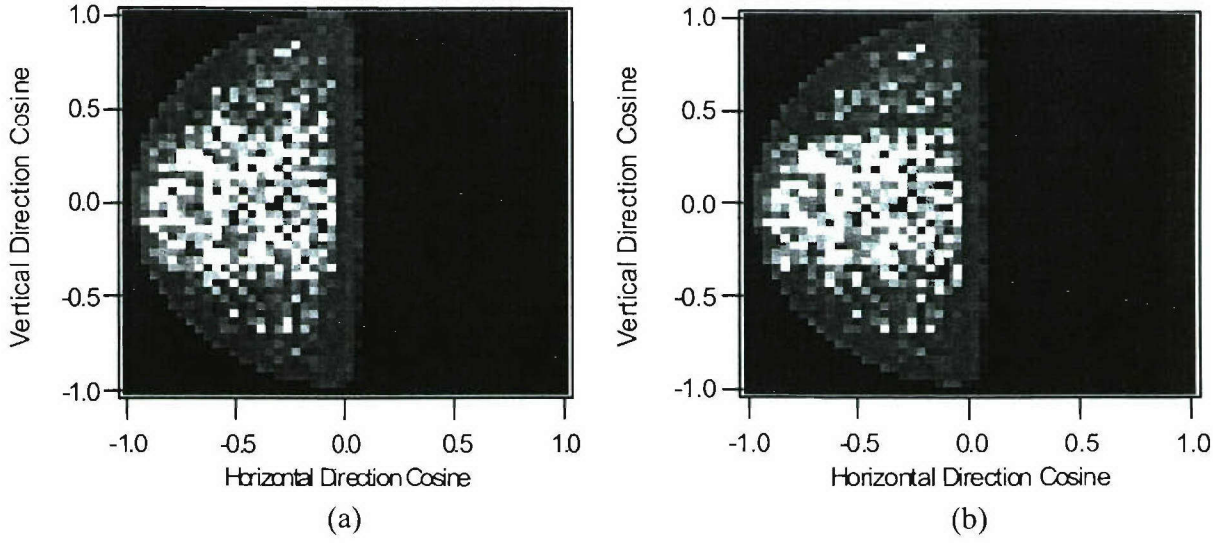

Figure 57 – Half-field angular distributions for narrow side-fire luminaire with fiber offset from center of luminaire by (a) 1% and (b) 10% of input fiber diameter.

REMAINING WORK PLANNED

For the remainder of the program, we will focus on further improvements to the small-scale side-fire luminaire with a protective window. We will continue to examine various beam expansion and homogonization methods, including structured diffusers from RPC Photonics and tapered fiber tips, to achieve broad angular extent with high efficiency. We will also order some custom-molded prototypes of the small-scale side-fire designs from an optical mold shop and characterize them for angular distribution and efficiency.